Synthesis, Characterization and Performance of Gelatin Biopolymer based Nanoparticle Formulations for Molecule Encapsulations

André T. Stevenson Jr.

Dissertation submitted to the faculty of the
Virginia Polytechnic Institute and State University
in partial fulfillment of the requirements for the degree of

Doctor of Philosophy
in
Materials Science and Engineering

Abby R. Whittington, Chair
Michael J. Friedlander
Pamela VandeVord
Gary R. Pickrell

March 13, 2018
Blacksburg, VA

Keywords: gelatin, nanoparticle, dispersity, glyceraldehyde, brain cells

Synthesis, Characterization and Performance of Gelatin Biopolymer based Nanoparticle Formulations for Molecule Encapsulations

André T. Stevenson Jr.

ABSTRACT (Academic)

Gelatin is one of the most common bulk biopolymers in the world finding use in food and pharmaceutical applications. Its ability to disperse in aqueous environments while also forming a thermo-reversible gel upon cooling allows for the encapsulation and emulsification of various substances into stable products. These properties along with a Generally Recognized as Safe (GRAS) certification by the Food and Drug Administration, have propelled gelatin nanoparticle (NP) research to encapsulate and deliver numerous food-based and pharmaceutical molecules.

While gelatin NPs have been shown to effectively protect molecules from premature enzymatic degradation, enhance therapeutic efficiency by crossing biological barriers such as the brain to treat brain injury, and maintain controlled release profiles which decrease side effects, the inability to obtain consistent gelatin NP properties substantially decreases its nanoscale translational potential. This is particularly troubling since NP properties dictate application and performance. Another need exists to stabilize gelatin NPs using alternative chemical crosslinkers to glutaraldehyde, which is reported to be toxic to cells.

Here, a materials science approach was implemented characterizing similar gelatins obtained from different manufacturers to determine correlations between their macroscale and nanoscale properties. Prior to chemical crosslinking gelatin samples with the lowest pre-crosslinked dispersity obtained the smallest average NP diameters (~71 nm), while samples with a higher dispersity obtained larger NP average diameters (>200 nm). From this work, a new method to obtain significant NP property consistency was developed based on vacuum filtration. To further increase the translational potential of gelatin NP formulations, crosslinking was performed using glyceraldehyde, a monosaccharide whose non-toxic nature was confirmed using brain cells. Glyceraldehyde crosslinked NPs were successfully prepared to meet specific design criteria for

traumatic brain injury treatment including the incorporation and slow release of a potential new therapeutic peptide.

Overall, these experimental findings reveal gelatin NP properties and their consistency are greatly influenced by the sample composition prior to NP synthesis. Gelatin NP property consistency paired with a non-toxic crosslinker for stability, is anticipated to provide smoother translations to industry use.

Synthesis, Characterization and Performance of Gelatin Biopolymer based Nanoparticle Formulations for Molecule Encapsulations

André T. Stevenson Jr.

ABSTRACT (General Audience Abstract)

Gelatin's ability to dissolve in water while also forming a gel upon cooling, produces "melt in your mouth" candies and frozen desserts, along with hard and soft capsules and tablets. This protein, which is extracted from pork skin and cattle hide, is categorized by a rigidity or stiffness value and remains one of the most common materials in food and pharmaceutical formulations. Its established use and safe certification are appealing characteristics for manipulation into nanoparticles (NPs) to encapsulate therapeutic molecules as medicine.

NPs are generally spherical materials, yet their abilities hold great promise to improve medical outcomes. These abilities include: protecting molecules from harsh locations like the stomach, improved therapeutic delivery through biological barriers such as the brain and *controlled* release for minimal side effects. NPs typically less than 200 nanometers (nm) overcome biological barriers more effectively than larger particles. For reference, 200 nm is equivalent to dividing the length of an ant (~4 millimeters) by 20,000. The potential applications of gelatin NPs to treat disease is impressive; however, an inability to consistently obtain ideal NP sizes (<200 nm average diameter) exists. Furthermore, gelatin NPs are commonly stabilized (or cross-linked) using toxic chemicals. The motivation for this research was to (1) contribute new understanding why ideal gelatin NPs are difficult to obtain and (2) form NPs using a non-toxic chemical for prospective brain injury treatment.

This dissertation determined low rigid and high rigid gelatin can consistently form NPs less than 200 nm, indicating rigidity alone is not a main factor for obtaining ideal NPs. Instead, characterization approaches indicated gelatin sample composition prior to NP formation must be

very uniform. As a result, filtering solutions prior to NP formation proved a new technique to prepare ideal NPs.

Glyceraldehyde is a sugar and has shown to be a non-toxic gelatin NP stabilizer. For the first time, glyceraldehyde's non-toxicity was shown using various brain cell types and NPs were formed to be ~130 nm. After incorporation of a new therapeutic molecule for brain injury treatment, average particles were ~149 nm with slow therapeutic release profiles determined in simulated body fluid.

Dedication

To my parents, André and Denise Stevenson, words can never express how grateful I am for the unconditional love, encouragement and guidance you have given me throughout my life. Without your continuous support, the successes I have been fortunate to achieve, including the finalization of this dissertation, would be limited. I greatly appreciate all that you have done and love you both very much.

To my brothers, Aaron and Andrew, thank you for supporting me in your own special way. There were times when your messages made me laugh uncontrollability, which was just what I needed to get through certain days in this graduate school journey. Though we get on each other's nerves at times, I love you both very much and am looking forward to growing as brothers.

To Aunt Rose, hearing your prospective after riveting *Game of Thrones* episodes was always entertaining! Thank you for thinking of me and checking in. I love you very much.

To my numerous teachers from elementary school, to high school, to college who also believed in me and inspired me to pursue graduate school, thank you deeply. Teachers and professors like you ensure the next generations will continually leave the world in a better place.

Acknowledgments

First, I wish to express my appreciation to my advisor, Dr. Abby Whittington. Thank you for welcoming me into your lab and allowing me to experience a range of projects from both industry and academia. You have been extremely accepting of my many research and non-research efforts, and our conversations where you, perhaps unknowingly, relieved my stresses were incredibly helpful. Early on in your lab, I began my first research project flying with you and our collaborators on a private jet to Washington, DC. What an incredible journey this has turned out to be! I am also very grateful to my committee members, Dr. Pamela VandeVord, Dr. Michael Friedlander and Dr. Gary Pickrell. I still remember how excited I was when each of you agreed to become a member on my committee. Thank you all for challenging me to think critically and for your unique input and advice.

Next, I want to thank my lab-mates, Shelley, Jewel, Nick, Jerry and Wyatt for your willingness to help with various tasks in lab, being supportive during my successes and frustrations and creating an overall wonderful experience during my time at Virginia Tech. I wish to especially acknowledge Shelley for being a great friend and teaching me cell culture, which turned out to be an extremely valuable technique in this dissertation. I am very thankful for the many friendships made at Virginia Tech both within Kelly Hall and also beyond.

I now want to thank several undergraduate research scholars for their hard work in the lab: Spencer Lewis, Ross Dickerman, Maria Bernero, Max Tarshis, Danny Jankus, Kevin Tong, Maeghan McDonough, Priya Ganesh and Casey Clark. Serving as your mentor was a wonderful experience and I know you will accomplish great things. I am also grateful to the Materials Science and Engineering Department for their unwavering support and guidance, including: Dr. Reynolds, Dr. Clark, Dr. Aning and Dr. Tallon. I also thank the office personnel including Cindy Perdue, Amy Hill and LeeAnn Ellis for handling the numerous supply orders among other tasks. I next want to sincerely thank my graduate coordinator, Kim Grandstaff, who has been an invaluable source of knowledge and support to ensure I am successful.

Thank you to my undergraduate research mentor Dr. Charleson Bell, who provided me with an incredible opportunity at Vanderbilt University to conduct nanoparticle research. I thank Dr. Todd Giorgio who was the principle investigator, for giving me the opportunity to work in his lab for approximately two years under Dr. Bell. This experience set my trajectory to earn a doctoral degree studying nanoparticles.

I want to acknowledge the College of Engineering New Horizon group, the Ellen Wade Graduate Studies Fellowship and the David W. Francis and Lillian Francis Memorial Scholarship for financial support.

I am profoundly grateful to Jesus Christ for life, determination, focus and humor provided to me, which were all needed in this research.

Finally, I'll thank the readers of this dissertation for being curious enough to explore what this work accomplishes. I hope the information provided here is useful to you and spurs innovative ideas to further scientific discovery.

Table of Contents

List of Figures

List of Tables

Chapter 1

Introduction

1.1 The General Role of Nanoparticles (NPs) for Therapeutic Molecule Delivery

Polymer NPs are materials so small they are invisible to the naked eye; yet, their nanoscale abilities hold great promise to create more efficient therapeutic delivery formulations. These abilities include (1) encapsulation of hydrophilic and poorly water-soluble hydrophobic molecules,[1] (2) protecting molecules from harsh biological environments (such as the stomach), (3) large surface area to volume ratio enabling targeted delivery via surface modifications,[2] (4) enhanced delivery across biological barriers[1, 3] and (5) therapeutic sustained release properties which decrease systemic exposure and side effects.[3-4] The research community has determined the nanoscale abilities mentioned above are predominantly influenced by NP physicochemical properties such as size, size distribution and surface charge.[1, 3, 5] Therefore, the ability to reproduce physicochemical properties is essential to maintaining NP function and for obtaining additional knowledge of NP size-effects on their transport, biological activity, and therapeutic efficiency.[5-6] For example, in nanomedicine applications after intravenous administration, circulating particles that are positively charged and have diameters 200 nm or greater activate the immune system more efficiently relative to smaller particles.[3] Once recognized by the complement system, opsonization occurs where NPs are marked by circulating blood proteins and ultimately removed by phagocytes.[3] Prolonged circulation increases NP probability to reach the targeted diseased tissue, ultimately improving therapeutic outcomes.[5] For particles that are able to evade detection during circulation, the 100-200 nm size range is large enough to avoid nonspecific accumulation by the liver[7-8] (with vascular fenestrations measuring 50-100 nm)[9] and the spleen (with 200-500 nm interendothelial cell slits).[7, 10]

1.2 Gelatin's Properties and Multifaceted Role for NP Encapsulation

In an effort to propel NP efficacy, the use of naturally derived materials known as biopolymers have merits of biocompatibility, biodegradability and low immunogenicity.[2] Gelatin is one particular biopolymer with a linear structure extracted from collagen (Figure 1.1),[11] the most abundant protein in animals.[12]

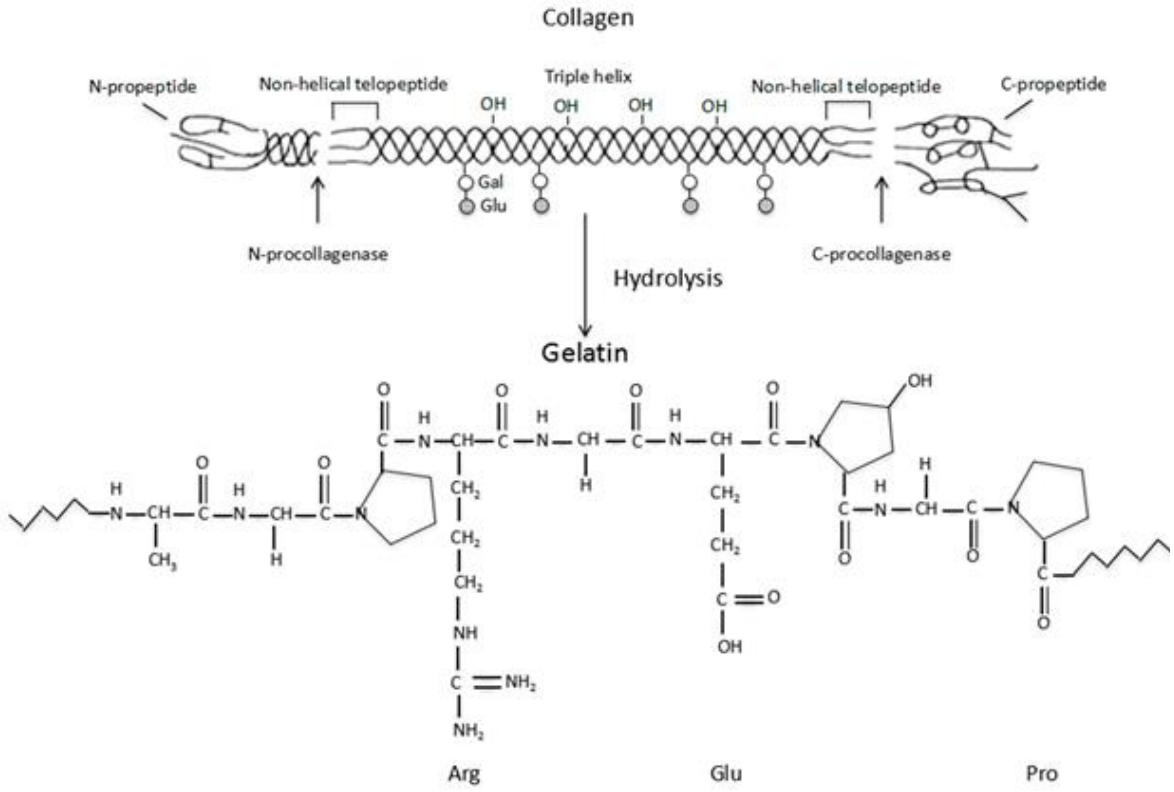

Figure 1.1. Schematic of collagen to gelatin conversion process. Reproduced via Open Source guidelines CC BY 4.0 from Wang, X.; Ao, Q.; Tian, X.; Fan, J.; Tong, H.; Hou, W.; Bai, S., Gelatin-Based Hydrogels for Organ 3D Bioprinting. Polymers 2017, 9 (9), 401.
Link: http://www.mdpi.com/2073-4360/9/9/401/htm

The two main types of gelatin are Type A derived from acid hydrolysis of pig skin and Type B derived from alkaline treatment of bovine hide, which produce slightly different amino acid compositions.[13] As a result, distinct isoelectric points (pI) are generated (Type A pI is 7-9 while Type B pI is ~4-5).[14] Additionally, the manufacturing process produces gelatin with molecular weight distributions characterized by bloom strength, which corresponds to the weight in grams to depress a gel a distance of 4 mm.[15,16] Low and medium gelatin bloom strengths are primarily used as food additives while higher blooms find use in pharmaceutical applications as hard and soft capsules and tablets.[17] Thus, gelatin's ability to encapsulate and emulsify numerous substances into stable products has prompted use for NP encapsulation and delivery of pharmaceutical and

food based molecules. Emulsification properties paired with high water capacity enable numerous synthesis techniques to prepare gelatin NP based formulations.

Site specific targeting potential and chemical modifications to enhance long term stability are additional benefits afforded to gelatin NPs through molecular conjugation of naturally incorporated ionizable groups.[14] Gelatin NP research has been directed toward stroke injury,[12] fungal keratitis,[18] topical ophthalmic use,[19] HIV,[20] cancer,[20] inflammation,[20] and malaria.[20] For food based approaches, gelatin NPs have encapsulated and protected anti-oxidative tea catechins from enzymatic digestion and improved the delivery of natural polyphenols.[21] The use of gelatin NPs represent an exciting materials approach to effectively protect and deliver both pharmaceutical and food based molecules.

1.3 Motivation and Aims

The extensive investigations of gelatin NPs for molecule encapsulation is impressive, yet the numerous gelatin types, average molecular weight ranges, and various synthesis techniques have created large variations in reported NP average diameters. For example, one research group might report 150 ± 5 nm particles while another group might report 235 ± 12 nm particles (outside the scope of nanomedicine relevancy) using similar gelatin types and synthesis methods. As a result, the experimental conditions which enable control of gelatin NP physicochemical properties remains highly inconsistent. This is particularly alarming as physicochemical properties dictate NP application and performance, ultimately affecting transport properties, biological activity, and therapeutic efficiency described above.[6, 21] Since the goal for any NP device is translation to industry, reproducible properties are necessary.[1] Chemical crosslinkers required for NP stability further inhibit translational potential as many are cytotoxic.

Altogether, this dissertation implements a materials science and engineering approach by characterizing macroscale and nanoscale gelatin to better understand why NP physicochemical properties are likely difficult to reproduce. Through this experimental design, a new method to control gelatin NP properties is presented, along with experimental recommendations to produce NPs crosslinked with a non-toxic crosslinker that meet specific design criteria. To accomplish these tasks, the following four aims were investigated:

Aim 1: Determine correlations between macroscale gelatin properties and average NP diameter.
Aim 2: Develop a new preparation method to reduce average NP diameter for gelatin particles greater than 200 nm.
Aim 3: Assess glyceraldehyde as a potential non-toxic chemical crosslinker using an established cellular assay.
Aim 4: Determine experimental conditions to form glyceraldehyde crosslinked gelatin NPs that meet specific design criteria for prospective traumatic brain injury treatment.

1.4 Organization of Proceeding Chapters

Chapter 2 provides background information on the three main techniques (circular dichroism, size exclusion chromatography, dynamic light scattering) used in this dissertation to characterize gelatin macroscale and nanoscale properties. Special attention is given to size exclusion chromatography and dynamic light scattering since both characterize different material properties, but have similar terminology. A review of the two common gelatin NP synthesis methods along with their nanoscale characterizations described in literature is presented next. The differing conclusions made by various studies are also presented to demonstrate additional insights regarding NP reproducibility are needed. Finally, several chemical crosslinkers commonly investigated for NP stability along with their proposed reaction mechanisms are discussed.

Chapter 3 contains a comprehensive analysis of gelatin macroscale and nanoscale properties to complete Aim 1. This chapter provides a new experimental design approach where similar gelatin types and bloom strengths were selected from different manufacturers as a means to identify correlations between macroscale and nanoscale properties. Theoretical calculations concerning gelatin aggregation and crosslinking are presented to provide additional insight regarding NP formation. This chapter contains results under peer review in *Nanoscale*.

Chapter 4 consists of Aim 2 and presents a new method to reduce gelatin NP physicochemical variation prior to NP synthesis termed filtration initiated selective homogeneity (FISH) desolvation. FISH desolvation acts on macroscale gelatin itself to control nanoscale properties, instead of relying upon traditional design parameters (pH, temperature, crosslinker concentration)

that have contributed to large NP variations and inconsistent conclusions. Two different gelatin types and blooms were synthesized into NPs and characterized. This chapter is currently under peer review in *Food Hydrocolloids,* so the work presented emphasizes gelatin NP encapsulation for the food industry. Although presented as such, the scope is not limited to solely food products given gelatin's described versatility.

Chapter 5 highlights gelatin's versatility by producing NPs with specific design considerations to potentially treat traumatic brain injury. To this end, the first section contains Aim 3 and assesses glyceraldehyde and glutaraldehyde viability using various brain cells. The second section contains Aim 4 and provides experimental approaches to obtain gelatin NPs using glyceraldehyde, along with their physicochemical properties after encapsulating a therapeutic molecule shown to heal injured murine brain tissue. Finally, additional insight regarding the production of gelatin NPs crosslinked with glyceraldehyde including experimental recommendations is presented. This chapter is in preparation for submission to journal.

Chapter 6 contains overall conclusions and significant impact of the described research. Future areas for investigation are also included.

References

1. Desai, N., Challenges in development of nanoparticle-based therapeutics. *The AAPS journal* **2012,** *14* (2), 282-95.
2. Nitta, S. K.; Numata, K., Biopolymer-based nanoparticles for drug/gene delivery and tissue engineering. *International journal of molecular sciences* **2013,** *14* (1), 1629-54.
3. Khanbabaie, R.; Jahanshahi, M., Revolutionary Impact of Nanodrug Delivery on Neuroscience. *Current Neuropharmacology* **2012,** *10* (4), 370-392.
4. Hudson, D.; Margaritis, A., Biopolymer nanoparticle production for controlled release of biopharmaceuticals. *Critical Reviews in Biotechnology* **2014,** *34* (2), 161-179.
5. Hickey, J. W.; Santos, J. L.; Williford, J.-M.; Mao, H.-Q., Control of polymeric nanoparticle size to improve therapeutic delivery. *Journal of Controlled Release* **2015,** *219*, 536-547.
6. Adjei, I. M.; Peetla, C.; Labhasetwar, V., Heterogeneity in nanoparticles influences biodistribution and targeting. *Nanomedicine (London, England)* **2014,** *9* (2), 267-278.
7. Blanco, E.; Shen, H.; Ferrari, M., Principles of nanoparticle design for overcoming biological barriers to drug delivery. *Nature biotechnology* **2015,** *33* (9), 941-951.
8. Petros, R. A.; DeSimone, J. M., Strategies in the design of nanoparticles for therapeutic applications. *Nature reviews. Drug discovery* **2010,** *9* (8), 615-27.
9. Braet, F.; Wisse, E.; Bomans, P.; Frederik, P.; Geerts, W.; Koster, A.; Soon, L.; Ringer, S., Contribution of high-resolution correlative imaging techniques in the study of the liver sieve in three-dimensions. *Microscopy research and technique* **2007,** *70* (3), 230-42.
10. Chen, L. T.; Weiss, L., The role of the sinus wall in the passage of erythrocytes through the spleen. *Blood* **1973,** *41* (4), 529-37.
11. Wang, X.; Ao, Q.; Tian, X.; Fan, J.; Tong, H.; Hou, W.; Bai, S., Gelatin-Based Hydrogels for Organ 3D Bioprinting. *Polymers* **2017,** *9* (9), 401.
12. Shoulders, M. D.; Raines, R. T., COLLAGEN STRUCTURE AND STABILITY. *Annual review of biochemistry* **2009,** *78*, 929-958.
13. Duconseille, A.; Astruc, T.; Quintana, N.; Meersman, F.; Sante-Lhoutellier, V., Gelatin structure and composition linked to hard capsule dissolution: A review. *Food Hydrocolloids* **2015,** *43*, 360-376.
14. Lohcharoenkal, W.; Wang, L.; Chen, Y. C.; Rojanasakul, Y., Protein Nanoparticles as Drug Delivery Carriers for Cancer Therapy. *BioMed Research International* **2014,** *2014*, 12.
15. Schrieber, R.; Gareis, H., From Collagen to Gelatine. In *Gelatine Handbook*, Wiley-VCH Verlag GmbH & Co. KGaA: 2007; pp 45-117.
16. von Hippel, P. H., The Macromolecular Chemistry of Gelatin. *Journal of the American Chemical Society* **1965,** *87* (8), 1824-1824.
17. (GMIA), G. M. I. o. A., Gelatin Handbook.
18. Ahsan, S. M.; Rao, C. M., Condition responsive nanoparticles for managing infection and inflammation in keratitis. *Nanoscale* **2017,** *9* (28), 9946-9959.
19. Vandervoort, J.; Ludwig, A., Preparation and evaluation of drug-loaded gelatin nanoparticles for topical ophthalmic use. *European Journal of Pharmaceutics and Biopharmaceutics* **2004,** *57* (2), 251-261.
20. Foox, M.; Zilberman, M., Drug delivery from gelatin-based systems. *Expert opinion on drug delivery* **2015,** *12* (9), 1547-63.
21. Elzoghby, A. O., Gelatin-based nanoparticles as drug and gene delivery systems: reviewing three decades of research. *Journal of controlled release : official journal of the Controlled Release Society* **2013,** *172* (3), 1075-91.

Chapter 2

Background and Literature Review

2.1 Introduction

Chapter 2 begins by providing background information describing the three main characterization techniques used in this manuscript. The relevant information each technique provides and their respective terminologies are given. After obtaining this basis, the next section describes common gelatin nanoparticle (NP) synthesis techniques and their nanoscale properties reported in the scientific literature. The scientific community uses many of the techniques described in this dissertation, so the terminologies presented beforehand are readily applied in the literature review section. Next, methods to chemically stabilize gelatin NPs, their proposed reaction schemes and toxicity assessment is presented. Chapter 2 concludes with a summary of the current knowledge and describes how the next chapters contribute significantly to the gelatin NP field.

2.2 Biopolymer Characterization

This dissertation utilizes three main techniques which include circular dichroism, size exclusion chromatography and dynamic light scattering to characterize macroscale and nanoscale properties. Circular dichroism is a relatively uncommon technique applied in NP dissertations. While size exclusion chromatography and dynamic light scattering are very common techniques in the NP community, similar terminology in the results they obtain have caused misunderstanding. The properties that each technique analyzes and their specific terminology will be discussed to provide clarity.

2.2.1 Circular Dichroism

Circular dichroism is a spectroscopic technique which measures the difference in absorption of left-handed and right-handed circularly polarized light.[1] Proteins contain amide (also known as peptide) bonds that absorb different intensities of polarized light in the far ultraviolet region (190-250 nm), producing a unique spectral signature. Circular dichroism determines if a protein's

secondary structure is an α-helix, β-sheet or random coil based on its spectral signature (Figure 2.1).[2]

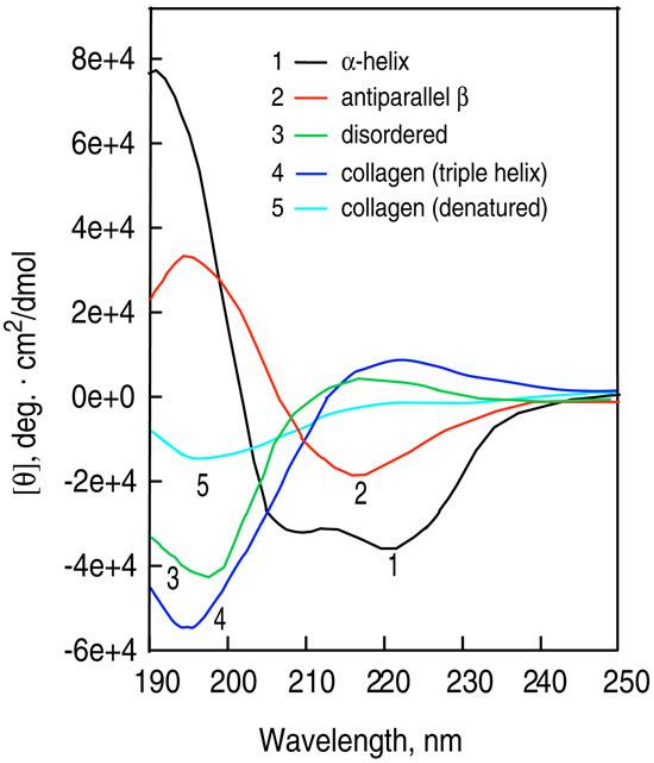

Figure 2.1. Representative spectra of protein secondary structures obtained from circular dichroism. From "Using circular dichroism spectra to estimate protein secondary structure," by N. J. Greenfield, 2006, Nature Protocols, 1, p. 2876. Copyright 2007 by Springer Nature. Adapted with permission via license number: 4316721408867. Link: https://www.ncbi.nlm.nih.gov/pmc/articles/PMC2728378/

2.2.2 Size Exclusion Chromatography

Size exclusion chromatography separates molecular weights from a sample based on size or hydrodynamic volume.[3] Biopolymer chain sizes smaller than the defined pore size will become

entrapped and eluted at a slower rate compared to larger chains.[4] The elution volume can be detected via multi-angle light scattering to obtain absolute molecular weights of a sample without requiring polymer calibration.

A variety of measurements characterizing the average biopolymer chain mass distribution such as the weight average molecular weight (M_w), number average molecular weight (M_n) and dispersity ($Đ$) are obtained via the following equations:

$$\overline{M_w} = \frac{\sum_{i=1}^{N} N_i {M_i}^2}{\sum_{i=1}^{N} N_i M_i} \qquad \text{Eq. 2.1}$$

$$\overline{M_n} = \frac{\sum_{i=1}^{N} N_i M_i}{\sum_{i=1}^{N} N_i} \qquad \text{Eq. 2.2}$$

$$Đ = \frac{\overline{M_w}}{\overline{M_n}} \qquad \text{Eq. 2.3}$$

where N_i is the number of molecules of mass M_i. The molecular weight dispersity, Đ, provides the distribution of chain sizes with a value of 1 indicating the biopolymer is 100% monodisperse. Values greater than 1 reveal a broader molecular weight profile.

2.2.3 Dynamic Light Scattering (DLS)

DLS – also known as photon correlation spectroscopy – has emerged as a simple table-top technique executable under ordinary lab environments to investigate the (hydrodynamic) size of NPs.[5] NPs are always under Brownian motion and will scatter laser light that is proportional to the 6^{th} power of their radii.[5] The intensity of the scattered light fluctuates with time and is autocorrelated using a time series where faster particle decay is associated with smaller particles and slower decays are associated with larger particles to obtain a size distribution and diffusion

coefficient (D_t). Particle diffusion can be converted to hydrodynamic diameter (D_h) via the Stokes Einstein equation:

$$D_h = \frac{k_B T}{3\pi\eta D_t} \qquad \text{Eq. 2.4}$$

where additional terms are Boltzmann's constant (k_B), absolute temperature (T) in Kelvin and viscosity (η). D_h is defined as the diameter of a hard sphere that diffuses at the same speed as the particle being measured.[5] The cumulants analysis provides the intensity-weighted mean diameter, known as the Z-Average size or Z-Average mean (Z_D), along with the polydispersity index (PDI) which are the major parameters produced by DLS.[6] Z-Average will be referred to as the "average NP diameter" or "average NP size" throughout this dissertation. In DLS, a PDI of 0 indicates sizes have no size distribution, while a value of 1 indicates the sample is highly polydispersed with multiple populations of NP widths. The PDI can be explained as the relative variance and expressed by the following equation:[5, 7]

$$PDI = \frac{\sigma^2}{{Z_D}^2} \qquad \text{Eq. 2.5}$$

where σ is the standard deviation of the hypothetical Gaussian distribution and Z_D is the intensity-weighted mean diameter.[7] The polymer NP community has proposed PDI values below 0.2 exhibit a narrow size distribution indicative of monodispersity.[8-10] While obtaining an average diameter and PDI does not mean that the distribution is Gaussian, smaller PDI values are a good indication that a Gaussian distribution might be a reasonable approximation of the real size distribution.[7] Additionally, DLS uses Mie theory to convert the NP size distribution by intensity, into a size distribution by volume, to describe the relative proportion of particles in a sample.[6, 11] For PDI values greater than 0.2, obtaining size distributions based on sample volume might prove practically useful[7, 12] especially since biopolymer NP pharmaceuticals typically require travel through tight barriers to reach diseased tissue.[13]

2.3 Gelatin NP Synthesis Background and Literature Review

Preparation of protein NPs is based on balancing the attractive and repulsive forces in the unfolded / denatured protein.[14] To prevent uncontrolled self-aggregation, noncovalent intramolecular hydrophobic interactions between amino acids must be reduced, typically through removal of tertiary structures using heat or pH.[15] Desolvation and emulsification are two synthesis routes from which protein based NPs, such as gelatin, can be prepared. This section describes each method, the NP physicochemical properties reported in the literature and the chemical routes for NP stability.

2.3.1 Gelatin NP Synthesis Methods

The scientific literature reveals numerous experimental methods with differing experimental outcomes and conclusions for gelatin NP preparations. Here, the various approaches the research community has implemented will be reviewed to show the significance and novelty of the work completed in this dissertation. After reviewing gelatin NP preparations and results, the mechanisms for chemical stability including relevancy to biological applications will be discussed.

2.3.1.1 Desolvation

Desolvation involves preparing an aqueous solution of gelatin and displacing the solvent by adding in an alcohol or salt.[16] The controlled addition of the desolvate allows the gelatin chains to thermodynamically self-associate once a critical concentration has been exceeded, leading to gelatin aggregates, which are subsequently crosslinked to produce NPs.[17] It is important that the gelatin concentration, c, be below the threshold level required to form a macroscopic gel, $c < c^*$, where c^* is the overlap concentration.[18] The overlap concentration is dependent on molecular weight, molecular weight dispersity, pH and co-solutes.[19] A $\leq$ 5% w/v gelatin solution is typically less than c^* based on the formation of NPs during the desolvation process.

Marty *et al.* (1978) was the first to prepare gelatin particles using ethanol as the desolvate, but NPs were difficult to achieve instead consisting of agglomerates[20] from ~470 nm-1080 nm with broad PDIs (0.2-0.48). Farrugia and Groves (1998, 1999) hypothesized gelatin's molecular weight heterogeneity was responsible for variations in experimental conditions required for gelatin NP *formation* and proposed 1) heating a gelatin solution to 37 °C would ensure the molecular weight

distribution remained relatively unaltered during NP synthesis and 2) higher molecular weight fractions of 700,000 Da were needed to from NPs between 220-250 nm with PDI values <0.2 at neutral pH.[20-21]

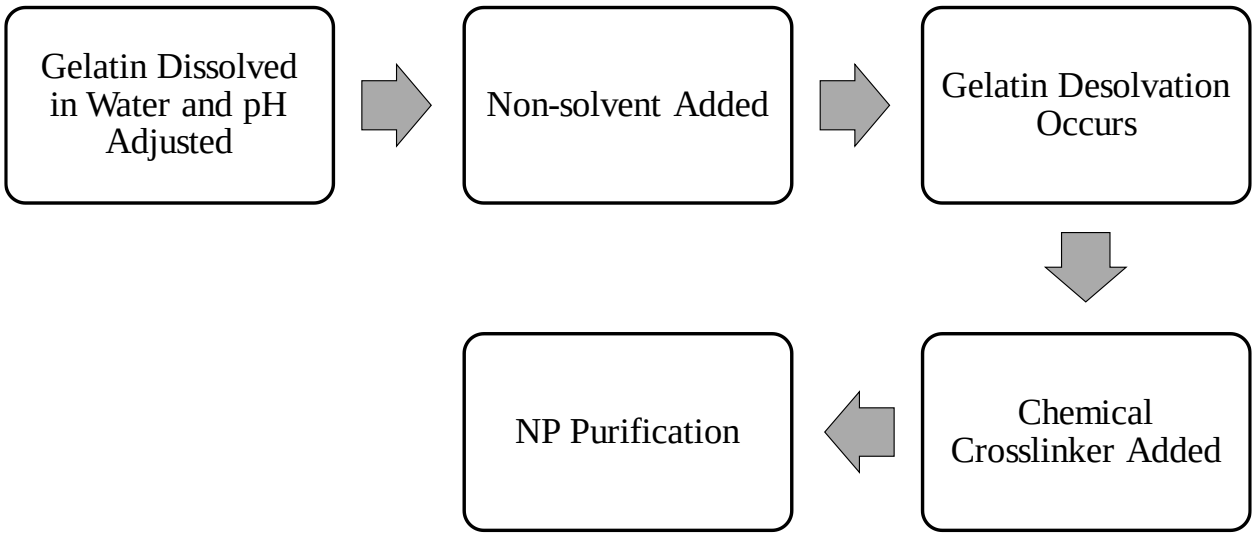

Figure 2.2. One-step desolvation method.

Though this one-step desolvation process (Figure 2.2) produced colloidal dispersions of individual gelatin NPs between 220-250 nm instead of multi-particulate aggreagates,[22] the low amount of gelatin used (0.2% w/w) and the lengthy investigation needed to determine the effect of time, temperature, pH and ethanol concentration for an adequate molecular weight distribution, were greatly inefficient. Thus, Coester *et al.* (2000) improved upon this method and developed the two step-desolvation process (Figure 2.3) where gelatin is initially dissolved in heated water and precipitated using acetone (the first desolvation).[23] Acetone addition produces what is described as high molecular weight sediment at the bottom, while a liquid low molecular weight region is left in solution at the top, which is then discarded. The sediment gelatin is then dissolved in heated water, the pH is adjusted away from the respective pI point (2.5 pH was used by Coester *et al.* for Type A 175 bloom gelatin)[23] and the second desolvation is initiated via dropwise acetone, followed by glutaraldehyde for chemical crosslinking. Coester *et al.* produced Type A 175 bloom strength gelatin particles with 277 nm diameters and a 0.08 PDI value.[23]

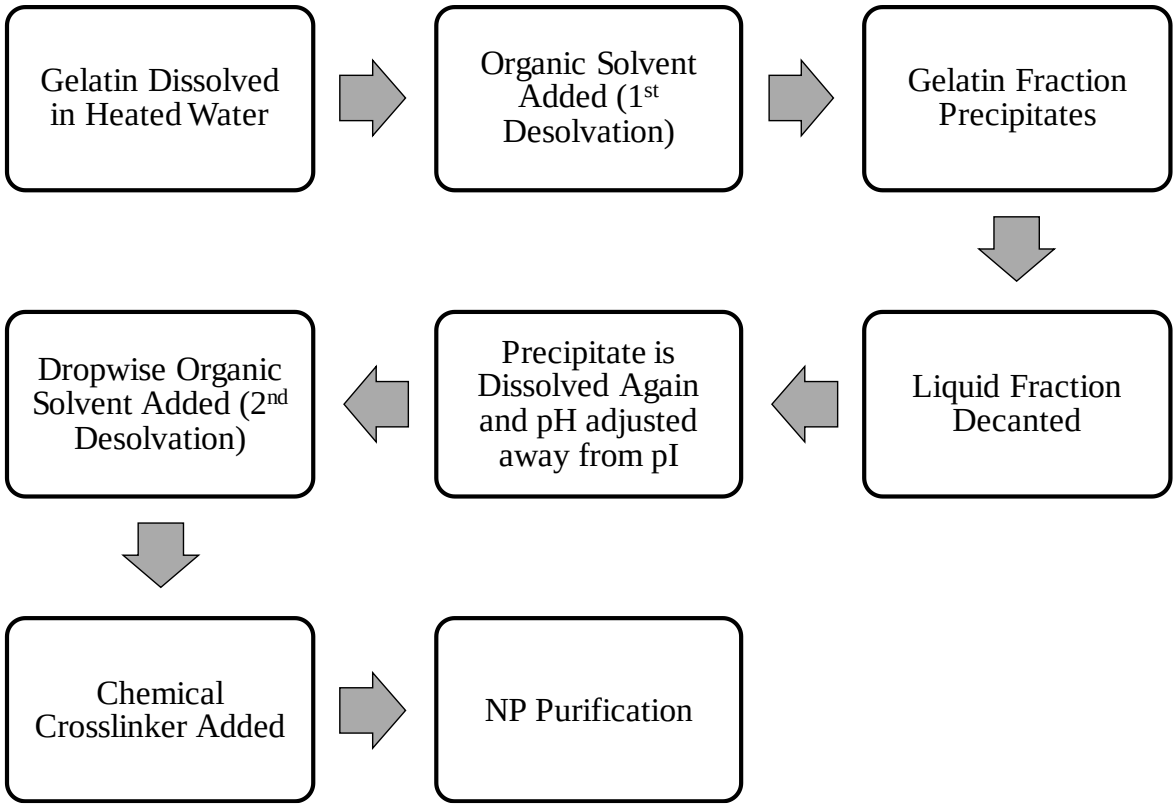

Figure 2.3. Two–step desolvation method.

After three months, the NP diameter and PDI was tested and both remained unchanged.[23] Removing low molecular weight fractions reduced the number of aggregates formed in the crosslinking phase and also prevented further secondary aggregation and flocculation during storage.[16] Coester *et al.* determined the molecular weight had a decisive influence on gelatin NP stability.[23] As a result of this work, additional information regarding NP formation was obtained, which included the lowering of pH was required to sufficiently prevent uncontrolled gelatin agglomeration of the gelatin, while the addition of acetone – a solvent with different polarity and hydrogen bond forming ability – replaces water molecules by dehydrating the gelatin chains until intermolecular aggregation forces overcome intermolecular electrostatic repulsion causing spontaneous gelatin chain precipitation.[22] These controlled aggregates can then be chemically stabilized to form typically homogeneous NPs with narrow size distributions within batches.

Since the invention of two-step desolvation, numerous studies have investigated the effects of various experimental conditions on NP size and distribution. Zwiorek's dissertation (2006)

describes the modification of pH, the first desolvation precipitation time, and second acetone addition amount, produced distinct populations of Type A 175 bloom strength NPs at 50 °C (108 ± 14 nm, 151 ± 2 nm, 293 ± 9.9 nm with all PDI values between 0.05 to 0.12).[24] Zwiorek determined that 100 and 300 nm were the lower and upper limits for the production of predicable NPs via two-step desolvation with the gelatin amount and pH being the two most critical factors.[24] Further, to investigate the effect of high molecular weight fractions for one-step desolvation, he obtained custom gelatin lots with the following profiles:

1) 40% of gelatin content with < 65,000 Da
2) 40% of gelatin content with < 65,000 Da + slight fraction with $>10^{10}$ Da
3) < 20% of gelatin content with < 65,000 Da

Gelatin NPs could only be formed using profile 3 with 181 ± 2.7 nm (PDI 0.007 ± 0.001) being the smallest size obtained.[24] Interestingly, the specific experimental conditions that formed the smallest NPs for Type A 175 bloom strength could not generate NPs for the custom gelatin profiles.[24] Altogether Zwiorek concluded that the absence or strong reduction of low molecular weight fractions < 65,000 Da and not a predominant presence of extra high molecular weight fractions could be determined as the essential factor for the preparation of stable and homogeneous NPs, refuting Farrugia and Groves.[24]

Saxena *et al.* (2005) investigated the effect of gelatin molecular weight differences on NP drug encapsulation efficiency.[25] Three different gelatin types and blooms were used including Type B 75, Type A 175 and 300.[25] Saxena *et al.* determined that all particles were between 200–300 nm, thus, gelatin type, their different pH, and isoelectric points did not influence overall NP formation.[25] This was attributed to the low acidic pH used for NP formation (~2.5), which is below the pI point of both gelatin types resulting in an overall net charge to facilitate chemical crosslinking with glutaraldehdyde.[25] Post gelatin NP incubation at increased temperatures maintained diameters (25 °C: 298 ± 15 nm, 50 °C: 278 ± 15 nm) which Saxena *et al.* attributed to constant electrostatic repulsion invariant of temperature by the Debye–Huckel equation:[25]

$$(\varepsilon T)^{-3/2} \approx 3\,x10^{-7} \qquad \text{Eq. 2.5}$$

where T is the temperature in Kelvin and ε is the relative permittivity or the amount of charge that can be held by a material relative to vacuum. At 25 °C and 50 °C, ε is 75 and 72 which suggests temperature has minimal effect on NP electrostatic interaction. With regard to encapsulation efficiency, the 300 bloom strength obtained nearly double incorporation compared to the 75 bloom strength (41 % vs ~26 %).[25] Drug release profiles also obtained differing results for the gelatin types with Type A showing higher release rates at physiological pH (7.4) compared to the Type B case, which were attributed to NP swelling in aqueous environments.[25]

Azarmi *et al.* (2006) used Type A 175 and Type B 225 bloom strength gelatin to study the effects of various production parameters such as temperature (40°C, 50°C, 60 °C), pH (2.5, 12) glutaraldehyde concentration (100-500 µL), desolvating agent (acetone, ethanol) and nature of gelatin had on NP properties.[26] From their study, temperature had a significant effect on NP diameter for both gelatins, as 40 °C produced the smallest NP sizes (Type A: 163 ± 24 nm, PDI:0.06 ± 0.007, Type B: 112 ± 21 nm, PDI: 0.09 ± 0.03).[26] This contrasts Zwiorek who found temperature did not have a significant effect on NP diameter.[24] Azarmi *et al.* proposed that at 40°C gelatin triple helical structures were sufficiently uncoiled, which decreases the viscosity of the solution allowing the desolvating agent to better control NP precipitation, compared to higher temperatures.[26] Gelatin type also produced differing NP properties. At 40 and 50 °C Type A NPs were generally larger compared to Type B NPs, but were of similar diameter when prepared at 60°C.[26] Finally, according to Azarmi *et al.*, acetone was the preferred desolvating agent producing generally smaller particles with lower PDIs compared to ethyl alcohol at 50°C – no information regarding desolvating agent comparison at 40 °C was provided.[26] Sahoo *et al.* (2015) attributed this phenomenon to the hydrogen bond forming differences between acetone and ethyl alcohol.[27] Acetone is a polar aprotic solvent, which means it cannot donate protons (H^+), while ethyl alcohol is an protic solvent donating its protons to reagents allowing for hydrogen bonding.[27] From this, the presence of hydrogen bonds facilitates the formation of larger networks and consequently larger particle sizes.[27]

Ahsan and Rao (2017) hypothesized the role of pH and desolvating agent could produce Type B 225 bloom strength NPs with different matrix densities, allowing for enzymatic modulation of drug release profiles.[28] A modified two-step desolvation process was used which involved

lyophilizing the high molecular weight fraction, dissolving in heated water (50 °C), filtering the 1% solution (0.22 µm), changing the pH, dropwise acetone and crosslinking.[28] By adjusting the pH to 4.0, particles were ~235 ± 2.2 nm (using ~55% acetone) while pH 3.25 produced ~185 ± 5.2 nm particles (using ~73% acetone) with prospectively different assembly mechansims.[28] At pH 4, Ahsan and Rao determined that after ~60% of dropwise acetone was added, the NP size remained constant, but the NP PDI increased which was hypothesized to be from additional free gelatin incorporation into the preformed NPs.[28] Ahsan and Rao described this formation as a high matrix dense core possibly acting as a nucleus upon which gelatin molecules are consequently added by extra acetone.[28] In contrast, pH 3.25 was proposed to yield a low matrix dense core of NPs with larger diameters possibly from incomplete extraction of water molecules.[28] Degradation studies determined the low matrix dense NPs with lower corresponding diameters had faster degradation kinetics compared to the larger NP dense cores. As a result, the high density matrix NPs were found to have a slow and sustained period of fluorescein release over 16 h compared to their lower density counterparts.[28] Contrary to previous studies however, NPs could not be generated at lower pH conditions (<3.5 for Type A and <3.0 for Type B).[28]

Injectable and biodegradable gels were prepared from two-step desolvated gelatin NPs by Wang *et al.* (2011) to investigate electrostatic self-assembly potential.[29] Hydrated Type A NPs were ~425 nm and Type B NPs were ~275 nm with less than 0.2 PDI.[29] Zeta potential measurements revealed at physiologically relevant pH (7.0 in this study) the respective NPs had opposite charges indicative of their distinct pI regions.[29] Upon mixing, the NPs showed a linear increase in diameter which resulted in electrostatic sedimentation of large aggregates after one hour.[29] To substantiate their claim that aggregation was initiated by electrostatic interactions, mixed gelatin NPs were dispersed in solutions with increasing ionic strength.[29] The highest ionic strength solution (100 mM NaCl) decreased NP diameter and dispersion extent while the lower ionic strengths lead to aggregation, which implied the electrical double layer surrounding charged particles is compressed with increasing ionic strength, thereby reducing the driving force for self –assembly and indicating aggregation is mainly driven by electrostatic interactions.[29] For gel formation, rheological experiments revealed that all dispersions of oppositely charged NPs obtained significantly higher elastic moduli compared to separate NP solutions, and shear thinning capability was obtained by high shear rates breaking electrostatic cohesive forces.[29] The generation of low viscosities allowed

NP dispersion to be injected through narrow syringes.[29] Finally, another unique property was the nanogel's self–healing ability where upon removal of the shear, near instantaneous gel rigidity was restored, attributed to the re-establishment of electrostatic interactions between oppositely charged NPs along with the re-arrangement of NP packing.[29]

2.3.1.2 Emulsification

An emulsion is a mixture of two immiscible liquids commonly an aqueous "water" phase and an organic "oil" phase which are dispersed in one another.[30] In gelatin NP synthesis, the aqueous solution contains gelatin which is then dispersed in oil (the continuous phase) under high speed homogenization or ultrasonic shear to form NPs at the water / oil interface.[14] Prior to crosslinking, the emulsion is cooled to below the gelling point of gelatin (<36 °C)[31] to facilitate particle formation (Figure 2.4).[32] Typically, emulsions contain emulsifiers – materials that concentrate at the phase interface to lower the interfacial tension – reducing the energy required to break the dispersed phase into particles and also preventing coalescence (the fusion of two or more particles into larger ones)[30] by generating a repulsive force between them.[30, 33] Because a high input of energy is required to form an emulsion, the process does not occur spontaneously, typically expressed via the Gibb's free energy (positive ΔG) equation below:[33]

$$\Delta G = \Delta H - T\Delta S \qquad \text{Eq. 2.7}$$

where ΔH is the change in enthalpy attributed to the amount of heat absorbed by the system, which is positive, and ΔS is the change in entropy, which is also positive since the generation of an emulsion increases the disorder of the system (assuming a constant pressure).

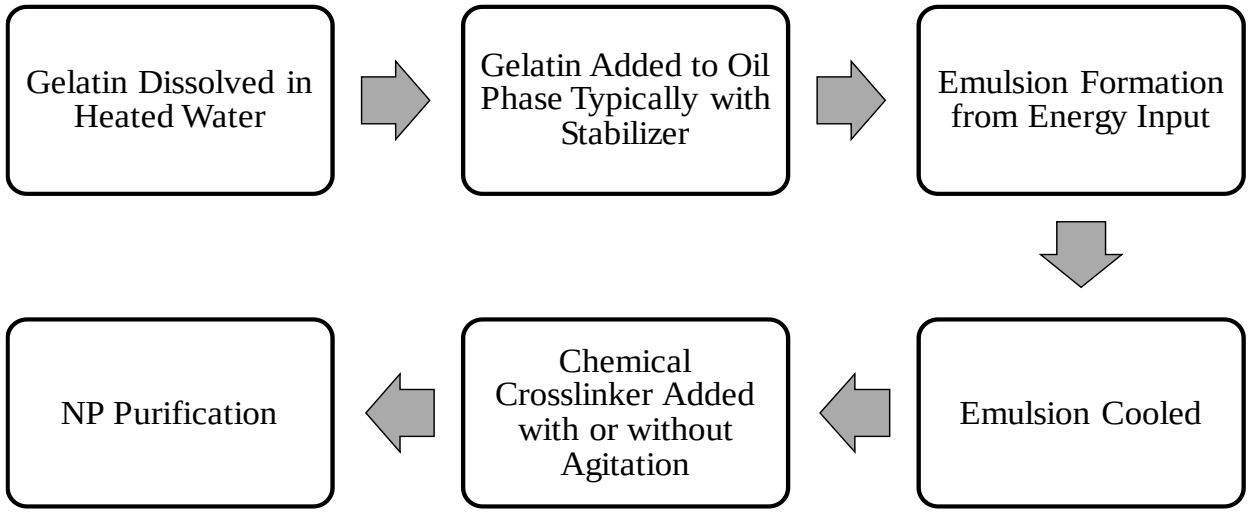

Figure 2.4. Water–in–oil emulsion method.

One of the first to adapt the water–in–oil emulsion technique for Type B gelatin NPs, instead of microparticles, was Tabata *et al.* (1981) producing diameters between 230–350 nm.[34] NPs must be extensively purified using organic solvents to remove the oil phase containing emulsifiers. Hydrophilic molecules can be encapsulated within the NPs by adding to the water phase, while hydrophobic compounds are incorporated by the double oil–water–oil method where the compound is added to the first oil phase, then emulsified with gelatin in water and finally added to another hydrophobic phase.[35] NP size distributions are affected by the time and speed of homogenization and the viscosity of the gelatin solution with 1–3% w/w gelatin being optimal.[32]
A modification of the water–in–oil emulsion process is solvent evaporation employed by Cascone *et al.* (2002) where the "oil phase" is an organic solvent mixture (1:1 of chloroform and toluene) containing a synthetic polymer stabilizer [such as poly (methyl methacrylate) (PMMA)].[36] The internal aqueous phase was Type B gelatin in phosphate buffered saline (PBS).[32, 36] The aqueous phase is added to the oil phase and following high speed homogenization, evaporation occurs under controlled conditions of temperature and pressure to produce NPs that can be chemically crosslinked.[37] While NPs were between 100–200 nm via scanning electron microscopy, numerous variables influenced the final product including the need for 25% (w/v) PMMA to prevent NP agglomeration during cooling but less than 30% to ensure recovery after washing.[36] Additionally, PMMA molecular weight (M_w) of 120,000 was selected to enhance emulsion stability.[36] A variety of emulsification techniques are available;[36, 38-41] however, the need to apply a range of intricate experimental methods to control particle size[17] such as: heating and cooling, a distinct oil phase with specific phase ratios, high speed processing, adequate time for homogenization, low particle yields and usually broad size distributions,[24,16] contribute to desolvation being the most popular gelatin NP synthesis method. For these reasons this dissertation applied desolvation to produce gelatin NPs.

2.3.2 Gelatin NP Chemical Stability

Since gelatin is a hydrophilic protein, it rapidly dissolves in aqueous environments; decreasing its sustained therapeutic release potential. Chemical crosslinking refers to the introduction of a covalent linkage between biopolymer functional groups effectively decreasing a biopolymer's solubility and degradation rate in aqueous solutions.[17] Non-zero-length and zero-length are two types of chemical crosslinkers which can be used to stabilize gelatin NPs. Non-zero-length

crosslinkers end up incorporated within the NP itself such as glutaraldehyde, glyceraldehyde and genipin while zero-length crosslinkers are not integrated within the final NP composition such as Ethyl-3-(3-dimethylaminopropyl)-carbodiimide (EDC)-N-hydroxysuccinimide (NHS). The proposed reaction schemes along with NP properties and toxicity experiments will be addressed in this section.

2.3.2.1 Glutaraldehyde

Glutaraldehyde is the most commonly used gelatin NP crosslinker as it is inexpensive, soluble in aqueous and organic solvents, and efficient. The NP studies cited above used glutaraldehyde extensively to enhance stability. Gelatin NPs have been shown to remain a stable suspension (un-agglomerated) for more than 10 months when stored between 2-8°C.[42] Glutaraldehyde crosslinking occurs in two proposed ways: by the formation of a Schiff base reaction of the aldehyde group (carbonyl of the glutaraldehyde) with the amino group of lysine or hydroxylysine in the gelatin (Figure 2.5),[43] and aldol condensation between two adjacent aldehydes.[43]

Figure 2.5. Glutaraldehyde structure and Schiff base formation schematic. Adapted from "Bonding of articular cartilage using a combination of biochemical degradation and surface cross-linking," by Englert et al., 2007, *Arthritis Research & Therapy, 9*. Copyright © 2007 Englert et al.; licensee BioMed Central Ltd. Adapted with permission under the Creative Commons Attribution License CC BY 2.0
Link: https://www.ncbi.nlm.nih.gov/pmc/articles/PMC2206351/

Glutaraldehyde's reactivity also extends to most biological materials, inducing either cell death (when cytotoxic) or mutagenesis (when carcinogenic).[17] Speer *et al.* (1980) showed that collagen sponges retain and release glutaraldehyde via hydrolysis that could be part of the covalent crosslink itself and possibly additional forms, inducing cytotoxicity in human fibroblasts at only 3 ppm.[17, 44] Additional *in vitro* and *in vivo* toxicity studies have determined high grade inflammation, edema, and necrosis to lung and liver tissue at glutaraldehyde concentrations of 10 µM to 0.002 M.[45] Biomaterials crosslinked with glutaraldehyde have resulted in increased inflammation and calcification when implanted *in vivo* in rabbit osteochondral defects.[45] Niknejad *et al.* (2015)

determined when epithelial cells were incubated overnight with albumin NPs crosslinked with glutaraldehyde (0.84 M) only 40.08% ± 6.6 were viable.[46] Furthermore, Khan *et al.* (2011) determined that human endothelial cell viability decreased as the amount of glutaraldehyde used to crosslink albumin NPs increased (using 1.5%, 3%, 4.5%, 6%, and 7.5% w/v), ultimately concluding that further research might be necessary to replace the application of glutaraldehyde with more biocompatible materials.[47] In an effort to reduce toxicity, the research community is actively investigating the use of less toxic crosslinkers.

2.3.2.2 Glyceraldehyde

Glyceraldehyde is a monosaccharide made by combining glycerol and one aldehyde. As simple sugars are a basic unit in biology, glyceraldehyde is considered non-toxic and has gained interest in NP crosslinking.[48] Kim *et al.* (2014) compared glutaraldehyde toxicity to various other crosslinkers (including glyceraldehyde) at the same concentration in four different cell lines (immortalized human corneal epithelial cells, human skin fibroblasts, primary bovine corneal endothelial cells, and immortalized human retinal pigment epithelial cells) and determined glyceraldehyde to be one of the least toxic while glutaraldehyde was one of the most toxic.[49] Their study consisted of incubating the cells for 24 h with the crosslinker molecules, followed by a 48 h recovery period.[49] In fact, glyceraldehyde crosslinked biomaterials have shown significantly decreased toxicity compared to glutaraldehyde after 7 days using human fibroblasts.[50] Glyceraldehyde crosslinks proteins similar to glutaraldehyde in that a Schiff base is initiated between the amino group of the protein and the sole aldehyde group of the glyceraldehyde (Figure 2.6). After Schiff Base formation, molecular Amadori rearrangements occur allowing for additional crosslinks forming ketosamines.[51] The resulting chemical linkages between aldehydes and amines is known as the Maillard reaction, which is also responsible for the browning effects of foods and desirable flavor components along with reaction side products.[17]

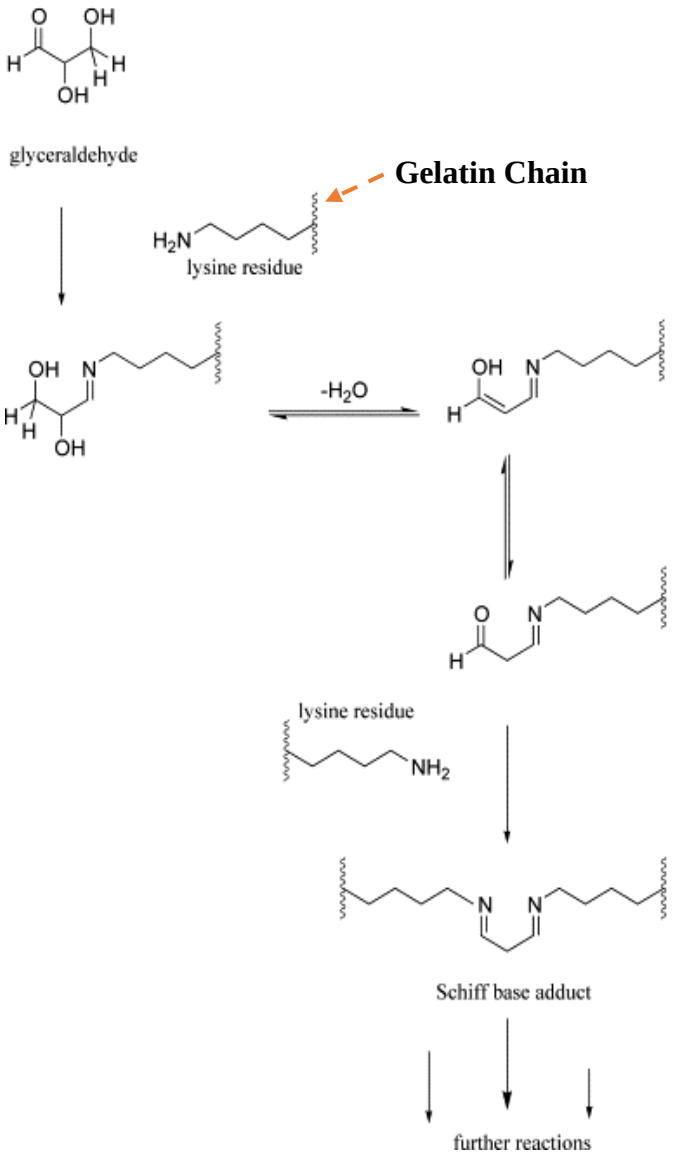

Figure 2.6. Proposed method for glyceraldehyde crosslinking of proteins. Adapted from "Maillard crosslinking of food proteins. I: the reaction of glutaraldehyde, formaldehyde and glyceraldehyde with ribonuclease, by Gerrard et al., 2002, *Food Chemistry, 79*, p.348. Copyright © 2002 Elsevier Science Ltd. Adapted with permission via license number 4316800724004.

Compared to glutaraldehyde crosslinking, the use of glyceraldehyde to stabilize gelatin NPs is limited. Recently Geh *et al.* (2016) showed it was possible to prepare glyceraldehyde crosslinked gelatin NPs using one-step desolvation conditions.[52] For their results, it took 65 h for glyceraldehyde (16 mg / mL solution) to produce 300-350 nm Type A 300 bloom strength gelatin

particles (pH 2.5-3).[52] The degree of crosslinking was estimated to be 40%.[52] To the contrary, Type B 300 bloom strength gelatin was crosslinked with glyceraldehyde (20 mg / mL) for 19 h and produced NPs between 200-250 nm with ~75% crosslinking.[52] Further, to scale up their desolvation process by five-fold, a paddle stirrer system that provided a tailored mixing intensity was used leading to greater control over the mixing efficiency.[52] As a result, Type B gelatin diameters between 200–250 nm and PDI values <0.15 were obtained.[52] The NPs were stored in purified water at 4 °C and were tested up to 35 days showing no significant increases in size or PDI.[52]

Two additional studies using glyceraldehyde for gelatin NP crosslinking involve emulsions. Zhao *et al.* (2012) utilized a novel water-in-water emulsion stabilized with poloxamer 188 to prepared gelatin NPs (type and bloom not provided) subsequently crosslinked with glyceraldehyde (1 mL, 10 % w/v). A 1:1 ratio of Poloxamer to gelatin produced 210 ± 10.2 nm particles with a 0.193 PDI and -23.1 ± 1.2 mV charge. Further, insulin was encapsulated within the NPs and obtained higher diameters (250 ± 7.5) and PDI (0.276).[41] Finally, Lu *et al.* (2015) also used a water-in-water emulsion technique with Poloxamer 188-grafted heparin copolymer with gelatin crosslinked glyceraldehyde (0.1% w/v) and the surfactant soy phosphatidylcholine.[53]

2.3.2.3 Genipin

Genipin is a natural crosslinker extracted from gardenia fruit that has been used in herbal medicine and fabrication of food dyes.[42] However, studies have determined it generates both toxic responses (comparable to glutaraldehyde)[43] and non-toxic responses that are substantially lower than glutaraldehyde.[43,54] Despite these discrepancies, gelatin-genipin crosslinking has been proposed to occur through two distinct steps involving 1) the Michael Reaction of a lysine amino group to the genipin ring structure forming a tertiary amine (Figure 2.7A) and 2) a subsequent much slower reaction resulting in crosslinking via a lysine amino group from a second gelatin chain (Figure 2.7B).[55]

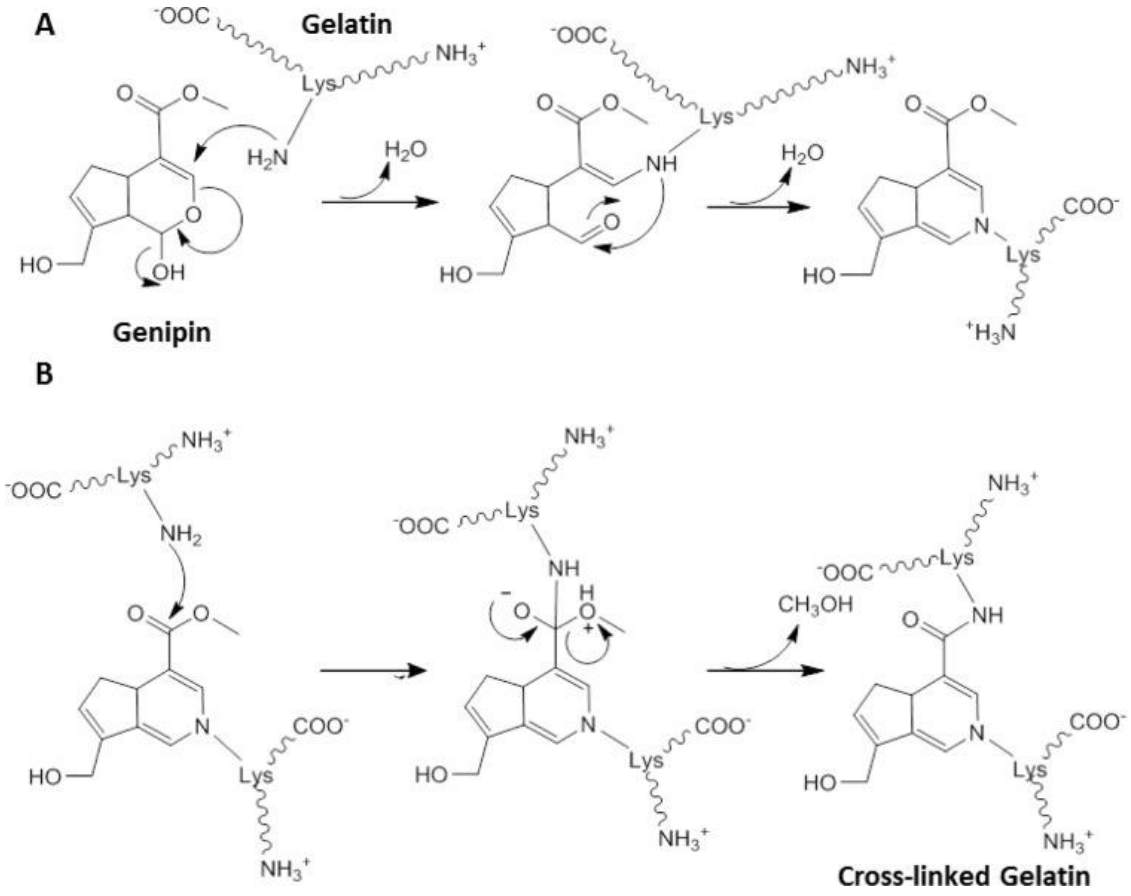

Figure 2.7. Proposed crosslinking reaction of gelatin with genipin. (A) The Michael reaction forms an intermediate which is furthered via a (B) secondary reaction consisting of lysine amine with genipin ester. Reproduced from "*Gelatin-Based Materials in Ocular Tissue Engineering*," by Rose et al., 2014, *Materials, 7*, p.3112. Copyright © 2014 by the authors. Licensee MDPI, Basel, Switzerland. Reproduced with permission under the Creative Commons Attribution License CC BY 3.0
Link: https://www.ncbi.nlm.nih.gov/pmc/articles/PMC5453355/

Won and Kim (2008) prepared recombinant human gelatin NPs via one-step desolvation (since the human form was said to have low and homogeneous molecular weight distribution) using genipin as a crosslinker.[56] Won and Kim determined the effect of gelatin and genipin concentration, desolvation amount and crosslink time on NP properties. They determined the optimal experimental conditions to be the following: 60% (v/v) ethanol, minimum 0.05% genipin and 0.05 % (w/v) gelatin to produce ~50 nm particles with a PDI l < 0.1.[56] NP zeta potential

measurements were neutral.[56] Though NP size reached steady state after 3 h, up to 3 days were needed to prevent particle disintegration.[56] After incorporating bovine serum albumin with a fluorescent tag into the particles, 80% extent of crosslinking was determined, diameters increased to 230 ± 11.2 nm and NPs became negatively charged (-21.8 ± 7.5 mV) in water.[56]

In an effort to replicate the work by Won and Kim, Geh *et al*. obtained between 280-370 nm particles using Type B 300 bloom strength gelatin (food grade based) crosslinked with genipin (20 mg / mL gelatin solution).[52] However, the NPs had poor colloidal stability with only 40% crosslinking.[52]

2.3.2.4 EDC-NHS

EDC and NHS are molecules that couple aspartic and glutamic acid carboxyl groups to amine groups and do not become part of the final bond.[57] As a result, this technique allows for gelatin to crosslink with itself forming a covalent amide bond (Figure 2.8).[55] An advantage of this technique is that all residues are water soluble, and can prospectively be washed out after crosslinking has concluded.[55] Compared to glutaraldehyde, gelatin gels crosslinked with EDC were well tolerated in primary rat iris pigment epithelial cultures and did not induce significant inflammatory responses even after 12 week implantation in the anterior chamber of a rabbit eye.[58]

Qazvini and Zinatloo (2011) prepared Type B gelatin (Bloom 80 – 120) NPs via two-step desolvation crosslinked with either glutaraldehyde (250 µL of 25% solution) or EDC/NHS (6.25 mL of 1.2% EDC:NHS).[59] Glutaraldehyde crosslinked NPs were 280 ± 11 nm, PDI: 0.45 ± 0.07, while EDC:NHS particles were 187 ± 7 nm, PDI: 0.14 ± 0.07).[59] The drastic size differences were attributed to the formation of crosslinks due to charge neutralization as EDC/NHS brings the reactant groups (—NH2, —COOH) close together enabling faster NP stabilization without further aggregation.[59] The authors also noted that any change in the conditions such as pH, temperature, desolvation agent, and ionic strength of the solution as well as gelatin type may cause different size characteristics.[59] Important experimental parameters that should be controlled when using EDC are pH (as hydrolysis is largely dependent on pH), the amount of EDC so that NPs do not aggregate due to their loss of electrostatic repulsive forces, and the ratio EDC/NHS to properly stabilize the particles in aqueous environments. [57] Numerous studies have enhanced the targeting

potential and overall performance of gelatin NPs by conjugating specific molecules to the gelatin surface via EDC/NHS chemistry prior to crosslinking via non-zero-length substances.[60-62]

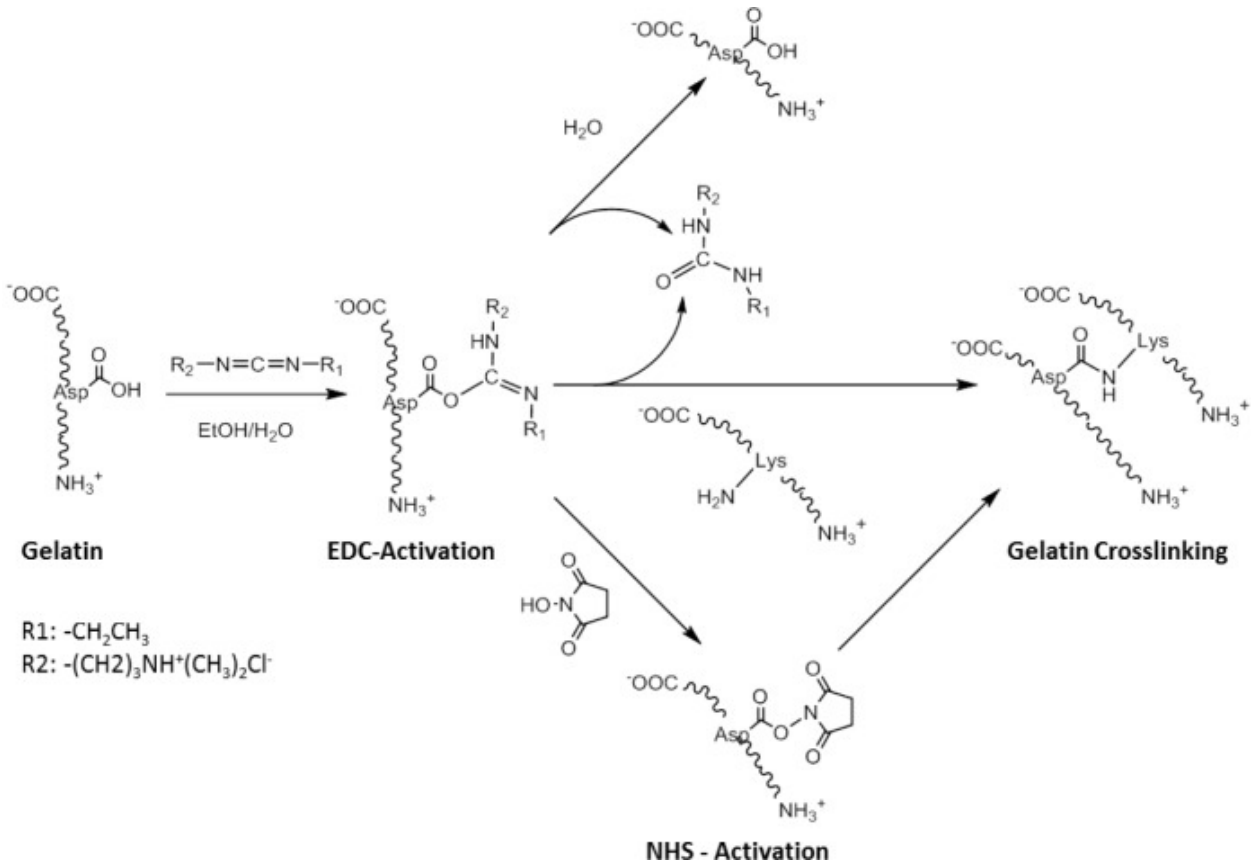

Figure 2.8. EDC/NHS crosslinking mechanism with gelatin results in amide bond formation between chains. Reproduced from "*Gelatin-Based Materials in Ocular Tissue Engineering*," by Rose et al., 2014, *Materials, 7*, p.3113. Copyright © 2014 by the authors. Licensee MDPI, Basel, Switzerland. Reproduced with permission under the Creative Commons Attribution License CC BY 3.0
Link: https://www.ncbi.nlm.nih.gov/pmc/articles/PMC5453355/

2.4 Overall Summary of Literature Review and Remaining Chapters

The investigation of gelatin NP properties based on altering experimental methods during and after NP formation have created numerous discrepancies in the literature. A significant gap in scientific knowledge regarding the most effective way(s) to control gelatin NP physicochemical properties exists. Chapter 3 essentially replicates the variation in NP physicochemical properties seen in the literature, by preparing gelatin NPs from similar bloom strengths obtained from

different manufactures. Through characterizing gelatin macroscale and nanoscale properties, novel correlations were developed to provide new insights regarding NP formation. While correlation does not make for causation, using the knowledge learned from Chapter 3, Chapter 4 describes a new desolvation method to prepare gelatin NPs with high consistency. Finally, to bring together the NP synthesis route with the biological aspect, Chapter 5 presents toxicity data comparing glutaraldehyde to glyceraldehyde and NP differences obtained, along with encapsulation and *in vitro* release of a new therapeutic molecule for potential traumatic brain injury treatment. Glyceraldehyde was chosen as the alternate crosslinker in this dissertation since limited study exists using NP desolvation. Furthermore, the potential applicability to food based products was appealing since it is a monosaccharide. Finally, Chapter 6 presents overall conclusions and additional areas for future work.

References

1. Rein, C. M.; Desai, U. R.; Church, F. C., Chapter Seven - Serpin–Glycosaminoglycan Interactions. In *Methods in Enzymology*, Whisstock, J. C.; Bird, P. I., Eds. Academic Press: 2011; Vol. 501, pp 105-137.
2. Greenfield, N. J., Using circular dichroism spectra to estimate protein secondary structure. *Nature protocols* **2006,** *1* (6), 2876-2890.
3. Nagy, K.; VÉKey, K., Chapter 5 - Separation methods A2 - Vékey, Károly. In *Medical Applications of Mass Spectrometry*, Telekes, A.; Vertes, A., Eds. Elsevier: Amsterdam, 2008; pp 61-92.
4. Fekete, S.; Beck, A.; Veuthey, J.-L.; Guillarme, D., Theory and practice of size exclusion chromatography for the analysis of protein aggregates. *Journal of Pharmaceutical and Biomedical Analysis* **2014,** *101*, 161-173.
5. Bhattacharjee, S., DLS and zeta potential – What they are and what they are not? *Journal of Controlled Release* **2016,** *235*, 337-351.
6. . Dynamic Light Scattering Common Terms Defined 2011.
7. Arzenšek D., P. R., Kuzman D. Dynamic light scattering and application to proteins in solutions 2010.
8. Danhier, F.; Lecouturier, N.; Vroman, B.; Jerome, C.; Marchand-Brynaert, J.; Feron, O.; Preat, V., Paclitaxel-loaded PEGylated PLGA-based nanoparticles: in vitro and in vivo evaluation. *Journal of controlled release : official journal of the Controlled Release Society* **2009,** *133* (1), 11-7.
9. Jain, A. K.; Thanki, K.; Jain, S., Co-encapsulation of Tamoxifen and Quercetin in Polymeric Nanoparticles: Implications on Oral Bioavailability, Antitumor Efficacy, and Drug-Induced Toxicity. *Molecular Pharmaceutics* **2013,** *10* (9), 3459-3474.
10. Panchal, J.; Kotarek, J.; Marszal, E.; Topp, E. M., Analyzing Subvisible Particles in Protein Drug Products: a Comparison of Dynamic Light Scattering (DLS) and Resonant Mass Measurement (RMM). *The AAPS Journal* **2014,** *16* (3), 440-451.
11. Nobbmann, U.; Morfesis, A., Light scattering and nanoparticles. *Materials Today* **2009,** *12* (5), 52-54.
12. Stetefeld, J.; McKenna, S. A.; Patel, T. R., Dynamic light scattering: a practical guide and applications in biomedical sciences. *Biophysical Reviews* **2016,** *8* (4), 409-427.
13. Blanco, E.; Shen, H.; Ferrari, M., Principles of nanoparticle design for overcoming biological barriers to drug delivery. *Nature biotechnology* **2015,** *33* (9), 941-951.
14. Lohcharoenkal, W.; Wang, L.; Chen, Y. C.; Rojanasakul, Y., Protein Nanoparticles as Drug Delivery Carriers for Cancer Therapy. *BioMed Research International* **2014,** *2014*, 12.
15. Ko, S.; Gunasekaran, S., Preparation of sub-100-nm β-lactoglobulin (BLG) nanoparticles. *Journal of microencapsulation* **2006,** *23* (8), 887-898.
16. Hudson, D.; Margaritis, A., Biopolymer nanoparticle production for controlled release of biopharmaceuticals. *Critical Reviews in Biotechnology* **2014,** *34* (2), 161-179.
17. Jones, O. G.; McClements, D. J., Functional Biopolymer Particles: Design, Fabrication, and Applications. *Comprehensive Reviews in Food Science and Food Safety* **2010,** *9* (4), 374-397.
18. Pelc, D.; Marion, S.; Pozek, M.; Basletic, M., Role of microscopic phase separation in gelation of aqueous gelatin solutions. *Soft Matter* **2014,** *10* (2), 348-356.
19. Haug, I. J.; Draget, K. I., 6 - Gelatin. In *Handbook of Hydrocolloids (Second edition)*, Woodhead Publishing: 2009; pp 142-163.
20. Marty, J. J.; Oppenheim, R. C.; Speiser, P., Nanoparticles--a new colloidal drug delivery system. *Pharmaceutica acta Helvetiae* **1978,** *53* (1), 17-23.
21. Farrugia, C. A.; Farrugia, I. V.; Groves, M. J., Comparison of the Molecular Weight Distribution of Gelatin Fractions by Size-exclusion Chromatography and Light Scattering. *Pharmacy and Pharmacology Communications* **1998,** *4* (12), 559-562.
22. Farrugia, C. A.; Groves, M. J., Gelatin behaviour in dilute aqueous solution: designing a nanoparticulate formulation. *The Journal of pharmacy and pharmacology* **1999,** *51* (6), 643-9.

23. Coester, C. J.; Langer, K.; van Briesen, H.; Kreuter, J., Gelatin nanoparticles by two step desolvation--a new preparation method, surface modifications and cell uptake. *Journal of microencapsulation* **2000,** *17* (2), 187-93.
24. Zwiorek, K. Gelatin Nanoparticles as Delivery System for Nucleotide-Based Drugs. Ludwig-Maximilians-University, 2006.
25. Saxena, A.; Sachin, K.; Bohidar, H. B.; Verma, A. K., Effect of molecular weight heterogeneity on drug encapsulation efficiency of gelatin nano-particles. *Colloids and Surfaces B: Biointerfaces* **2005,** *45* (1), 42-48.
26. Azarmi, S.; Huang, Y.; Chen, H.; McQuarrie, S.; Abrams, D.; Roa, W.; Finlay, W. H.; Miller, G. G.; Lobenberg, R., Optimization of a two-step desolvation method for preparing gelatin nanoparticles and cell uptake studies in 143B osteosarcoma cancer cells. *Journal of pharmacy & pharmaceutical sciences : a publication of the Canadian Society for Pharmaceutical Sciences, Societe canadienne des sciences pharmaceutiques* **2006,** *9* (1), 124-32.
27. Sahoo, N.; Sahoo, R. K.; Biswas, N.; Guha, A.; Kuotsu, K., Recent advancement of gelatin nanoparticles in drug and vaccine delivery. *International Journal of Biological Macromolecules* **2015,** *81*, 317-331.
28. Ahsan, S. M.; Rao, C. M., The role of surface charge in the desolvation process of gelatin: implications in nanoparticle synthesis and modulation of drug release. *International Journal of Nanomedicine* **2017,** *12*, 795-808.
29. Wang, H.; Hansen, M. B.; Löwik, D. W. P. M.; van Hest, J. C. M.; Li, Y.; Jansen, J. A.; Leeuwenburgh, S. C. G., Oppositely Charged Gelatin Nanospheres as Building Blocks for Injectable and Biodegradable Gels. *Advanced Materials* **2011,** *23* (12), H119-H124.
30. Tadros, T. F., Emulsion Formation, Stability, and Rheology. In *Emulsion Formation and Stability*, Wiley-VCH Verlag GmbH & Co. KGaA: 2013; pp 1-75.
31. Li, J. K.; Wang, N.; Wu, X. S., Gelatin nanoencapsulation of protein/peptide drugs using an emulsifier-free emulsion method. *Journal of microencapsulation* **1998,** *15* (2), 163-72.
32. Kommareddy, S.; Shenoy, D. B.; Amiji, M. M., Gelatin Nanoparticles and Their Biofunctionalization. In *Nanotechnologies for the Life Sciences*, Wiley-VCH Verlag GmbH & Co. KGaA: 2007.
33. *Emulsions and Emulsification - Technical Brief*; Particle Sciences: 2009.
34. Toshio, Y.; Mitsuru, H.; Shozo, M.; Hitoshi, S., Specific delivery of mitomycin c to the liver, spleen and lung: Nano- and m1crospherical carriers of gelatin. *International Journal of Pharmaceutics* **1981,** *8* (2), 131-141.
35. Vassileva, E. D.; Koseva, N. S., Chapter 6 - Sonochemically born proteinaceous micro- and nanocapsules. In *Advances in Protein Chemistry and Structural Biology*, Donev, R., Ed. Academic Press: 2010; Vol. 80, pp 205-252.
36. Cascone, M. G.; Lazzeri, L.; Carmignani, C.; Zhu, Z., Gelatin nanoparticles produced by a simple W/O emulsion as delivery system for methotrexate. *Journal of materials science. Materials in medicine* **2002,** *13* (5), 523-6.
37. Nicolas, J.; Mura, S.; Brambilla, D.; Mackiewicz, N.; Couvreur, P., Design, functionalization strategies and biomedical applications of targeted biodegradable/biocompatible polymer-based nanocarriers for drug delivery. *Chemical Society Reviews* **2013,** *42* (3), 1147-1235.
38. Bajpai, A. K.; Choubey, J., Design of gelatin nanoparticles as swelling controlled delivery system for chloroquine phosphate. *Journal of materials science. Materials in medicine* **2006,** *17* (4), 345-58.
39. El-Shabouri, M. H., Positively charged nanoparticles for improving the oral bioavailability of cyclosporin-A. *International Journal of Pharmaceutics* **2002,** *249* (1), 101-108.
40. Ethirajan, A.; Schoeller, K.; Musyanovych, A.; Ziener, U.; Landfester, K., Synthesis and Optimization of Gelatin Nanoparticles Using the Miniemulsion Process. *Biomacromolecules* **2008,** *9* (9), 2383-2389.
41. Zhao, Y.-Z.; Li, X.; Lu, C.-T.; Xu, Y.-Y.; Lv, H.-F.; Dai, D.-D.; Zhang, L.; Sun, C.-Z.; Yang, W.; Li, X.-K.; Zhao, Y.-P.; Fu, H.-X.; Cai, L.; Lin, M.; Chen, L.-J.; Zhang, M., Experiment on the feasibility

of using modified gelatin nanoparticles as insulin pulmonary administration system for diabetes therapy. *Acta Diabetologica* **2012,** *49* (4), 315-325.
42. Elzoghby, A. O., Gelatin-based nanoparticles as drug and gene delivery systems: reviewing three decades of research. *Journal of controlled release : official journal of the Controlled Release Society* **2013,** *172* (3), 1075-91.
43. Englert, C.; Blunk, T.; Muller, R.; von Glasser, S. S.; Baumer, J.; Fierlbeck, J.; Heid, I. M.; Nerlich, M.; Hammer, J., Bonding of articular cartilage using a combination of biochemical degradation and surface cross-linking. *Arthritis research & therapy* **2007,** *9* (3), R47.
44. Speer, D. P.; Chvapil, M.; Eskelson, C. D.; Ulreich, J., Biological effects of residual glutaraldehyde in glutaraldehyde-tanned collagen biomaterials. *Journal of Biomedical Materials Research* **1980,** *14* (6), 753-764.
45. Furst, W.; Banerjee, A., Release of glutaraldehyde from an albumin-glutaraldehyde tissue adhesive causes significant in vitro and in vivo toxicity. *The Annals of thoracic surgery* **2005,** *79* (5), 1522-8; discussion 1529.
46. Niknejad, H.; Mahmoudzadeh, R., Comparison of Different Crosslinking Methods for Preparation of Docetaxel-loaded Albumin Nanoparticles. *Iranian journal of pharmaceutical research : IJPR* **2015,** *14* (2), 385-94.
47. Khan, A. A.; Paul, A.; Abbasi, S.; Prakash, S., Mitotic and antiapoptotic effects of nanoparticles coencapsulating human VEGF and human angiopoietin-1 on vascular endothelial cells. *International Journal of Nanomedicine* **2011,** *6*, 1069-1081.
48. Sharma, P. P.; Sharma, A.; Solanki, P. R., Recent Trends of Gelatin Nanoparticles in Biomedical Applications. In *Advances in Nanomaterials*, Husain, M.; Khan, Z. H., Eds. Springer India: New Delhi, 2016; pp 365-381.
49. Kim, M.; Takaoka, A.; Hoang, Q. V.; Trokel, S. L.; Paik, D. C., Pharmacologic Alternatives to Riboflavin Photochemical Corneal Cross-Linking: A Comparison Study of Cell Toxicity Thresholds. *Investigative Ophthalmology & Visual Science* **2014,** *55* (5), 3247-3257.
50. Sisson, K.; Zhang, C.; Farach-Carson, M. C.; Chase, D. B.; Rabolt, J. F., Evaluation of cross-linking methods for electrospun gelatin on cell growth and viability. *Biomacromolecules* **2009,** *10* (7), 1675-80.
51. Gerrard, J. A., Maillard crosslinking of food proteins. I: the reaction of glutaraldehyde, formaldehyde and glyceraldehyde with ribonuclease. *Food chemistry* **2002,** *v. 79* (no. 3), pp. 343-349-2002 v.79 no.3.
52. Geh, K. J.; Hubert, M.; Winter, G., Optimisation of one-step desolvation and scale-up of gelatine nanoparticle production. *Journal of microencapsulation* **2016,** *33* (7), 595-604.
53. Lu, C. T.; Jin, R. R.; Jiang, Y. N.; Lin, Q.; Yu, W. Z.; Mao, K. L.; Tian, F. R.; Zhao, Y. P.; Zhao, Y. Z., Gelatin nanoparticle-mediated intranasal delivery of substance P protects against 6-hydroxydopamine-induced apoptosis: an in vitro and in vivo study. *Drug design, development and therapy* **2015,** *9*, 1955-62.
54. Tsai, C. C.; Huang, R. N.; Sung, H. W.; Liang, H. C., In vitro evaluation of the genotoxicity of a naturally occurring crosslinking agent (genipin) for biologic tissue fixation. *J Biomed Mater Res* **2000,** *52* (1), 58-65.
55. Rose, J. B.; Pacelli, S.; El Haj, A. J.; Dua, H. S.; Hopkinson, A.; White, L. J.; Rose, F. R. A. J., Gelatin-Based Materials in Ocular Tissue Engineering. *Materials* **2014,** *7* (4), 3106-3135.
56. Won, Y. W.; Kim, Y. H., Recombinant human gelatin nanoparticles as a protein drug carrier. *Journal of controlled release : official journal of the Controlled Release Society* **2008,** *127* (2), 154-61.
57. Conde, J.; Dias, J. T.; Grazú, V.; Moros, M.; Baptista, P. V.; de la Fuente, J. M., Revisiting 30 years of biofunctionalization and surface chemistry of inorganic nanoparticles for nanomedicine. *Frontiers in Chemistry* **2014,** *2*, 48.
58. Lai, J. Y., Biocompatibility of chemically cross-linked gelatin hydrogels for ophthalmic use. *Journal of materials science. Materials in medicine* **2010,** *21* (6), 1899-911.

59. Taheri Qazvini, N.; Zinatloo, S., Synthesis and characterization of gelatin nanoparticles using CDI/NHS as a non-toxic cross-linking system. *Journal of Materials Science: Materials in Medicine* **2011,** *22* (1), 63-69.
60. Wong, C.; Stylianopoulos, T.; Cui, J.; Martin, J.; Chauhan, V. P.; Jiang, W.; Popović, Z.; Jain, R. K.; Bawendi, M. G.; Fukumura, D., Multistage nanoparticle delivery system for deep penetration into tumor tissue. *Proceedings of the National Academy of Sciences* **2011,** *108* (6), 2426.
61. Park, C.; Vo, C. L.; Kang, T.; Oh, E.; Lee, B. J., New method and characterization of self-assembled gelatin-oleic nanoparticles using a desolvation method via carbodiimide/N-hydroxysuccinimide (EDC/NHS) reaction. *European journal of pharmaceutics and biopharmaceutics : official journal of Arbeitsgemeinschaft fur Pharmazeutische Verfahrenstechnik e.V* **2015,** *89*, 365-73.
62. Nahar, M.; Dubey, V.; Mishra, D.; Mishra, P. K.; Dube, A.; Jain, N. K., In vitro evaluation of surface functionalized gelatin nanoparticles for macrophage targeting in the therapy of visceral leishmaniasis. *Journal of drug targeting* **2010,** *18* (2), 93-105.

Chapter 3

The correlation between gelatin macroscale differences and nanoparticle properties: providing insight to biopolymer variability

This chapter contains results and concepts under peer review in Nanoscale

Abstract

From therapeutic delivery to sustainable packaging, manipulation of biopolymers into nanostructures, imparts biocompatibility into numerous materials with minimal environmental pollution during processing. While biopolymers are appealing natural based materials, the lack of nanoparticle (NP) physicochemical consistency has decreased their nanoscale translation into actual products. Insights regarding macroscale and nanoscale property variation of gelatin, one of the most common biopolymers already utilized in its bulk form, is presented. Novel correlations between macroscale and nanoscale properties were made by characterizing similar gelatin rigidities obtained from different manufacturers. Samples with significant differences in clarity, indicating sample purity, obtained the largest deviations in NP diameter. Furthermore, a statistically significant positive correlation between macroscale molecular weight dispersity and NP diameter was determined. New theoretical calculations proposing the limited number of gelatin chains that can aggregate and subsequently crosslinked for NP formation was presented as one possible reason to substantiate the correlation analysis. NP charge and crosslinking extent were also associated based on diameter. Lower gelatin sample molecular weight dispersities produced statistically smaller average diameters (<75 nm), higher average electrostatic charges (~30 mV) and crosslinking extents (~95%), which were independent of gelatin rigidity; conclusions not shown in literature. This study demonstrates that the molecular weight composition of the starting material is one significant factor affecting gelatin nanoscale properties and must be characterized prior to NP preparation. Identifying gelatin macroscale and nanoscale correlations offers one route toward greater physicochemical property control and reproducibility of new NP formulations for industry translation.

3.1 Introduction

The continual growth of nanotechnology is increasing the likelihood of human and environmental interaction with engineered nanomaterials.[1] Biopolymers are naturally occurring materials formed during the life cycles of animals, plants, bacteria or fungi;[2] thus, their inherent biocompatibility and minimal environmental pollution during processing,[3] are attractive sources for manipulation into nanostructures. The scientific community has explored the use of biopolymer nanomaterials for: therapeutic delivery to treat disease,[4-6] food preservation to mask certain odors and tastes,[7-8] waste water treatment to absorb potentially toxic substances,[9] and recently nanogenerators for self-powered biomedical devices.[10] Nanoparticles (NPs) are spherical structures of which proteins, polysaccharides, and other biopolymers have garnered the most impact. While their vast exploration is impressive, the difficulty in obtaining consistent NP physicochemical properties, such as size and charge, has hindered biopolymer nanoscale translation into actual products.

Out of all the biopolymers, gelatin's unique ability to disperse in aqueous environments while also forming a thermo-reversible gel upon cooling, already proves useful as a bulk material in food and pharmaceutical formulations.[11-16] Two traditional gelatin types exist from the partial hydrolysis of collagen in the skin and bones of animals.[13-14] Type A gelatin is obtained from acidic treatment of porcine skin while Type B is obtained from alkaline treatment of bovine hide or bone, accounting for its 25% higher carboxylic acid content.[17] Since the polypeptide chains obtained during hydrolysis depends on the extraction time, gelatin is categorized by bloom strength (simply known as bloom in this chapter), which measures gel rigidity, and is related to its average molecular mass (from ~20,000 Da to ~100,000 Da).[12, 15]

Gelatin NP formation involves a common desolvation process, similar to other biopolymers, where an organic desolvating agent causes molecular chains to aggregate and are subsequently crosslinked for stability.[18-20] Since the introduction of desolvation, studies have investigated the influence of experimental methods on biopolymer NP properties.[21-22] For example, Saxena *et al.* determined variations made in several parameters like molecular weight of gelatin, temperature, and pH do not bring about any significant change in diameter since all particles were between 200-300 nm.[23] On the other hand, Azarmi *et al.* determined temperature and gelatin type were the most important factors to prepare NPs with different average diameters (~100-300 nm) and minimal

size distributions.[22] These contradictory results are particularly troubling as the design of biopolymer-based NPs with specific sizes, size distributions, and charges is critical to determine their respective application and function.[18] For example, in healthcare applications, NPs that are positively charged in physiologic pH and >200 nm activate the immune system more efficiently relative to smaller NPs.[24] Immune system activation leads to decreased NP circulation due to opsonization leading to clearance from the body likely before its desired effect can occur.[25] Alternatively, particles with ~100 nm average diameters and negative charges in physiologic pH generally prove long lasting in the body.[25]

Over the past few decades the scientific community has prepared biopolymer NPs with physicochemical variability[26] lacking consensus for such inconsistencies. Therefore, the purpose of this work was to offer new reasoning behind biopolymer NP physicochemical inconsistency by identifying correlations between macroscale and nanoscale differences. Theoretical calculations based on chain aggregation and chemical crosslinking aided the correlation analysis. Gelatin was selected to validate the overall characterization approach, due to its complexity and vast application.[27] In all, a characterization emphasis is expected to reveal potential screening methods that can be utilized by research labs and large scale manufacturers to determine if NP physicochemical properties might be replicable using different gelatin batches.

3.2 Materials

Gelatin was purchased from Sigma-Aldrich (St. Louis, MO) or provided as a gift from Vyse Gelatin Company (Schiller Park, IL). Glutaraldehyde (25%), acetone, and TNBS assay (4%) solution, were obtained from Fisher Scientific or Sigma-Aldrich. Carbon gold coated 200 mesh TEM grids were obtained from Electron Microscopy Sciences (Hatfield, PA).

3.3 Experimental Section

3.3.1 Gelatin NP Synthesis

Gelatin NPs were synthesized using two-step desolvation with some modifications. Briefly, gelatin (1.25 g) was added to distilled water (25 mL) with a stir bar (~12.7 mm by ~3 mm, 600 rpm) and heated to ~40 °C until dissolved. Afterwards, the solution was removed from heat and acetone (25 mL) was added and left for 24 h to precipitate the high molecular weight fraction. The supernatant was decanted and the remaining gelatin sediment was re-dissolved in distilled water (25 mL) using the same stir bar and speed as before. After dissolution, the pH was adjusted to ~2.5 (1 M HCl) and acetone was added dropwise (3 mL/min, 1000 rpm) until the Tyndall effect was visualized (usually ~80 mL acetone). Glutaraldehyde (25 wt. %, 250 µL) was added to the solution at room temperature while stirring at 600 rpm for 24 h. After crosslinking, acetone was removed from solution via rotary evaporation (RV120, 36°C, 40 rpm). This process was repeated separately three times for each gelatin.

3.3.2 NP Morphology, Diameter, PDI and Charge Analysis

Gelatin NP morphology was assessed using TEM. Post purified solutions (8 µL) were added to gold coated carbon grids. Excess sample was removed via kimwipe after 3 min and left to dry for ~24 h. Samples were then negatively stained with lead citrate (8%) for 2 min and imaged using a JEOL JEM-1400 TEM (JEOL Ltd., Tokyo, Japan).

Gelatin NP Z-Average size (described as NP diameter or size hereafter), PDI, and zeta potential was measured by Malvern Zetasizer Nano ZS90 (λ = 633 nm, protein analysis method) at a 173° Backscatter (NIBS) after adding the NP suspension (100 µL) to deionized water (900 µL). At least three measurements ($n \geq 3$) of each sample per trial was measured. To determine statistical significance between gelatin bloom average NP diameters, a one-way ANOVA with Games-Howell multiple comparison test due to unequal variance was performed in Minitab 18. Statistical significance was determined if $p < 0.01$. Two-sample t-tests were used to determine statistical significance of gelatin NP charges to SB75 and VB275 for $p < 0.01$.

3.3.3 Gelatin NP Quantification of Free Amine Groups

Post purified gelatin NP solutions were prepared and diluted with 1 mL deionized water. Additional reagents were added according to Won *et al*. (1 mL of 4% w/v sodium hydrogen carbonate pH 8.5, 1 mL of 0.1% v/v TNBS).[28] After reacting for 2 h at ~40 °C and 400 rpm, the solutions were centrifuged (100,000 x g, 15 min). Part of the supernatant (560 µL) was diluted in deionized water (1 mL) and absorbance measured at 349 nm using UV-Vis (BioTek Multi-Mode, Winooski, VT). The moles of lysine and degree of crosslinking was calculated using a calibration curve where SB225 and VB275 macroscale gelatin was dissolved in deionized water (0, 0.5, 5% w/v). After dissolution, the same procedure was carried out as the NP solutions (1 mL deionized water dilution, 1 mL 4% sodium hydrogen carbonate pH 8.5, 1 mL 0.1% TNBS, 2 h reaction, 15 min centrifugation). The moles of lysine (L) was calculated via the following modified equation (Eq. 3.1):[29]

$$L = \frac{2\ x\ Abs\ [349\ nm]\ \ x\ 0.02}{\varepsilon\ x\ b\ x\ g}$$

where Abs [349 nm] is the absorbance value at 349 nm, ε is the molar attenuation (or molar absorption) coefficient for 2,4,6-trinitrophenyl lysine (1.4×10^4) in units of $M^{-1}cm^{-1}$, b is the cell path length of 1 in units of cm, and g is the sample weight of 0.494 in grams. Crosslinking extent (%) was determined by the following equation (Eq. 3.2):

$$Lysine\ Amine\ Crosslinking\ (\%) = \left(\frac{L_{control} - L_{0.494g\ NP}}{L_{control}}\right) * 100\%$$

where $L_{control}$ is the determined moles of lysine using the 5% w/v macroscale gelatin sample (SB225 used for SB225 NPs and VB275 used for all other NPs to provide excellent crosslinking estimates) and $L_{0.494g\ NP}$ is the moles of lysine calculated from each NP solution using the prepared standard curve. Three to five measurements (n = 3-5) were analyzed from each gelatin bloom NP suspension.

3.3.4 Gelatin Secondary Structure and Macroscale Charge Analysis

To evaluate gelatin secondary structure, circular dichroism (Jasco J-810), was performed. Gelatin samples (5% of 0.125 mg / mL in distilled water, 40 °C, pH 6-7 and ~2.5) were added to a 1 mm

path length cuvette and scanned (room temperature, 250 nm-190 nm, 1 nm data pitch, standard sensitivity, 2 sec D.I.T, 1.00 nm bandwidth, 20 nm/min scanning speed, distilled water baseline correction). Three trials were prepared with each gelatin at each pH along with three scans (n = 3) per trial. Data is expressed as mean residue ellipticity [θ], $deg^1cm^2dmol^{-1}$ which normalizes results by concentration for comparison. A mean residual weight of 91.2 for gelatin was used for conversion.[30-31] To determine macroscale charge, gelatin (100 mg) was added to 2 mL distilled water and pH adjusted with 1M HCl to 2.5. Samples (1 mL, neutral and acidic) were placed in the Malvern ZetaSizer Nano ZS90 and measured ($n \geq 3$) as described above.

3.3.5 Gelatin Clarity

Samples were prepared and analyzed according to the Gelatin Manufacturer's Institute of American (GMIA) protocol.[32] Two separate trials with three measurements each (n = 3) were performed and measured using UV-Vis (Agilent Cary 60, Santa Clara, CA) at 640 nm. Statistical significance was determined using two-sample t-tests assuming unequal variance at $p < 0.05$ within same / similar gelatin blooms using Minitab 18.

3.3.6 Gelatin Molecular Weight Analysis and Chain Size Estimation

Gelatins were dissolved at ~40 °C (1 mg mL^{-1}) in vacuum filtered buffer (ultrapure water, 0.2 M $NaNO_3$, 0.1 M NaH_2PO_4) and pH adjusted to 7.[33] The dissolved gelatin samples were syringe filtered (0.45 µm) to remove dust. The solutions (20 µL) were then passed through an Agilent PL aquagel–OH 40 column with a Waters 2414 refractive index detector and Wyatt miniDAWN TREOS MALS. Gelatin refractive index increment (dn / dc) of 0.18 was estimated.[34-35] Molecular weights and Đ were determined via SEC light scattering and analyzed in Millennium software. Theoretical gelatin NP diameters based on the number of chains that aggregate and are subsequently crosslinked was calculated by first determining the minimum gelatin chain radius via Eq. 3.3:[36]

$$R_{minimum} = 0.066 * M_n^{1/3}$$

where $R_{minimum}$ is the minimum radius of a gelatin chain and M_n is the number average molecular weight. Using $R_{minimum}$, the number of gelatin chains that aggregate and are crosslinked within a NP was determined via Eq. 3.4:

$$D_H = 2^* R_{mininum} * x_{gelatin\ chains}$$

where D_H is the hydrodynamic diameter and $x_{gelatin\ chains}$ are the number of gelatin chains that can aggregate and be crosslinked for NP formation.

Sample Calculation:

a) Because SB75 (low molecular weight gelatin, confirmed from SEC analysis, Table 3.3) and VB275 (high molecular weight gelatin, confirmed from SEC analysis, Table 3.3) produced the same average D_H (Table 3.1), the number of gelatin chains that can form a NP was assumed to be similar.

b) The average D_H for SB75 and VB275 was 71 nm. Using the $R_{mininum}$ values calculated from SEC (Table 3), the number of gelatin chains for SB75 and VB275 was calculated as follows:

$$x_{SB75\_gelatin\ chains} = 71\ nm / (2.13 * 2\ nm) = 16.7 = 17$$
$$x_{VB275\_gelatin\ chains} = 71\ nm / (2.73 * 2\ nm) = 13.0 = 13$$

c) Glutaraldehyde can crosslink between 13 and 17 aggregated gelatin chains. Theoretical NP diameter ranges were calculated (Table 3.3) for each gelatin using 13 and 17 chains.

3.3.7 Pre-crosslinked Volume & PDI Distributions, Correlation Strength Analysis

Analysis of gelatin sample chain dispersity before adding glutaraldehyde crosslinker was assessed via the Malvern Zetasizer Nano ZS90 as described above. After dropwise acetone addition, 100 µL gelatin suspension was added to 900 µL deionized water and PDIs were measured at 40 °C. Two separate trials for each gelatin were analyzed with at least three measurements each ($n \geq 3$). Outliers were removed via Grubbs test ($p < 0.05$) with confirmation via boxplot in Minitab 18 (two values removed from SA300 and one value removed from VA300). Statistical significance was determined via the Kruskal-Wallis non-parametric test with statistical significance determined if $p < 0.05$ with Steel-Dwass pairwise comparisons. For one-way ANOVA, equal variances were confirmed without assuming a normal distribution. Pairwise comparisons were determined using Tukey's post hoc test in Minitab 18. Correlation tests (Spearman rank and Pearson) were performed in Minitab 18 with statistical significance determined if $p < 0.05$.

3.4 Results and Discussion

3.4.1 NP Synthesis and Characterization

Two-step desolvation is one of the most common gelatin NP synthesis techniques; however, inconsistency in the literature regarding NP diameter and incomplete experimental methods exists.[26] The motivation for this section was to determine if gelatin NP physicochemical property differences exist between similar gelatin blooms selected from different manufacturers. Gelatins with low (50-125), medium (175-225), and high (225-300) blooms were purchased from Sigma-Aldrich and Vyse. The following nomenclature was used: the first letter denotes gelatin manufacturer, the second letter denotes gelatin type, and the final number denotes bloom strength. For example, Sigma Type B bloom 75 is SB75. Selecting similar gelatin blooms from different manufacturers increased the likelihood of sample macroscale variability.

Gelatin NPs were synthesized and characterized after complete removal of acetone. Transmission electron microscopy (TEM) shows all NPs have generally spherical morphologies (Figure 3.1). SB75 (Figure 3.1A) and VB275 (Figure 3.1D) have the smallest NP sizes (<100 nm diameters) while all other NPs are ≥ 200 nm (Figure 3.1B, C, E, F).

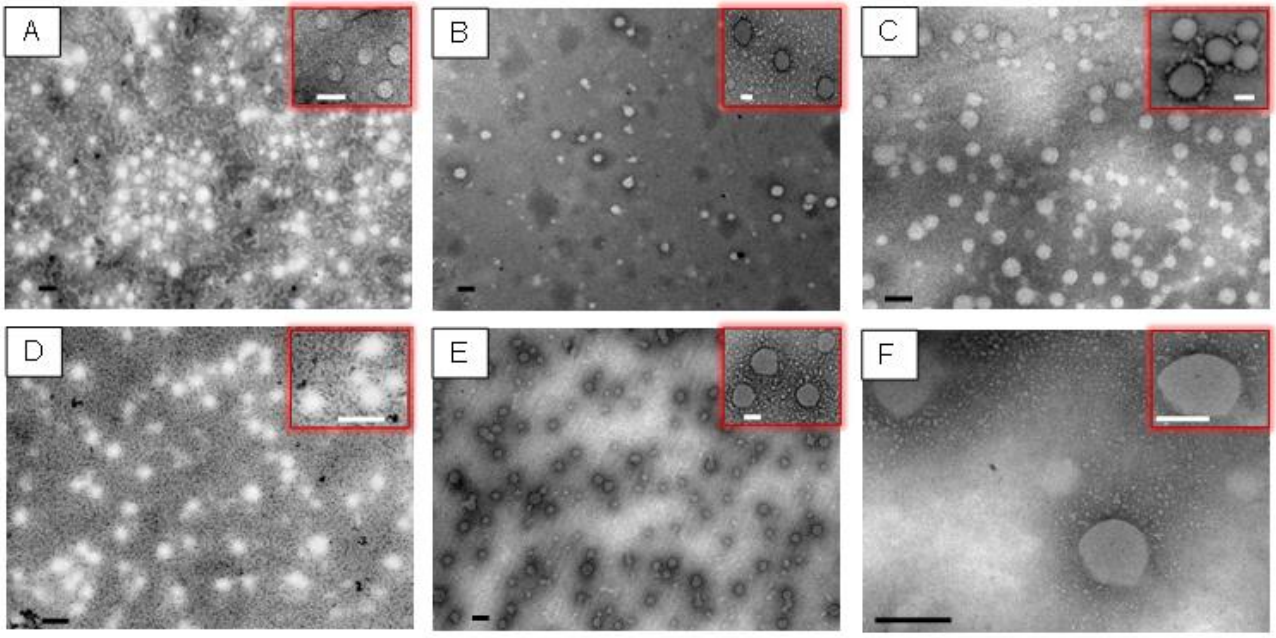

Figure 3.1. Representative TEM images of gelatin NPs show overall spherical morphology. (A) SB75, (B) VB85, (C) SB225, (D) VB275, (E) SA300, (F) VA300. SB75 and VB275 have diameters less than 100 nm while all other NPs have diameters greater or equal to 200 nm. Black scale bars represent 200 nm while inset white scale bars represent 100 nm. Overview TEMs taken at 30kV except for VA300 (100 kV). Insert square TEMs taken at 100-150 kV.

Dynamic light scattering for average size / diameter and laser doppler electrophoresis for charge analysis were used to characterize gelatin NPs in aqueous solutions. Two interesting characterization phenomenon were determined. Firstly, similar gelatin blooms have significantly different average NP diameters ($p<0.01$) shown in Table 3.1 (SB75 and VB85, SB225 and VB275). Only SA300 and VA300 have average diameters that are not statistically different. Secondly, low and high gelatin blooms (SB75 and VB275) consistently produced the smallest (~71 nm) average diameters (Table 3.1). All gelatin NPs have polydispersity indices (PDIs) less than 0.2 indicating diameters follow a narrow size distribution,[37] commonly attributed to removal of low molecular weight gelatin prior to NP formation using the desolvation process.[38] Zeta potential measurements reveal SB75 and VB275 NPs have statistically higher charges ($p < 0.01$) compared to all other NPs (Table 3.1).

Table 3.1. Post purified Gelatin NP Physicochemical Properties (pH 2.5~3.5) using Malvern Zetasizer ZS90

Gelatin	$Size_{\_diameter}$ (nm)	PDI	Zeta Potential (mV)
SB75	69.5 ± 1.2 †	0.13 ± 0.03	29.3 ± 1.5
VB85	225 ± 7.3 #	0.10 ± 0.03	22.1 ± 0.57
SB225	218 ± 5.7 #	0.12 ± 0.02	22.2 ± 0.77
VB275	72.7 ± 2.9 †	0.12 ± 0.01	30.7 ± 2.4
SA300	312 ± 12.7 @	0.11 ± 0.02	23.9 ± 0.83
VA300	352.3±12.6 @	0.11 ± 0.02	22.4 ± 1.8

Size statistics: Gelatins that do not share the same symbol were determined to be statistically significant via one-way ANOVA at $p < 0.01$. Three separate trials conducted with $n = 3$ measurements per trial. Data represent mean ± standard deviation.

Zeta Potential statistics: ● represents all pairs significantly different to SB75 and VB275 via two-sample t-test at $p < 0.01$. Three separate trials with $n = 3$-5 measurements per trial. Data represent mean ± standard deviation.

This is the very first study directly comparing gelatin NP physicochemical properties between similar gelatin blooms from different manufacturers. Also, based on extensive literature review, this work is the first to prepare, characterize and report Vyse gelatin nanoscale properties. Previous studies have applied two-step desolvation to synthesize NPs using Sigma-Aldrich gelatin. There are contradictory results comparing gelatin bloom to NP diameter. Saxena *et al.* determined NP

diameters remain constant between 200- 300 nm invariant of pH post synthesis, temperature post synthesis, and molecular weight (SB75, SA175, and SA300 were tested).[23] To purify their NPs, Saxena *et al.* used centrifugation without mentioning speed and length of time.[23] The amount of force applied to the pre-purified NPs could explain why sub-100 nm particles for SB75 were not observed. This dissertation determined centrifugation and washing with acetone / water caused large increases in sizes. To prevent such size increases, less destructive methods, such as rotary evaporation for purification, were required. Unlike the discrepancy between the SB75 NP diameters, SA300 NP diameters are both consistently ~300 nm, which suggests higher bloom gelatins might be more resistant to centrifugal force.

Similar to the results obtained in this dissertation Wang *et al.* obtained ~250 nm diameters for SB225[37] while Azarmi *et at.* obtained significantly lower diameters of 112 ± 21 nm.[22] The experimental methods between studies were similar except for the following conditions: 1) The length of time for the first desolvation was not included by Azarmi *et al.* (the precipitate was removed after 24 h in this dissertation), 2) The dropwise acetone rate was not included[39] (3 mL/ min was use in this study), and 3) The amount of time the NPs were crosslinked. Azarmi *et al.* crosslinked their gelatin NPs for 12 h,[22] while this research used 24 h[39] to mimic the length of time for the first desolvation step. The average zeta potential values reported here are all slightly higher compared to Azarmi *et al.* (20 mV versus ~15 mV for relevant gelatin samples), which suggests the NP method presented in this dissertation produces particles that might be less susceptible to aggregation overtime.

The valuable experimental approach preparing NPs of similar gelatin blooms obtained from different manufactures is prominently revealed in Figure 3.2. Here, a scatterplot of gelatin NP diameter versus bloom with an additional categorization by company is presented. Interestingly, gelatin samples from Sigma-Aldrich appear to follow a positive correlation where average NP diameter increases with bloom. Researchers might conclude the bloom-NP diameter association is universal for all gelatin samples using the experimental conditions applied. However, these results are misleading as Vyse gelatin revealed no observed trend.

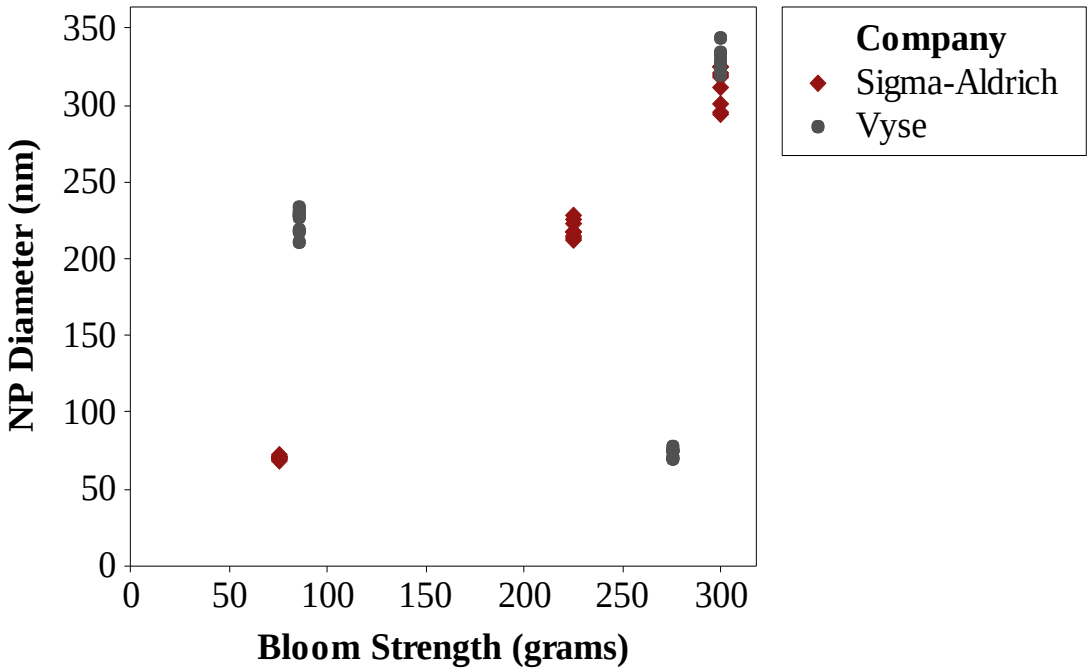

Figure 3.2. Scatterplot of Gelatin NP Diameter vs Bloom Strength and Company. Adequate gelatin batch variability was achieved as there is no overall association between average NP diameter and the company from which gelatin was obtained.

Ultimately, this single study both refutes and corroborates previously discussed conclusions by Saxena *et al*. and indicates discrepancies in how to control gelatin NP diameter exist, as most studies prepare NPs from one company, one specific bloom and / or one particular batch. To fully determine if manipulated experimental protocols impact gelatin NP diameter, multiple gelatin batches (either from similar or different companies) should be selected. This study sought to obtain gelatin variation by selecting similar blooms from different manufactures, instead of selecting multiple similar blooms from the same manufacturer. Comparing gelatin NP diameter between respective company reveals an inability to predict particle diameter, confirming adequate variation was achieved.

Overall, similar gelatin blooms from different manufacturers produced significantly different average NP diameters (except for SA300 and VA300). Additionally, low and high blooms (SB75 and VB275) produced the smallest diameters with highest zeta potentials. Gelatin NP solutions were next characterized to determine glutaraldehyde crosslinking extent.

3.4.2 Gelatin NP Quantification of Free Amine Groups

Similar to other biopolymers, gelatin is often crosslinked with glutaraldehyde to create suspensions of stable spheres resistant to aqueous and enzymatic degradation. A Schiff Base forms between glutaraldehyde carbonyl groups and gelatin amino groups in lysine or hydroxylysine preventing 1) premature therapeutic release due to swelling[22] and 2) NP agglomeration shown for over 10 months.[40] Significant differences in gelatin NP diameter between similar blooms warranted an understanding of glutaraldehyde crosslinking efficiency. Calibration curves of macroscale gelatin (defined as its uncrosslinked form) were created (0, 0.5, 5% w/v) shown in Figure 3.3.

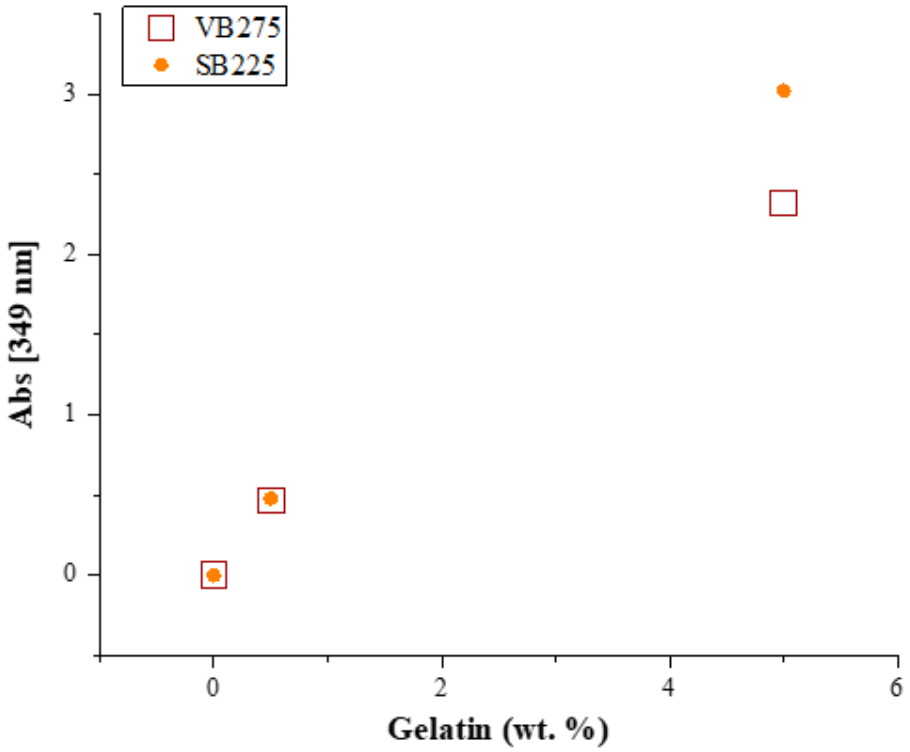

Figure 3.3. Gelatin absorbance using TNBS assay. As gelatin concentration increases so does the absorbance values using TNBS assay. n = 3 measurements averaged.

Interestingly, macroscale SB225 at 5% w/v had a higher absorbance value compared to VB275 (Figure 3.3). This might indicate the incorporation of non-gelatin contaminants such as skin proteoglycans or residual collagen during the manufacturing process.[41] The final standard curve was generated after calculating the moles of lysine (Figure 3.4A). After allowing TNBS to react

with the post purified gelatin NPs, three distinct color changes occurred indicative of TNBS and lysine interaction.[42] SB75 and VB275 produced a faint yellow hue (Figure 3.4Bi), VB85 and SB225 produced an orange hue (Figure 3.4Bii), and SA300 & VA300 produced a dark orange hue (Figure 3.4Biii). The color changes correspond to the specific grouping of NP sizes where the smallest NPs (SB75 and VB275) had the least amount of free moles of lysine while the largest NPs had the greatest amount of free lysine content (Figure 3.4C). As expected, the smallest NPs (SB785 and VB275) with the least amount of available lysine had the highest degree of crosslinking, while the largest NPs (SA300 and VA300) with the highest concentrations of available amino groups were crosslinked the least (Figure 3.4D).

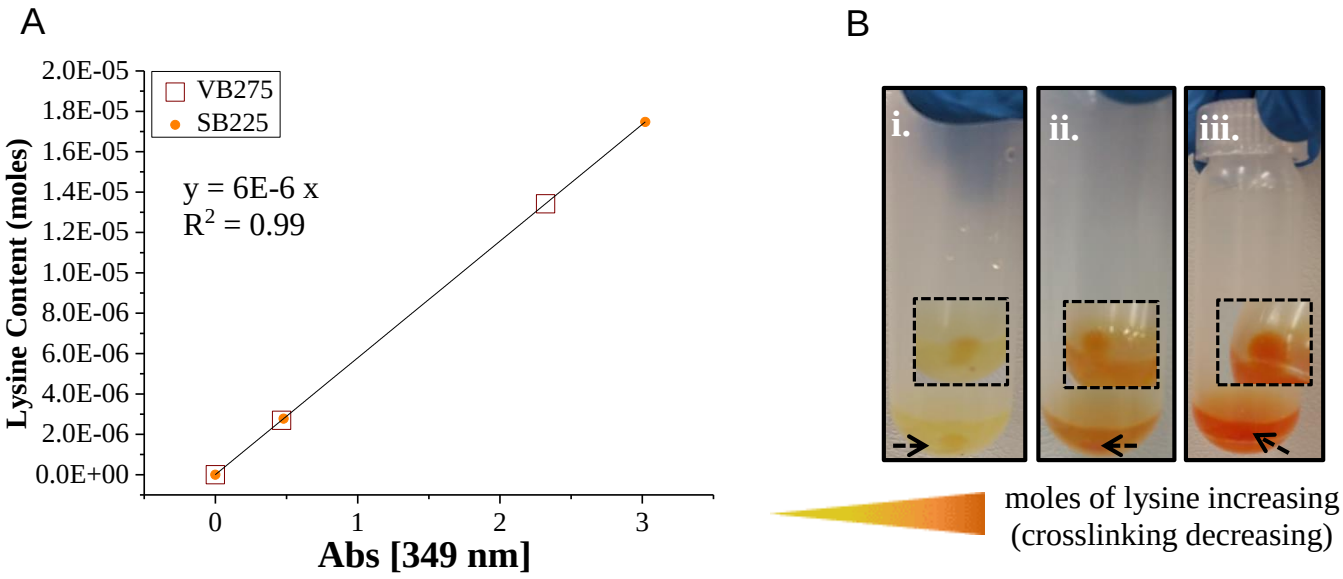

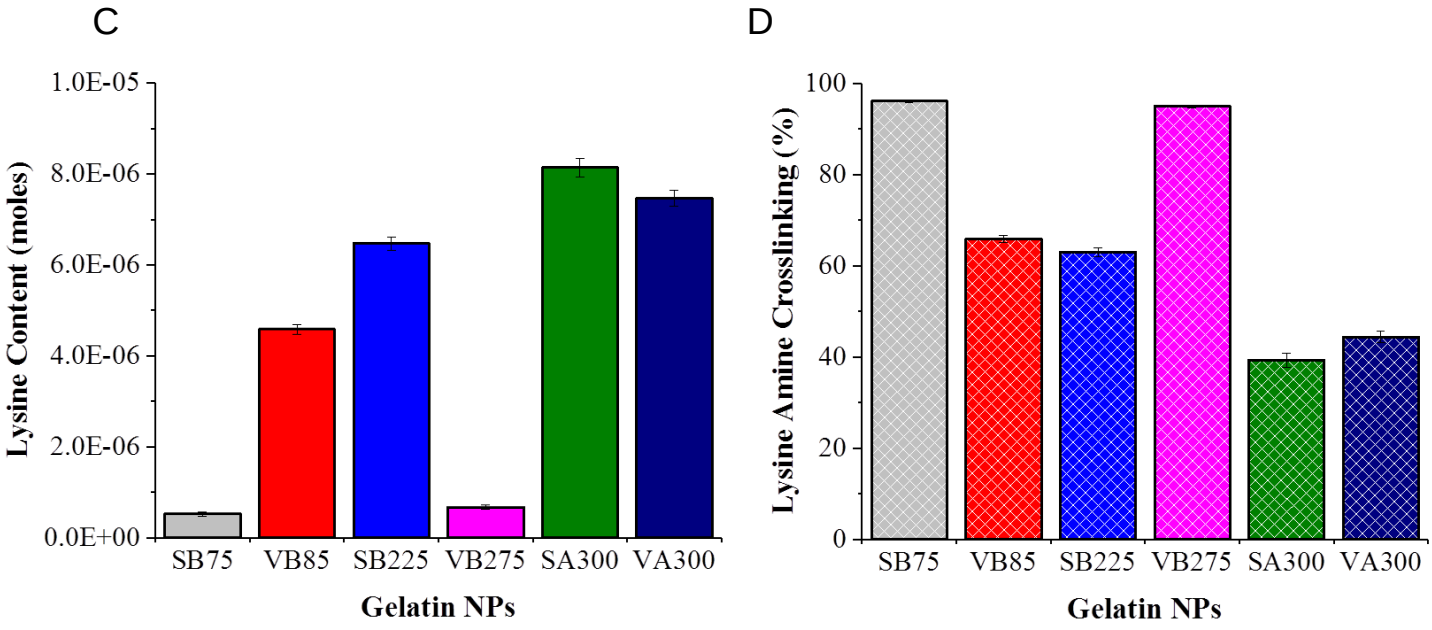

Figure 3.4. TNBS assay reveals large differences in free moles of lysine and amine group crosslinking between NPs. (A) Moles of lysine detection increases linearly with TNBS absorbance. (B) Representative optical images of TNBS interacting with gelatin NPs. Inserts reveal NP pellet formation after centrifugation. Only the solutions were used for absorbance measurements. Each single image represents the NP pairs described. (i) SB75 and VB275 produced the same faint yellow hue indicating low free lysine content (C). (ii) VB85 and SB225 solutions appear orange revealing moderate detection of free lysine moles (C). (iii) SA300 and VA300 solutions appear dark orange corresponding to high lysine detection (C). (D) SB75 and VB275 had the highest degree of crosslinking, VB85 and SB225 had moderate crosslinking while SA300 and VA300 were the least crosslinked. Overall, an inverse relationship exists as lower moles of lysine correspond to higher crosslinking (and smaller NP diameters). n=3-5 measurements per gelatin bloom NP suspension. Data represent mean ± standard deviation.

Previous studies have reported NP crosslinking using different experimental procedures of the same gelatin type, showing ~80% crosslinking after dispersing lyophilized samples in TNBS solution.[22, 28] Initial attempts to replicate earlier crosslinking procedures consisted of freezing post purified NP solutions (15 mL) and lyophilizing for 48 h. The NP solution became a dense foam material (Figure 3.5A) and crosslinking was confirmed to be ~80% for all NPs (Figure 3.5B). Though these results are consistent with literature, it was hypothesized the lyophilization process was destructive to the NP structure since all solutions were frozen at -20 °C followed by sublimation (-60 °C, 0.06 mbar). Temperatures below gelatin's gel point (< 30 °C)[43-44] causes physical inter-chain entanglements of disordered random coils producing a gel.[45] Lyophilizing an entangled frozen network of gelatin NPs produced the same degree of crosslinking likely overriding the covalent stabilization process of glutaraldehyde. As a result, the alternative method using NP solutions along with raw gelatin weight percent's to generate a standard curve obtained more representative crosslinking effects. Results suggest glutaraldehyde can crosslink both low bloom strength (SB75) and high bloom strength (VB275) gelatin leading to sub-100 nm average diameters. This likely indicates high molecular weight (or bloom) gelatin is not a significant influencer for small NP formation as previously described.[46] Furthermore, the differences in glutaraldehyde crosslinking between similar gelatin bloom strengths (which correspond to differences in NP physicochemical properties discussed earlier) suggest there are dissimilarities in fundamental gelatin properties. Therefore, we next characterized macroscale gelatin properties and identified correlations to their NP physicochemical properties.

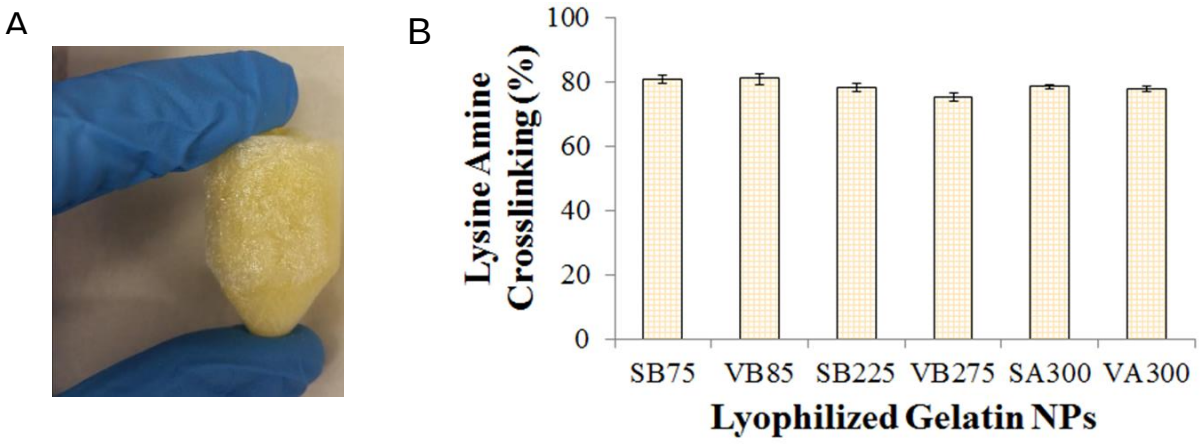

Figure 3.5. Lyophilized NPs. (A) Representative dry foam of gelatin NPs after lyophilizing solution for 2 days. (B) All lyophilized NPs were ~80% crosslinked. n = 3-5 measurements per sample. Data represent mean ± standard deviation.

3.4.3 Macroscale Gelatin Secondary and Tertiary Structures from Circular Dichroism

Gelatin's structure can vary from one sample to another due to the chemical process by which collagen is broken into irregularly shaped polypeptide chains.[47] Therefore, it was necessary to characterize gelatin structural responses in aqueous solutions. Circular dichroism is a spectroscopic technique providing the secondary and tertiary structures of chiral molecules by measuring the difference in absorbance between left handed and right handed circularly polarized light. Gelatin is a denatured protein with triple helical morphology indicated by a positive peak at ~222 nm and a random coil conformation indicated by a negative peak at ~205 nm.[48] Macroscale gelatins were dissolved at 40 °C in distilled water at neutral pH. Following dissolution, samples were equilibrated to room temperature and half the solution was removed and adjusted to acidic conditions (pH 2.5) similarly to the NP synthesis procedure.

At neutral pH, the higher gelatin bloom strengths (VB275, VA300, SA300) have slight peaks at ~220 nm while the lower bloom strengths show no peak at 220 nm, indicating minimal triple helical structure (Figure 3.6A). The results indicate heating solutions to ~40 °C denatures gelatin chains, which is confirmed by Pelc *et al.*[44] and more recently by Ahsan *et al.*[49] There was significant random coil morphology with all gelatin samples with their corresponding intensity based on bloom strength (Figure 3.6A). Generally, as the bloom strength increases, so does the degree of random coil. Thus, structural characterization at neutral pH conditions reveal random coil intensity can serve as an indirect method to confirm low, middle, and high bloom gelatin.

After adjusting the pH to 2.5, a slight decrease in triple helical content was seen which indicates further denaturation. Interestingly, the random coil intensity decreased for all gelatin samples as well, with middle and high bloom samples (SB225, VB275, SA300, VA300) showing prominent reductions **(**Figure 3.6B).

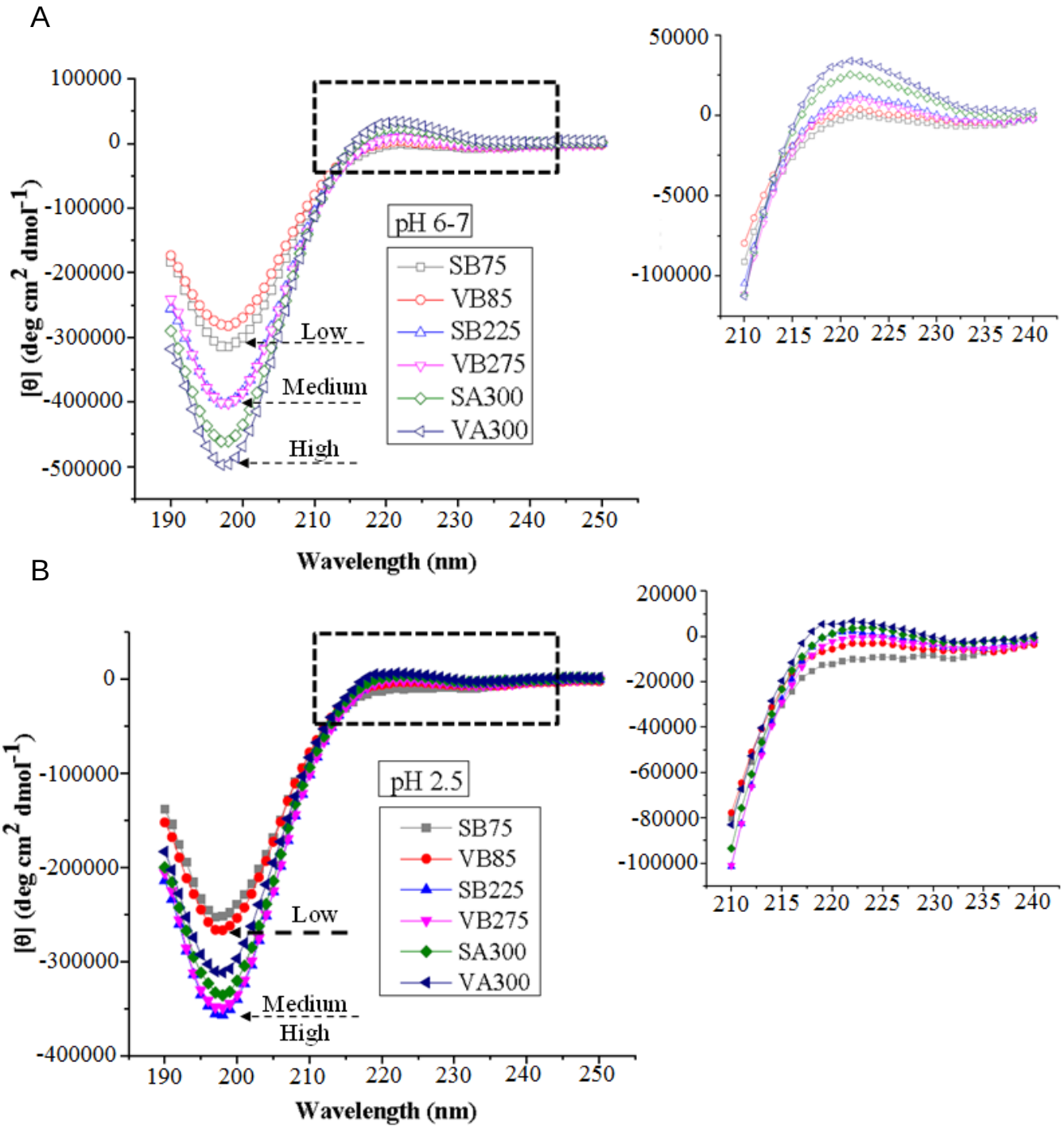

Figure 3.6. Circular dichroism confirms analogous macroscale gelatin structures in aqueous solutions. (A) Gelatins at pH 6-7 have three distinct regions of random coil intensity by bloom. Insert reveals at most moderate triple helical content likely due to heat denaturation. (B) Gelatins at pH 2.5 have random coil (and triple helical) reductions indicating chemical denaturation and likely chain stacking due to protonation of amine groups. Insert reveal further reductions in triple helical content as well. All gelatin samples respond similarly in aqueous environments indicating analogous structures. n = 3 separate trials with 3 scans per trial.

Gelatin macroscale zeta potential measurements were conducted to offer one possible explanation for random coil reductions in acidic pH. Gelatin's isolectric point (pI) is the pH at which there is zero net charge. The pI of Type B gelatin is 4.7-5.4 while the pI of Type A gelatin is 7-9.[16] All gelatins have modest charges (~0 ± 4 mV) (Figure 3.7) in distilled water (pH 6-7). In acidic solutions, amine groups undergo protonation resulting in net positive charges for all gelatins (Figure 3.7). Further, results suggest protein charge and the degree of random coil are associated. One possible explanation is due to gelatin chain flexibility. Gelatin Type B chains can persist for a 2 nm distance before changing direction while Type A chains can persist for 10 nm before changing direction.[50] These highly flexible chains containing charged amine groups have a greater propensity to overlap and interact with negatively charged segments.[23, 50] The intra chain association results in chain stacking at acidic conditions, which likely reduces some of the random coil intensity in the overall gelatin structure. Circular dichroism has shown all gelatin bloom strengths respond similarly to pH changes, which suggests all structures are consistent after their respective manufacturing processes.

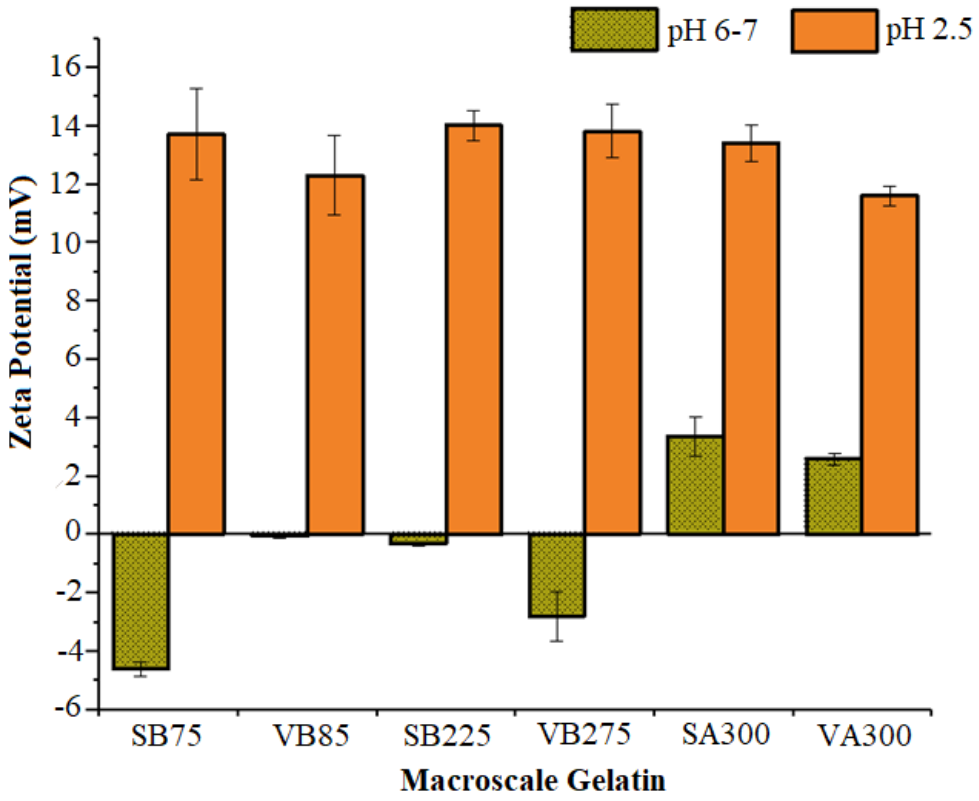

Figure 3.7. Macroscale gelatin zeta potential measurements reveal pH dependency. Type A and Type B gelatin have modest charge (0±4 mV) in distilled water (pH 6-7). Acidic environments (pH 2.5) are significantly below gelatin pIs leading to protonation of amine groups and net positive charges. n = 3-5 measurements per sample. Data represent mean ± standard deviation.

3.4.5 Gelatin Clarity

Clarity is a material property utilized by manufacturers to determine gelatin purification after its extraction and processing.[32] Very high clarity (up to 98 and 99%)[51-52] which is determined via percent transmittance, indicates minimal substances that scatter light and causes cloudiness in solutions.[53] To determine adequate gelatin extraction and investigate whether impurities might impact nanoscale properties, two separate solutions of each gelatin bloom were dissolved, heated, and percent transmittance at 640 nm was measured three times according to Gelatin Manufacturers Institute of America protocol.[32] Transmittance values were compared using a two-sample t-test between similar gelatin blooms since their respective processing conditions were assumed to be conserved between manufactures. As shown in Table 3.2, most gelatin solutions have average transmittance values below 93% indicating the presence of possible inorganic salts, non-

collagenous proteins, or mucosubstance contaminants, which have been shown to exist in gelatin.[41, 54-55] Additionally, there are significant differences ($p<0.05$) in transmittance values for SB75 and VB85 along with SB225 and VB275 (Table 3.2). These gelatins also have the largest differences in NP diameters within their respective bloom strengths (Table 3.1). Non-gelatin protein and mucosubstance contaminants, which reduce gelatin clarity, contain amine groups and are thus susceptible to chemical crosslinking. Glutaraldehyde crosslinking with protein contaminants could prevent adequate reactions with gelatin leading to larger NP diameters and lower crosslinking efficiencies. SA300 and VA300 have nearly the same average transmittance (~93%) and have the closest differences in NP diameter (~40 nm). Overall, this suggests that percent transmittance might be a suitable technique to screen macroscale gelatin batches before beginning the NP synthesis procedure to determine if diameters might be replicable from literature. For example, if the transmittance of a completely separate VB275 gelatin solution is significantly < 87% then this could indicate corresponding NP diameters might be larger than 70 nm.

SB75 and VB275 have the highest transmittance with their respective bloom strengths and overall smallest NP diameters. Conversely, SA300 and VA300 have high transmittance and the largest NP diameters. Together, this likely indicates that sample purity is one component, but not a significant material property contributing to NP property differences.

Table 3.2. Macroscale Gelatin Clarity

Gelatin	Clarity (% Transmittance)[a]	[b]Average Gelatin Diameter (nm)
SB75	94.3 ± 0.63 †	69.5 ± 1.2
VB85	88.0 ± 0.23 †	225 ± 7.3
SB225	68.3 ± 1.1 †	218 ± 5.7
VB275	86.7 ± 1.6 †	72.7 ± 2.9
SA300	93.3 ± 1.2	312 ± 12.7
VA300	93.4 ± 0.28	352 ± 12.6

[a] n = 2 separate trials with 3 measurements per trial.
Data represent mean ± standard deviation.
† signifies statistically significant at $p < 0.05$ using two-sample t-test.
[b] Diameter measurements from Table 3.1 added for reference.

3.4.6 Gelatin Molecular Weight Analysis and Chain Size Estimation

Following clarity measurements indicating likely presence of scattering impurities in gelatin solutions, it was necessary to obtain absolute molecular weight and dispersity of each sample. SEC separates sample components based on size and calculates number average molecular weight (M_n), weight average molecular weight (M_w), and dispersity, Đ (M_w / M_n) with a value of 1 in SEC signifies uniform molecular mass. Absolute molecular weights obtained from SEC light scattering detection were used to compare each gelatin's estimated average molecular weight based on bloom strength. Compared to all other gelatins, SB75, VB85 and VB275 have M_n values closer to their respective theoretical molecular masses based on bloom strength while all samples have M_w values >100,000 Da (Table 3.3). Gelatin is a heterogeneous protein and its molecular weight distribution varies according to variations in raw material and gelatin pretreatment and extraction conditions.[56-57] Therefore, a range of commercial gelatin molecular weights have been reported from 40,000 to 80,000 for M_n to 20,000 to 200,000 for M_w.[58] One of the earliest studies to compare commercial gelatin molecular weights from Sigma Chemical Company was Farrugia *et al.* determining molecular weights (M_n, M_w) >100,000 Da and average Đ's between 4.3 and 8.5 for every gelatin they tested (SB225, SB60, SA60).[46] Interestingly, within similar blooms, lower Đ's correspond to higher clarity measurements (SB75 vs VB85, SB225 vs VB275, SA300 vs VA300). Overall, this further suggests lower clarity might account for protein contaminants leading to broader molecular weight distributions. Additionally, these same pairs had similar Đ's and obtained similar average NP diameters suggesting the ability to 1) replicate NP diameters and 2) obtain small sub-100 nm particles is heavily influenced by solution composition. Theoretical calculations further substantiated this analysis.

Table 3.3. Macroscale Gelatin Absolute Molecular Weight, Dispersity, and Minimum Theoretical Sizes

Gelatin	[a]Molecular Mass (Da)	[b]M_n (Da)	[b]M_w (Da)	[c]Đ ([b]M_w/[b]M_n)	[d]$R_{minimum}$ (nm)	[e]D_H (nm)
SB75	30000	33700	113400	3.4	2.13	69.7 - 72.5
VB85	34000	26800	118200	4.4	1.98	51.3 - 67.2
SB225	50000	28300	113000	4.0	2.01	52.3 - 68.4
VB275	61111	71000	207900	2.9	2.73	71.1 - 92.9
SA300	92307	38500	126100	3.3	2.23	57.9 - 75.8
VA300	92307	53800	186300	3.5	2.49	64.8 - 84.7

a: Theoretical average molecular mass based on bloom strength
b: Experimentally determined number average and weight average molecular weight
c: Dispersity, Đ calculated by dividing $^{b}M_w$ / $^{b}M_n$
d: Estimated minimum gelatin chain radius,[40] $R_{mininum} = 0.066 * M_n^{1/3}$ (Eq. 3.3)
e: Min. theoretical diameter after crosslinking of 13 and 17 gelatin chains (x), $D_H = 2* R_{mininum} * x$ (Eq. 3.4)

From the molecular weight data, the minimum theoretical radius of a gelatin chain was calculated (Table 3, Eq. 3.3).[36] The calculations are within reason as Diaz-Calderón *et al.* determined the minimum radius for Type B 220 gelatin under single strand configuration was 2.5 nm via dynamic light scattering.[59] Because low molecular weight (SB75, M_n 33,700 Da) and high molecular weight (VB275, M_n 71,000 Da) gelatin produced the smallest average NP diameters, this indicated glutaraldehyde can crosslink and form into particles roughly the same number of gelatin chain aggregates. Therefore, a new equation that determined NP diameter is equal to the diameter of a single gelatin chain multiplied by the number of chains within the particle (Eq. 3.4) was produced. Using SB75 and VB275 as a baseline (71 nm average diameter), the number of gelatin chains formed in a single NP was 17 for SB75 and 13 for VB275. Accordingly, using the M_n of each gelatin and the number of aggregated chains (13 and 17), their minimum theoretical NP diameters were calculated to all be sub-100 nm (Table 3.3). It is important to note this calculation is based on the assumption that all gelatins (VB85, SB225, SA300, VA300) have the same molecular weight dispersity as SB75 and VB275, since these gelatins produced the minimum NP diameter out of all other blooms in this study. Regarding molecular weight uniformity, within Type B samples, SB75 and VB275 have the lowest Đ's indicating less variation in their molecular masses (Table 3.3). Again, these samples produced the same NP diameters and were the smallest (Table 1.1). Interestingly, Type A samples also had relatively low Đ's compared to the entire gelatin data

set (Table 3.3), but produced large average NP diameters (Table 1.1). During the extraction process of Type A gelatin, acidic conditions precipitate out low molecular weight fractions while higher molecular weight fractions remain in solution.[55] **Altogether, this indicates the following:** 1) SB75 and VB275 have higher contents of low molecular weight fractions that are removed after the first desolvation step in NP synthesis and 2) All other gelatins have broader contents of high molecular weight fractions (likely from both gelatin and protein contaminants) that remain in the sample due to their higher densities even after the first desolvation step.

This is the first study to propose mathematically that glutaraldehyde crosslinking is constant between gelatin NP blooms and suggests a high level of dependency on macroscale molecular weight composition. Based on these results, variations in pre-crosslinked gelatin suspensions (after dropwise acetone, but before glutaraldehyde addition), indicating a range of higher molecular weights, were hypothesized to produce larger NP diameters. Testing pre-crosslinked distributions was the final characterization study.

3.4.7 Gelatin Pre-crosslinked Volume and PDI Distributions

Bloom strength corresponds to the average molecular weight of gelatin. Though two-step desolvation removes low molecular weight gelatin fractions after the first desolvation step, [21] depending on the polymer sample dispersity, a range of molecular weights can undergo dehydration via dropwise acetone and finally crosslinking via glutaraldehyde during NP synthesis. Pre-crosslinked qualitative volume distributions along with PDI values were obtained by adding gelatin solutions (100 µL) to deionized water (900 µL) and measuring at 40 °C using dynamic light scattering. Two separate trials of each gelatin was taken with n = 3 to 6 measurements per trial. As shown in Figure 3.8, SB75 and VB275 have one main volume peak in their pre-crosslinked samples indicating most of the solution consists of one component. All other gelatins have at least two distinct peaks corresponding to multiple volume distributions in their pre-crosslinked solutions. As expected, VB85, SB225, and SA300 have broad distributions in their higher diameter regions indicating large molecular weight components within their samples. Results indicate that while the desolvation process likely removes low molecular weight gelatin, the ability to control molecular weight dispersity prior to crosslinking, holds substantial importance for producing consistent NP properties.

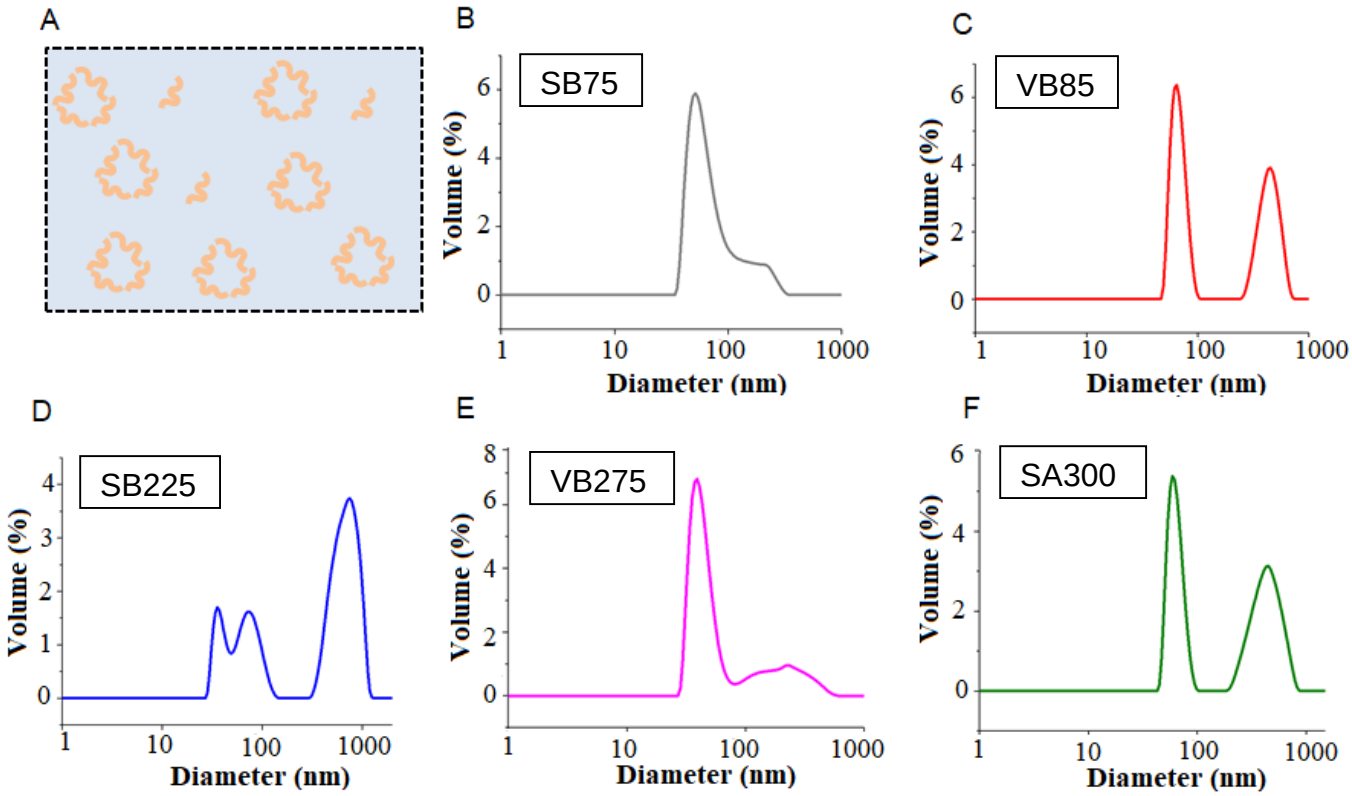

Figure 3.8. Representative volume distributions of pre-crosslinked gelatin solutions. (A) Pictorial representation of highly monodispersed gelatin chain aggregates prior to chemical crosslinking. (B) SB75 and (E) VB275 have one main component in their sample indicated by only one peak. All other gelatin samples (C) VB85, (D) SB225 and (F) SA300 have multiple peaks indicating a variety of components – likely different molecular weight gelatin chains and / or non-gelatin protein contaminates. VA300 was too polydispersed to generate a representative profile.

3.4.8 Quantitative Pre-crosslinked PDI Analysis

Potential outliers were identified using a boxplot, confirmed via Grubb's test ($p < 0.05$), and removed from the data set (one point removed from SA300 and two points removed from VA300). SB75 and VB275 had considerably lower pre-crosslinked PDI averages compared to all other gelatins (Figure 3.9A). Since there was significant non-normality in the VA300 data set, the non-parametric equivalent to the one-way ANOVA, known as the Kruskal-Wallis test,[60] along with Steel-Dwass pairwise comparison test (equivalent to Tukey's test),[61] was used to assess statistical significance ($p < 0.05$). The Kruskal-Wallis test calculates an average rank of the pre-crosslinked PDI within each group (the smallest value is given a rank of 1, the second smallest value is given a rank of 2, etc.) and compares each group to the average rank of all measurements. Furthermore, the z-value provides a numerical assessment comparing each bloom's average rank to the average rank of all observations.

A

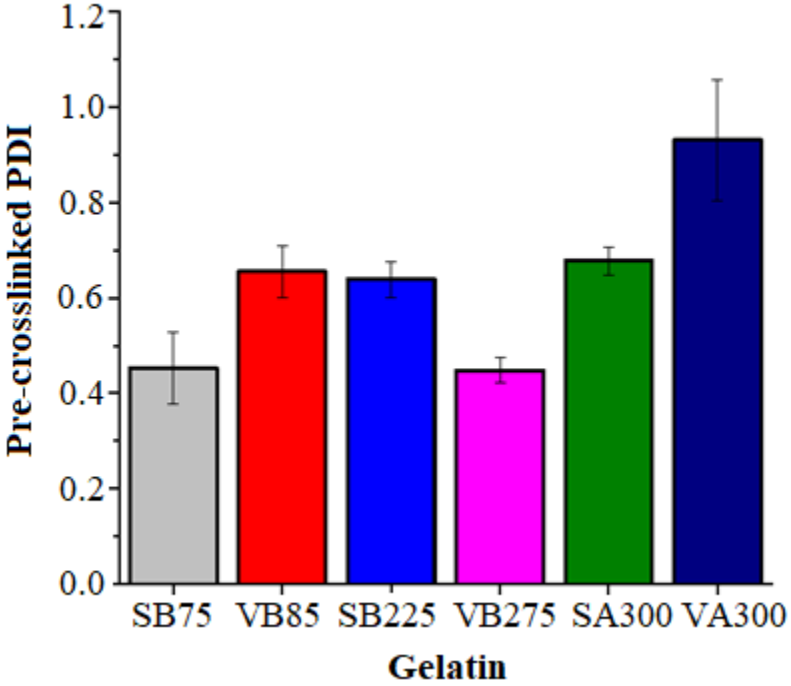

B

Pre-crosslinked PDI Kruskal-Wallis Analysis

Gelatin	Median	Average Rank		Z
SB75	0.447	11.2	⌂	-3.47
VB85	0.65	31.5	#, @	1.07
SB225	0.636	29.9	†, @	1.01
VB275	0.449	10.6	⌂	-3.61
SA300	0.664	34.2	†, #	1.84
VA300	1	46.4		4.1
Overall	-	25.5		-

Figure 3.9. Pre-crosslinked PDI quantitative and statistical analysis. (A) Gelatin pre-crosslinked PDI bar graph shows SB75 and VB275 have the lowest PDIs. (B) Pre-crosslinked PDI table of the Kruskal-Wallis summary statistics shows SB75 and VB275 have the lowest average rank indicated by negative z-values. VB85 & SB225 have averages ranks slightly above the overall rank while SA300 and VA300 have average ranks much larger than the overall rank. Lower pre-crosslinked PDI measurements indicate SB75 and VB275 have lower gelatin chain distributions prior to glutaraldehyde crosslinking. Gelatin pre-crosslinked PDIs that do not share the same symbol were determined to be statistically significant ($p \leq 0.05$). Two separate trials with n = 3-5 measurements per trial included. Data represent mean ± standard deviation.

SB75 and VB275 had average rank values lower than the overall rank (indicated by negative z -values), VB85 and SB225 had average rank values slightly higher than the average rank (slight positive z-value), and SA300 and VA300 had average rank values much higher than the average rank (highest positive z-values) (Figure 3.9B). Furthermore, the Steel-Dwass multiple comparison ranking test showed that similar gelatin blooms had statistically different average ranks calculated from their pre-crosslinked PDIs (Figure 3.9B). Similarly, these trends correspond with the average NP diameter data for the entire gelatin population. SB75 and VB275 had statistically smaller diameters (between 69.5 to 72.7 nm), VB85 and SB225 had average diameters in the middle (218 to 225 nm), while SA300 and VA300 had the largest average diameters (>300 nm). Though ANOVA is robust against non-normal data,[62-63] it does not rank a group's data set to the entire population, which was a valuable asset for this analysis. Nevertheless, the one-way ANOVA obtained the same pairwise comparisons as the Kruskal- Wallis test (Figure 3.10).

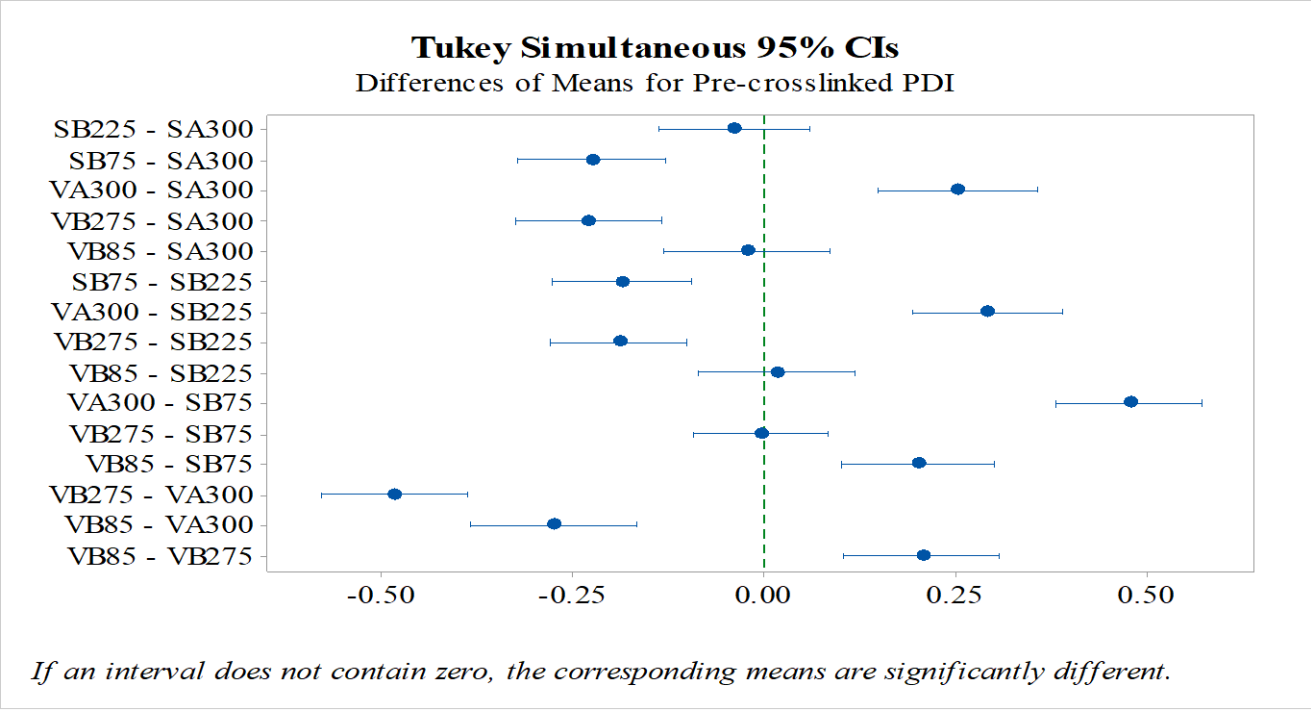

Figure 3.10. One–way ANOVA with Tukey's pairwise comparison for gelatin pre-crosslinked PDI values. Statistical significance yields the same results for the pairs compared to Kruskal-Wallis test (Figure 3.9B). Two separate trials with n = 3 to 6 measurements per trial included. Data represent mean ± standard deviation.

3.4.9 Pre-crosslinked PDI and NP Diameter Correlation Analysis

Graphical comparison of pre-crosslinked PDI and NP diameter was observed using a scatterplot with three upper PDI deviations identified by triangles (Figure 3.11). The triangle deviations are likely due to inefficient sample stabilization during the first measurement. As expected, increases in gelatin pre-crosslinked PDIs were similarly charted with increases in average NP diameter. Because the pre-crosslinked PDI and NP diameter data sets were not normally distributed, the non-parametric equivalent to linear regression, known as the Spearman's rank-order correlation test was performed to quantitatively determine the strength of observed trends.[64] A Spearman's correlation test makes no assumptions regarding distribution of the data, but assesses the degree of monotonicity — the degree to which the dependent variable (NP diameter) increases or decreases as the independent variable (pre-crosslinked PDI) increases. A Spearman correlation coefficient, ρ, of zero indicates no association, while ± 1 indicates a perfect positive or negative association. Pre-crosslinked PDI and NP diameter were highly correlated since ρ equaled 0.82,[65] which was determined to be significant as $p = 0.000$.

The well-known Pearson correlation test, which determines the strength and direction of a linear relationship, has been shown to be robust against non-normally distributed data.[64] A Pearson coefficient, r, closer to ± 1 reveals strong linearity. A Pearson correlation test revealed high positive linearity determined to be statistically significant ($r = 0.83$, $p = 0.000$) between pre-crosslinked PDI and NP diameter. All coefficient values assessing correlation strength and direction are similar for both tests suggesting either method is appropriate. Table 3.4 contains a summary of the correlation tests and reveals minimal increases in correlation coefficients after removal of triangle deviations shown in Figure 3.11.

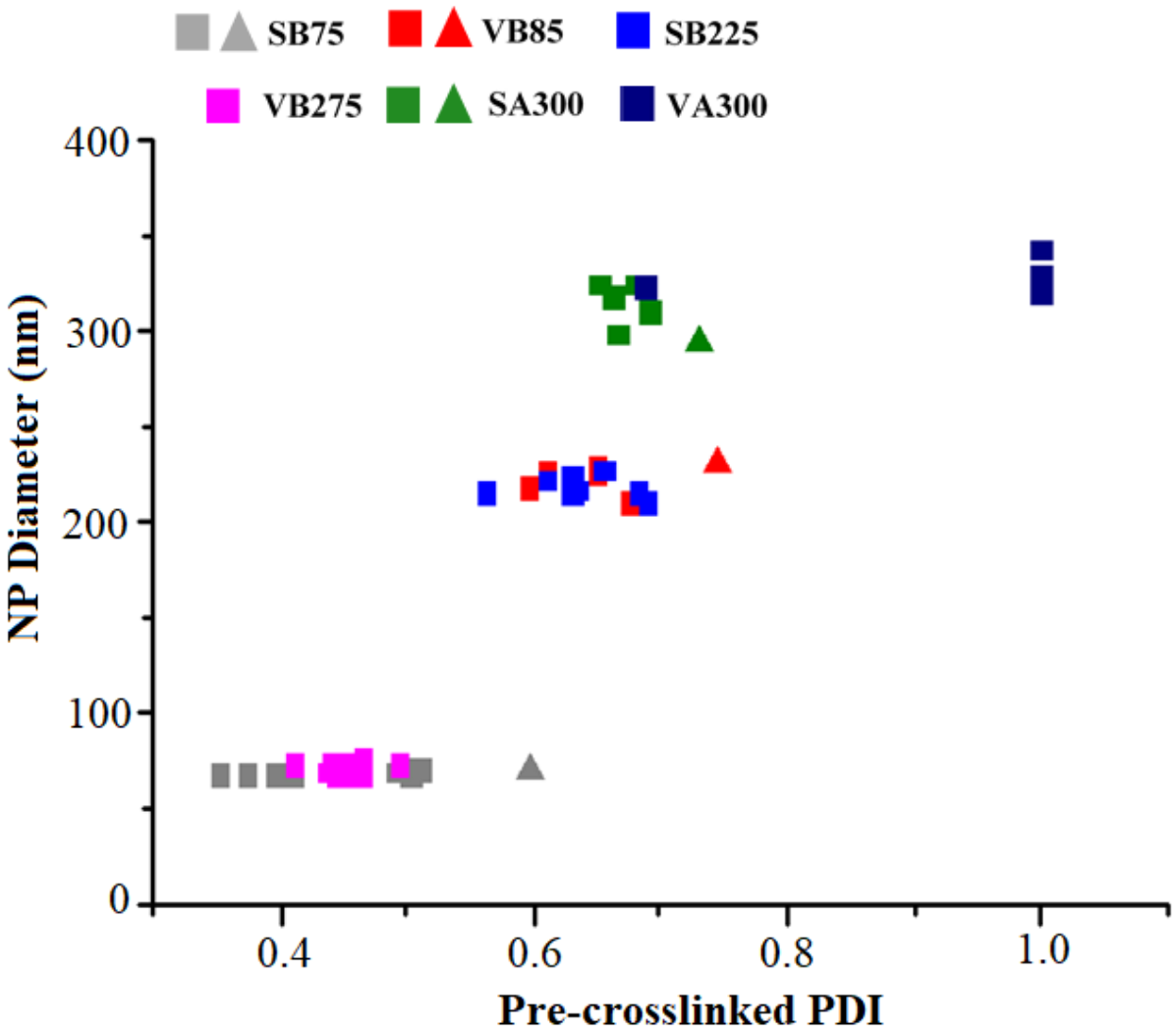

Figure 3.11. Graphical analysis of pre-crosslinked PDI versus NP diameter indicates a correlation exists. Sample deviations identified as triangles led to slight increases in coefficient values once removed from the data, indicating minimal effect on the overall analysis (Table 3.4). Total data points include 43.

Table 3.4. Quantitative Correlation Strength Analysis

Test Used	Coefficient Value	p-value
Spearman_triangle deviations removed	$\rho = 0.87$	0.00
Spearman_triangle deviations kept	$\rho = 0.82$	0.00
Pearson_triangle deviations removed	$r = 0.86$	0.00
Pearson_triangle deviations kept	$r = 0.83$	0.00

Figure 3.12 offers a pictorial representation of pre-crosslinked gelatin PDIs and corresponding NP diameters. More homogeneous molecular weight compositions in pre-crosslinked samples (equating to lower PDIs) lead to smaller NPs as determined for both low molecular weight (SB75) and higher molecular weight (VB275) gelatin. Heterogeneous molecular weight compositions in pre-crosslinked samples (equating to higher PDIs) lead to larger NPs (VB85, SB225, SA300, and VA300). Gelatin sample heterogeneity might consist of various gelatin molecular weights, non-gelatin proteins or leftover collagen, which can all be crosslinked into the overall NP via glutaraldehyde.

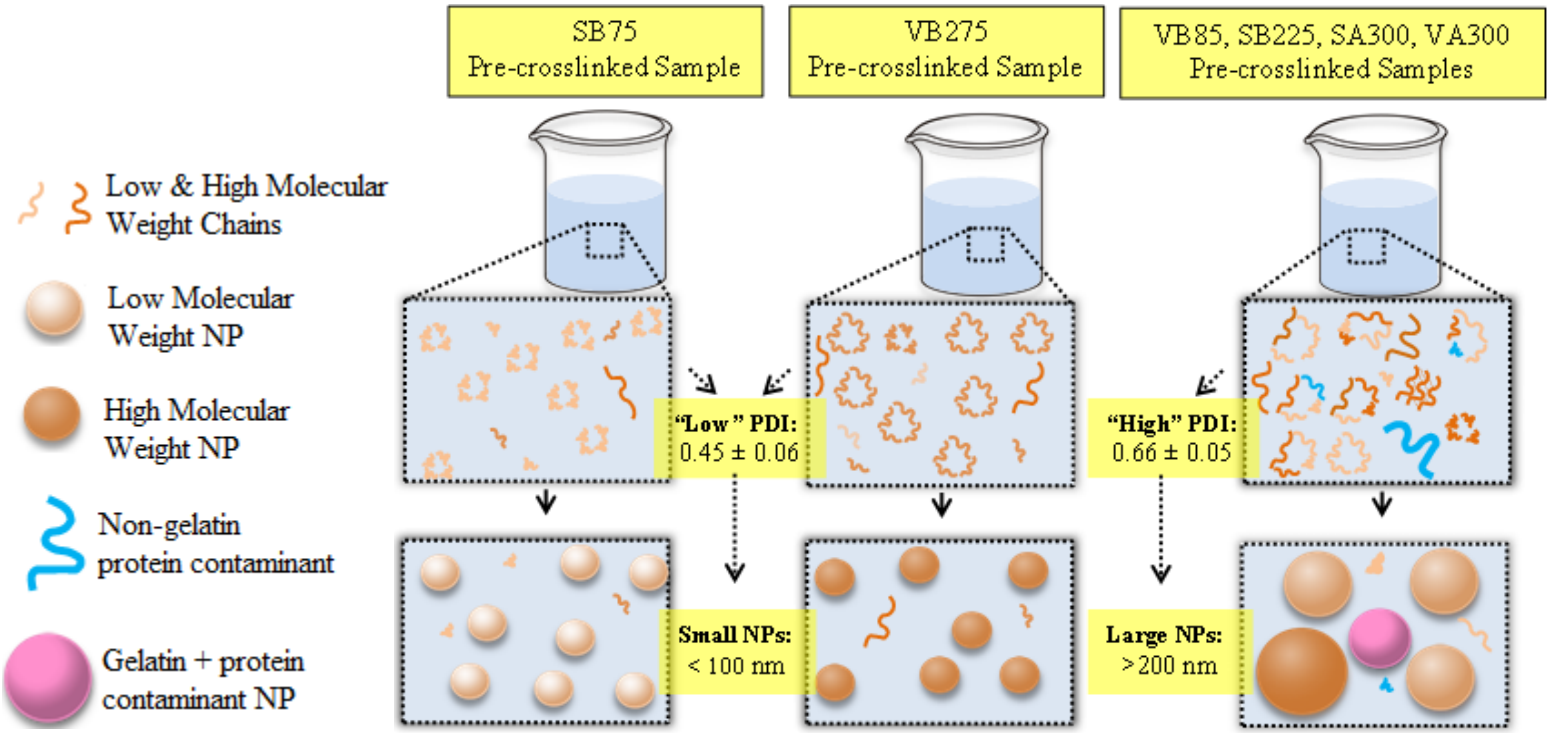

Figure 3.12. Pictorial representation of pre-crosslinked gelatin samples and NP diameters. More homogeneous samples have lower pre-crosslinked PDIs and smaller NP diameters. Our results suggest a critical pre-crosslinked PDI threshold exists corresponding to NPs either <100 nm or >200 nm. Four molecular weight chains shown for simplicity.

In literature, similar gelatin blooms have shown to have very different molecular weights and viscosities, with Phillips and Williams concluding no good correlation exists between 1) gelatin bloom and average molecular weight and 2) gelatin bloom and molecular weight distribution.[66] One relatively recent study by Eysturskard *et al.* determined positive and negative linear relationships exist between gelatin and its mechanical properties based on low and high molecular weight content.[67] The work presented in this dissertation is the first to determine that sample dispersity has an important role in the ability to replicate NP diameters and produce sub-100 nm particles from low and high bloom gelatin.

3.5 Conclusions

The implementation of a materials science characterization approach provided in-depth analysis of gelatin macroscale and NP physicochemical properties. Characterization revealed significantly lower clarity measurements between similar gelatin bloom strengths (except for SA300 and VA300), possibly from non-gelatin contaminants, leading to greater Đ via size exclusion chromatography. Furthermore, this research is the first to show that gelatin macroscale pre-crosslinked dispersity is very strongly correlated to NP diameter, so future studies should resist framing correlation studies by gelatin type and bloom strength without characterizing sample dispersity (indirectly from clarity measurements and directly using size exclusion chromatography, for example). Interestingly, low bloom strength (SB75) and high bloom strength (VB275) gelatin produced consistent sub-100 nm particles revealing a particular pre-crosslinked PDI threshold exists. Similar average rank measurements of pre-cross-linked PDIs produced statistically similar NP diameters, which was independent of gelatin bloom strength and type. The sample dispersity suggests a mechanism to determine if diameters might be over or under the 200 nm threshold for nanomedicine relevancy.[68-69]

In an effort to reduce gelatin heterogeneity, Pouradier and Vent developed a fractionation approach where alcohol separates gelatin fractions as a coacervate (second liquid phase) which can be removed from the bulk liquid.[55] Additionally, monodisperse gelatin has been described by mild heating of citrate-extracted ichthyocol solutions resulting in the breakdown of long thin collagen protofibrils.[55] Methods that can be applied specifically in NP synthesis include 1) adding

in another desolvation step after the first precipitation has occurred (prior to dropwise acetone) and 2) reducing the amount of time acetone is left to incubate with the gelatin. The experimental process here left the first acetone addition in gelatin for 24 h. Based on molecular weight heterogeneity, reducing the time might prevent higher molecular weight fractions from precipitating.

The fundamental characterizations outlined are likely applicable to other biopolymers that can form NPs via desolvation,[70-72] along with synthetic polymers with high molecular weight distributions.[73] Properly characterizing and identifying correlations between macroscale and nanoscale properties offers a new approach to potentially reduce polymer NP physicochemical inconsistencies, allowing for smoother translations into the manufacturing of new formulations.[74]

References

1. Nel, A. E.; Madler, L.; Velegol, D.; Xia, T.; Hoek, E. M. V.; Somasundaran, P.; Klaessig, F.; Castranova, V.; Thompson, M., Understanding biophysicochemical interactions at the nano-bio interface. *Nat Mater* **2009,** *8* (7), 543-557.
2. Patil, G. V., Biopolymer albumin for diagnosis and in drug delivery. *Drug Development Research* **2003,** *58* (3), 219-247.
3. Mohan, S.; Oluwafemi, O.; Kalarikkal, N.; Thomas, S.; Songca, S., *Biopolymers – Application in Nanoscience and Nanotechnology*. 2016.
4. Nitta, S. K.; Numata, K., Biopolymer-Based Nanoparticles for Drug/Gene Delivery and Tissue Engineering. *International Journal of Molecular Sciences* **2013,** *14* (1), 1629-1654.
5. Faridi Esfanjani, A.; Mahdi Jafari, S., *Biopolymer Nano-particles and Natural Nano-carriers for Nano-encapsulation of Phenolic Compounds*. 2016; Vol. 146.
6. Soest, J. J. G. v., The Development of Biopolymer-Based Nanostructured Materials: Plastics, Gels, IPNs, and Nanofoams. In *Feedstocks for the Future*, American Chemical Society: 2006; Vol. 921, pp 288-303.
7. Li, X.; Li, M.; Liu, J.; Ji, N.; Liang, C.; Sun, Q.; Xiong, L., Preparation of Hollow Biopolymer Nanospheres Employing Starch Nanoparticle Templates for Enhancement of Phenolic Acid Antioxidant Activities. *Journal of Agricultural and Food Chemistry* **2017,** *65* (19), 3868-3882.
8. Mary, S. K.; Pothan, L. A.; Thomas, S., Applications of Starch Nanoparticles and Starch-Based Bionanocomposites. In *Biopolymer Nanocomposites*, John Wiley & Sons, Inc.: 2013; pp 293-308.
9. Qian, J., Hollow Micro-/Nano-Particles from Biopolymers: Fabrication and Applications. In *Lightweight Materials from Biopolymers and Biofibers*, American Chemical Society: 2014; Vol. 1175, pp 257-287.
10. Bao, Y.; Wang, R.; Lu, Y.; Wu, W., Lignin biopolymer based triboelectric nanogenerators. *APL Materials* **2017,** *5* (7), 074109.
11. Gómez-Guillén, M. C.; Giménez, B.; López-Caballero, M. E.; Montero, M. P., Functional and bioactive properties of collagen and gelatin from alternative sources: A review. *Food Hydrocolloids* **2011,** *25* (8), 1813-1827.
12. Schrieber, R.; Gareis, H., From Collagen to Gelatine. In *Gelatine Handbook*, Wiley-VCH Verlag GmbH & Co. KGaA: 2007; pp 45-117.
13. Advanced Polymers in Medicine

Puoci, F., Ed. Springer: Switzerland, 2015.
14. Leuenberger, B. H., Investigation of viscosity and gelation properties of different mammalian and fish gelatins. *Food Hydrocolloids* **1991,** *5* (4), 353-361.
15. von Hippel, P. H., The Macromolecular Chemistry of Gelatin. *Journal of the American Chemical Society* **1965,** *87* (8), 1824-1824.
16. (GMIA), G. M. I. o. A., Gelatin Handbook. 2012; pp 1-25.
17. Ehrlich, H., Marine Gelatins. In *Biological Materials of Marine Origin: Vertebrates*, Springer Netherlands: Dordrecht, 2015; pp 343-359.
18. Jones, O. G.; McClements, D. J., Functional Biopolymer Particles: Design, Fabrication, and Applications. *Comprehensive Reviews in Food Science and Food Safety* **2010,** *9* (4), 374-397.
19. Husain, M.; Khan, Z. H., *Advances in nanomaterials*. Springer: India, 2016.
20. Hu, B.; Huang, Q.-r., Biopolymer based nano-delivery systems for enhancing bioavailability of nutraceuticals. *Chinese Journal of Polymer Science* **2013,** *31* (9), 1190-1203.
21. Coester, C. J.; Langer, K.; van Briesen, H.; Kreuter, J., Gelatin nanoparticles by two step desolvation--a new preparation method, surface modifications and cell uptake. *Journal of microencapsulation* **2000,** *17* (2), 187-93.
22. Azarmi, S.; Huang, Y.; Chen, H.; McQuarrie, S.; Abrams, D.; Roa, W.; Finlay, W. H.; Miller, G. G.; Lobenberg, R., Optimization of a two-step desolvation method for preparing gelatin nanoparticles and

cell uptake studies in 143B osteosarcoma cancer cells. *Journal of pharmacy & pharmaceutical sciences : a publication of the Canadian Society for Pharmaceutical Sciences, Societe canadienne des sciences pharmaceutiques* **2006,** *9* (1), 124-32.
23. Saxena, A.; Sachin, K.; Bohidar, H. B.; Verma, A. K., Effect of molecular weight heterogeneity on drug encapsulation efficiency of gelatin nano-particles. *Colloids and Surfaces B: Biointerfaces* **2005,** *45* (1), 42-48.
24. Khanbabaie, R.; Jahanshahi, M., Revolutionary Impact of Nanodrug Delivery on Neuroscience. *Current Neuropharmacology* **2012,** *10* (4), 370-392.
25. Blanco, E.; Shen, H.; Ferrari, M., Principles of nanoparticle design for overcoming biological barriers to drug delivery. *Nature biotechnology* **2015,** *33* (9), 941-51.
26. Geh, K. J.; Hubert, M.; Winter, G., Optimisation of one-step desolvation and scale-up of gelatine nanoparticle production. *Journal of microencapsulation* **2016,** *33* (7), 595-604.
27. Duconseille, A.; Astruc, T.; Quintana, N.; Meersman, F.; Sante-Lhoutellier, V., Gelatin structure and composition linked to hard capsule dissolution: A review. *Food Hydrocolloids* **2015,** *43*, 360-376.
28. Won, Y. W.; Kim, Y. H., Recombinant human gelatin nanoparticles as a protein drug carrier. *J Control Release* **2008,** *127* (2), 154-61.
29. Tronci, G.; Russell, S. J.; Wood, D. J., Photo-active collagen systems with controlled triple helix architecture. *Journal of Materials Chemistry B* **2013,** *1* (30), 3705-3715.
30. Nishio, T.; Hayashi, R., Regeneration of a Collagen-like Circular Dichroism Spectrum from Industrial Gelatin. *Agricultural and Biological Chemistry* **1985,** *49* (6), 1675-1682.
31. Wüstneck, R.; Wetzel, R.; Buder, E.; Hermel, H., The modification of the triple helical structure of gelatin in aqueous solution I. The influence of anionic surfactants, pH-value, and temperature. *Colloid and Polymer Science* **1988,** *266* (11), 1061-1067.
32. Standard Testing Methods for Edible Gelatin: Official Procedure of the Gelatin Manufacturers Institute of America, Inc. GMIA: Revised July 2013.
33. ANALYSIS OF POLYMERS BY GPC/SEC PHARMACEUTICAL APPLICATIONS. Technologies, A., Ed. 2015.
34. Boedtker, H.; Doty, P., A Study of Gelatin Molecules, Aggregates and Gels. *The Journal of Physical Chemistry* **1954,** *58* (11), 968-983.
35. Tumolo, T.; Angnes, L.; Baptista, M. S., Determination of the refractive index increment (dn/dc) of molecule and macromolecule solutions by surface plasmon resonance. *Analytical Biochemistry* **2004,** *333* (2), 273-279.
36. Erickson, H. P., Size and shape of protein molecules at the nanometer level determined by sedimentation, gel filtration, and electron microscopy. *Biological procedures online* **2009,** *11*, 32-51.
37. Wang, H.; Hansen, M. B.; Löwik, D. W. P. M.; van Hest, J. C. M.; Li, Y.; Jansen, J. A.; Leeuwenburgh, S. C. G., Oppositely Charged Gelatin Nanospheres as Building Blocks for Injectable and Biodegradable Gels. *Advanced Materials* **2011,** *23* (12), H119-H124.
38. Azimi, B.; Nourpanah, P.; Rabiee, M.; Arbab, S., Producing gelatin nanoparticles as delivery system for bovine serum albumin. *Iranian biomedical journal* **2014,** *18* (1), 34-40.
39. Shutava, T. G.; Balkundi, S. S.; Vangala, P.; Steffan, J. J.; Bigelow, R. L.; Cardelli, J. A.; O'Neal, D. P.; Lvov, Y. M., Layer-by-Layer-Coated Gelatin Nanoparticles as a Vehicle for Delivery of Natural Polyphenols. *ACS Nano* **2009,** *3* (7), 1877-85.
40. Elzoghby, A. O., Gelatin-based nanoparticles as drug and gene delivery systems: Reviewing three decades of research. *Journal of Controlled Release* **2013,** *172* (3), 1075-1091.
41. Pearson, C. H.; Gibson, G. J., Proteoglycans of bovine periodontal ligament and skin. Occurrence of different hybrid-sulphated galactosaminoglycans in distinct proteoglycans. *The Biochemical journal* **1982,** *201* (1), 27-37.
42. Kanjee, U.; Houry, W. A., An Assay for Measuring the Activity of Escherichia coli Inducible Lysine Decarboxyase. *Journal of Visualized Experiments : JoVE* **2010,** (46), 2094.
43. Djabourov, M.; Leblond, J.; Papon, P., Gelation of aqueous gelatin solutions. I. Structural investigation. *J. Phys. France* **1988,** *49* (2), 319-332.

44. Pelc, D.; Marion, S.; Pozek, M.; Basletic, M., Role of microscopic phase separation in gelation of aqueous gelatin solutions. *Soft Matter* **2014,** *10* (2), 348-356.
45. Saha D, B. S., Hydrocolloids as thickening and gelling agents in food: a critical review. *Journal of Food Science and Technology* **2010,** *47* (6), 587-597.
46. Farrugia, C. A.; Farrugia, I. V.; Groves, M. J., Comparison of the Molecular Weight Distribution of Gelatin Fractions by Size-exclusion Chromatography and Light Scattering. *Pharmacy and Pharmacology Communications* **1998,** *4* (12), 559-562.
47. Meyerhofer, D., Holographic Recording Materials

1ed.; Smith, H. M., Ed. Springer-Verlag: Berlin Heidelberg, 1977; Vol. 20.
48. Ramamourthy Gopal, J. S. P., Chang Ho Seo,Yoonkyung Park, Applications of Circular Dichroism for Structural Analysis of Gelatin and Antimicrobial Peptides. *International Journal of Molecular Sciences* **2012,** *13*.
49. Ahsan, S. M.; Rao, C. M., Structural studies on aqueous gelatin solutions: Implications in designing a thermo-responsive nanoparticulate formulation. *Int J Biol Macromol* **2016**.
50. Rawat, K.; Pathak, J.; Bohidar, H. B., Effect of persistence length on binding of DNA to polyions and overcharging of their intermolecular complexes in aqueous and in 1-methyl-3-octyl imidazolium chloride ionic liquid solutions. *Physical Chemistry Chemical Physics* **2013,** *15* (29), 12262-12273.
51. Jobling, A., Inedible meat by-products. Advances in meat research, vol. 8. Edited by A. M. Pearson and T. R. Dutson. Elsevier Science Publishers, London, 1992. pp. xx + 416, price UK£105.00. ISBN 1-85166-767-9. *Polymer International* **1994,** *33* (1), 117-117.
52. Avena-Bustillos, R. J.; Olsen, C. W.; Olson, D. A.; Chiou, B.; Yee, E.; Bechtel, P. J.; McHugh, T. H., Water Vapor Permeability of Mammalian and Fish Gelatin Films. *Journal of Food Science* **2006,** *71* (4), E202-E207.
53. Cole, C. G. B.; Roberts, J. J., Gelatine colour measurement. *Meat Science* **1997,** *45* (1), 23-31.
54. Eastoe, J. E., and Leach, A. A, Chemical constitution of gelatin. Academic Press: London, 1977.
55. Idson, B.; Braswell, E., Gelatin. *Advances in Food Research* **1957,** *7*, 235-338.
56. Meng, Y.; Cloutier, S., Chapter 20 - Gelatin and Other Proteins for Microencapsulation. In *Microencapsulation in the Food Industry*, Academic Press: San Diego, 2014; pp 227-239.
57. Olijve, J.; Mori, F.; Toda, Y., Influence of the Molecular-Weight Distribution of Gelatin on Emulsion Stability. *Journal of Colloid and Interface Science* **2001,** *243* (2), 476-482.
58. Pharmaceutical capsules. 2nd ed.; Podczeck, F.; Jones, B. E., Eds. Pharmaceutical Press: London 2004; p. 272.
59. Díaz-Calderón, P.; Caballero, L.; Melo, F.; Enrione, J., Molecular configuration of gelatin–water suspensions at low concentration. *Food Hydrocolloids* **2014,** *39* (Supplement C), 171-179.
60. Corder, G. W.; Foreman, D. I., Comparing More than Two Unrelated Samples: The Kruskal–Wallis H-Test. In *Nonparametric Statistics for Non-Statisticians*, John Wiley & Sons, Inc.: 2009; pp 99-121.
61. Day, R. W.; Quinn, G. P., Comparisons of Treatments After an Analysis of Variance in Ecology. *Ecological Monographs* **1989,** *59* (4), 433-463.
62. Blanca, M. J.; Alarcon, R.; Arnau, J.; Bono, R.; Bendayan, R., Non-normal data: Is ANOVA still a valid option? *Psicothema* **2017,** *29* (4), 552-557.
63. Santiago, E., What Should I Do If My Data is Not Normal. In *The Minitab Blog*, Minitab: 2015; Vol. 2018.
64. McDonald, J. H., *Handbook of Biological Statistics*. Sparky House Publishing: Baltimore.
65. Hinkle, D. E.; Wiersma, W.; Jurs, S. G., Applied statistics for the behavioral sciences. 5th ed. ed.; Houghton Mifflin ;[Hi Marketing] (distributor): Boston, Mass. [London] :, 2003. HathiTrust Digital Library, Limited view (search only) http://catalog.hathitrust.org/api/volumes/oclc/50716608.html.
66. Haug, I. J.; Draget, K. I., 5 - Gelatin. In *Handbook of Food Proteins*, Woodhead Publishing: 2011; pp 92-115.

67. Eysturskarð, J.; Haug, I. J.; Ulset, A.-S.; Joensen, H.; Draget, K. I., Mechanical Properties of Mammalian and Fish Gelatins as a Function of the Contents of α-Chain, β-Chain, and Low and High Molecular Weight Fractions. *Food Biophysics* **2010,** *5* (1), 9-16.
68. Petros, R. A.; DeSimone, J. M., Strategies in the design of nanoparticles for therapeutic applications. *Nature reviews. Drug discovery* **2010,** *9* (8), 615-27.
69. Desai, N., Challenges in Development of Nanoparticle-Based Therapeutics. *The AAPS Journal* **2012,** *14* (2), 282-295.
70. Grenha, A., Chitosan nanoparticles: a survey of preparation methods. *Journal of Drug Targeting* **2012,** *20* (4), 291-300.
71. Mukherji, G.; Murthy, R. S. R.; Miglani, B. D., Preparation and evaluation of cellulose nanospheres containing 5-fluorouracil. *International Journal of Pharmaceutics* **1990,** *65* (1), 1-5.
72. Yu, Z.; Yu, M.; Zhang, Z.; Hong, G.; Xiong, Q., Bovine serum albumin nanoparticles as controlled release carrier for local drug delivery to the inner ear. *Nanoscale Research Letters* **2014,** *9* (1), 343-343.
73. Nandagiri, V.; Chiono, V.; Gentile, P.; Montevecchi, F.; Ciardelli, G., Biomaterials of Natural Origin in Regenerative Medicine. In *Polymeric Biomaterials*, CRC Press: 2013; pp 271-308.
74. Logothetidis, S., Nanotechnology: Principles and Applications. In *Nanostructured Materials and Their Applications*, Logothetidis, S., Ed. Springer Berlin Heidelberg: Berlin, Heidelberg, 2012; pp 1-22.

Chapter 4

Filtration Initiated Selective Homogeneity (FISH) Desolvation: a new method to prepare gelatin nanoparticles with high physicochemical consistency

This chapter contains sections under peer review in Food Hydrocolloids

Abstract

Biopolymer nanoparticles (NPs) have garnered much interest in the food industry as encapsulating materials for flavors, nutraceuticals and other bioactive compounds. The ability to control and reproduce NP physicochemical properties is a crucial step in the utilization of nanoscale formulations for food based and sustainable packaging applications. Conventional preparations of gelatin NPs involve a range of solution based methods with inconsistent nanoscale properties. Integrating a filtration step prior to gelatin NP formation obtained highly consistent physicochemical properties between two different gelatin types. The average diameter of the entire population was 143 ± 12 nm with a low polydispersity index of 0.07 ± 0.03. Volume distributions revealed a single peak confirming the existence of one NP composition. Gelatin NPs obtained high chemical crosslinking extents (≥ 87%) with synonymous chemical bonding determined via FTIR. Rhodamine 110 fluorescent agent incorporation maintained consistent diameters (~140 nm) with significantly higher fluorescence measurements compared to empty particles. The results indicate that greater control and reproducibility of gelatin nanoscale properties is highly dependent on gelatin molecular weight homogeneity prior to NP synthesis. The production of consistent NP properties is anticipated to propel the translation of gelatin NPs as bioactive encapsulators in food and sustainable packaging applications.

4.1 Introduction

Biologically derived proteins (such as gelatin, albumin and hyaluronic acid) and polysaccharides (such as chitosan, cellulose and starch) are increasingly attractive biopolymers for nanotechnology applications in food based products. Their inherent degradability and low immunogenicity [1] have been explored as nanoparticles (NPs) by researchers to encapsulate, protect and release a variety of food based bioactive compounds.[2] These compounds include colorants, flavors and nutraceuticals for human and animal consumption,[2] and odor eliminators in sustainable packaging. Furthermore, NPs that are negatively charged and / or less than 200 nm more readily overcome biological barriers, such as 1) the mucous membrane in the gastrointestinal tract, or 2) untimely removal by the spleen. [3-4] Thus, these physicochemical properties substantially increase the bioavailability of encapsulated nutraceuticals to potentially inhibit chronic diseases and improve human performance.[2]

Gelatin, a protein obtained from collagen hydrolysis, is one particularly unique hydrocolloid as its gel forming ability already proves valuable in a wide range of food industry products.[5] Its established use and Generally recognized as safe (GRAS) certification by the Food and Drug Administration has prompted the development of numerous gelatin NP preparation techniques.[6] Decades of research has obtained two step desolvation as the most common NP preparation method due to its relatively straightforward synthesis.[7-8] The use of a desolvation agent to remove low molecular weight fractions, allows the remaining high molecular weight precipitate to form ~100 to 300 nm particles after chemical crosslinking.[6, 9] Experimental modifications to pH, crosslinker concentration and desolvation agent are routinely employed to obtain desirable NP sizes (typically less than 200 nm), charges (higher charges indicate greater NP stability) and chemical bonding.[6, 10] Chapter 3 reported that molecular weight dispersity is significantly correlated to gelatin NP diameter in particular, so NP preparation adjustments are batch to batch dependent given gelatin's large molecular weight heterogeneities. While gelatin NP translation to human food products is probable given their use to treat diseases in canines[11] and horses,[12] their use is impeded as numerous experimental factors impart significant variability in NP preparation and efficacy. [7, 13] Altogether these findings highlight that improved methods to obtain consistent NP physicochemical properties are needed.

Chapter 4 describes a vacuum filtration method to prepare gelatin NPs with high consistency, known as filtration initiated selective homogeneity (FISH) desolvation. Instead of relying upon various chemical methods to control NP properties, FISH physically acts upon gelatin itself to reduce molecular weight heterogeneity. As a result, gelatin chains with more similar molecular weight aggregate during the preparation process and undergo chemical stabilization. FISH desolvation is proven using two different gelatins that had the highest molecular weight dispersities and largest NP diameters (~220-350 nm) shown in Chapter 3. The ease of FISH desolvation along with its production of consistent NP properties may propel the translation of gelatin NPs as bioactive encapsulators in food and sustainable packaging applications.

4.2 Experimental Section

4.2.1 Materials

Vyse Type A (porcine derived) 300 bloom strength gelatin, referred here as VA300, was obtained from Vyse Gelatin Company (Schiller Park, IL). Sigma Aldrich Type B (bovine derived) 225 bloom strength gelatin, referred here as SB225, was obtained from Sigma Aldrich (St. Louis, MO). Filter papers (Whatman grade 50 cellulose filter paper with a 2.7 µm nominal particle retention along with nylon membrane 1.0 µm pore size) were purchased from GE Healthcare Life Sciences (Little Chalfont, United Kingdom). Rhodamine 110, glutaraldehyde (25%), acetone, PBS (with Ca, Mg) and trinitrobenzenesulfonic acid (TNBS) assay solution (4%) were obtained from Fisher Scientific or Sigma Aldrich. Carbon gold coated 200 mesh TEM grids were obtained from Electron Microscopy Sciences (Hatfield, PA).

4.3 Methods

4.3.1 Preparation of NPs

Gelatin (0.7 g) was added to distilled water (25 mL) with heating (~ 40°C) and stirring (600 rpm, 12.7 mm x 3 mm stir bar) until dissolved (~ 20 minutes). After briefly wetting the respective filter paper and placing inside a Büchner funnel, the entire gelatin solution was vacuum filtered. Additional distilled water (17 mL) was added to the filtrate with heating and stirring as previously described. The pH was lowered to 2.5 (1M HCl), dropwise acetone added until the Tyndall effect was visualized (~90 mL, 3 mL/min) followed by glutaraldehyde (250 µL of 25%). After crosslinking (24 h, room temperature), solutions were rotovapped, centrifuged (7 mL, 100,000 x

g, 15 min) and dispersed in phosphate buffered saline (PBS). Each gelatin type was prepared into NPs twice per filter paper. For encapsulation, rhodamine 110 (1 mM, 500 µL) was added to cellulose filtered gelatin solutions after pH adjustment. Purification was performed as described above.

4.4 Characterization

4.4.1 Imaging of Filter Paper

Filter papers were imaged optically (Olympus IX7, Tokyo, Japan) and with a JCM 5000 NeosScope^{TM} table top SEM (JEOL, Tokyo, Japan).

4.4.2 Dynamic Light Scattering (DLS) and Transmission Electron Microscopy (TEM)

Gelatin NP Z-Average mean (diameter), polydispersity indices (PDIs), volume distributions and charges were carried out using a Malvern ZetaSizer Nano ZS90 (λ = 633 nm, protein analysis method) after 10x dilution. At least five total measurements were obtained ($n \geq 5$). Practical significance was calculated via an effect size estimate. NP morphology was assessed using a JEOL JEM-1400 TEM (JEOL Ltd., Tokyo, Japan) previously described in Chapter 3.

4.4.3 Fourier Transform Infrared Spectroscopy (FTIR)

FTIR measurements of PBS dispersed NPs were carried out using a Nicolet iS5 with iD7 ATR (Thermo Fisher Scientific, Waltham, MA) and 32 scans.

4.4.4 Crosslinking (%)

NP solution absorbance measurements were analyzed using a microplate reader (BioTek Multi-Mode, Winooski, VT) to calculate crosslinking extent previously described in Chapter 3. Briefly, a calibration curve using gelatin concentrations was first produced to quantify the free moles of lysine. Next, NPs in PBS (0.494 g) were added to TNBS and $NaHCO_3$, reacted for 2 h at ~ 40 °C, centrifuged (100,000 x g, 30 min) to remove the NP pellet and absorbance measured at 349 nm. Three measurements were obtained (n = 3).

4.4.5. Encapsulation Efficiency (%) and NP Fluorescence

Encapsulation efficiency was calculated[14] from a rhodamine 110 (Rho) calibration curve ($R^2 \geq 0.99$) after measuring supernatant fluorescence (Excitation: 475 nm, Emission: 520, Sensitivity setting: 50). NP fluorescence (- Rho, + Rho) was measured after centrifugation and dispersion in water. Two-sample t-tests were used to determine significant differences in NP fluorescence measurements with a 99% confidence interval in Minitab 18. Three measurements were obtained (n = 3).

4.5 Results and Discussion

4.5.1 FISH Desolvation Process Compared to Two-step Desolvation

Shown in Figure 4.1, FISH essentially substitutes the first desolvation step, where gelatin is precipitated typically in acetone, for vacuum filtration to physically reduce molecular weight chain dispersity. Extensive reading of the scientific literature revealed a profound lack of specificity regarding the first desolvation step, such as length of time for appropriate precipitation, amount of organic solvent added, and method of decanting. As a result, the first desolvation step is a likely contributor to the lack of reproducibility which has been noted as one shortcoming for two-step desolvation.[7] Vacuum filtration also significantly reduces gelatin NP preparation times by 24 h since gelatin induced precipitation using an organic solvent is not required.

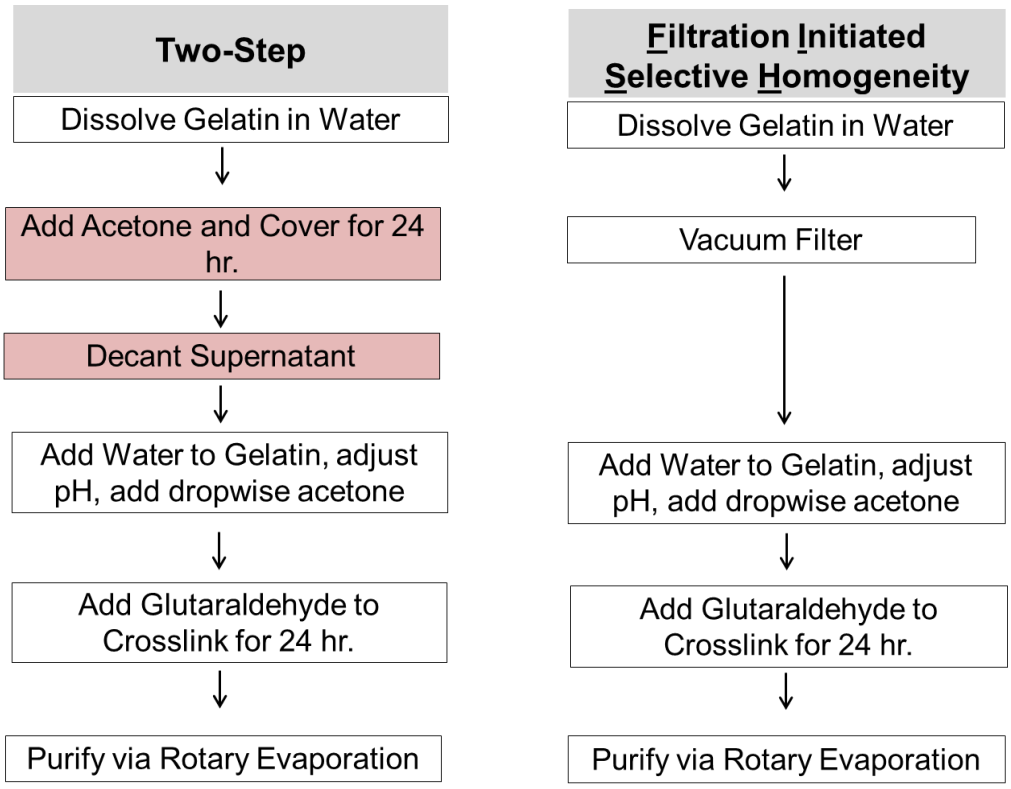

Figure 4.1. Two-Step vs FISH Desolvation schematic comparison. Red highlight indicates the experimental steps removed using FISH.

4.5.2 Filter Paper Morphology and FISH Desolvation

Two distinct types of Whatman filter paper (hardened cellulose with 2.7 µm pore size and nylon with 1 µm pore size) were used to determine the role of polymer type, morphology, and pore size on gelatin filtration efficiency. These distinct types of filters were utilized as both were developed to maintain integrity when wet and are compatible for Büchner funnel separation of aqueous solutions. Both filter papers had pore sizes inconsistent from their packaging (Figure 4.2). Cellulose filter paper had large gaps between fibers with much smaller pore sizes actually within the fibers themselves (Figure 4.2). Nylon filter paper contained varying, non-interconnected rather large openings (> 2 µm) with smaller pores in the bigger structures (Figure 4.2).

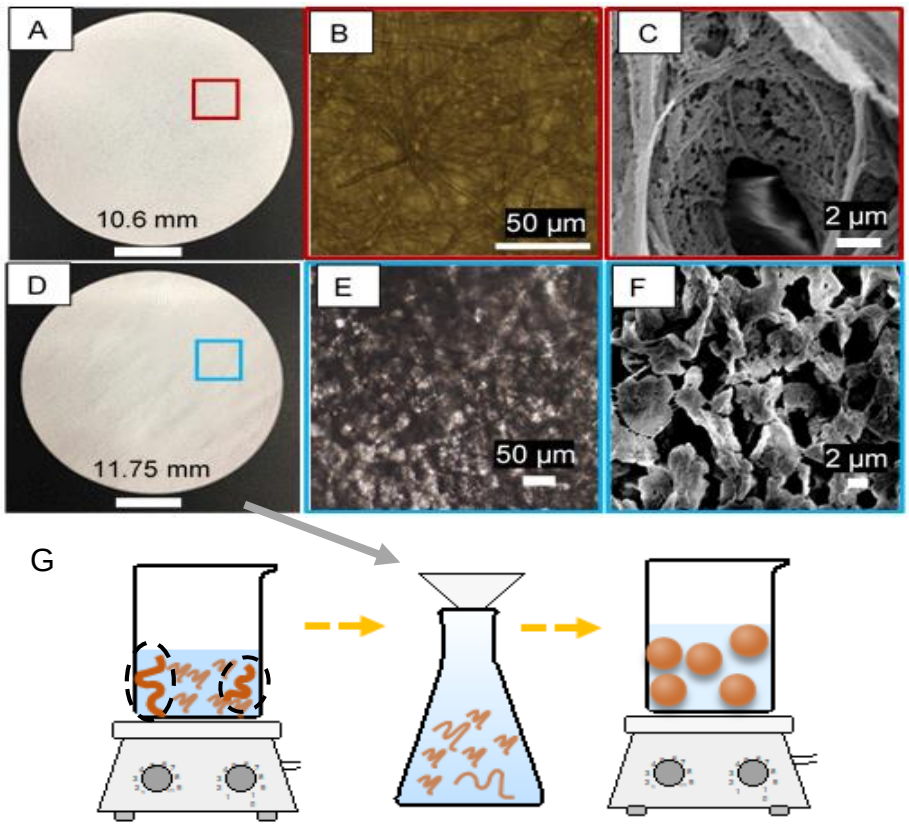

Figure 4.2. Filter paper imaging and FISH desolvation. (A:C) Optical and SEM images of cellulose filter paper. (D:F) Optical and SEM images of nylon filter paper. (G) Schematic of FISH desolvation process. Gelatin is dissolved and vacuum filtered removing chains larger than pore sizes (identified by dashed black ovals) prior to NP synthesis.

FISH desolvation is shown in Figure 4.2G and is based on decreasing molecular weight heterogeneity by removing gelatin chain lengths larger than the filter pore size. Theoretical calculations determining the molecular weight cutoff is shown below in Figure 4.3 based on gelatin contour length (L_c)[15] and degree of polymerization calculated from size exclusion chromatography (Chapter 3, Table 3.3). Assuming the largest pore size is 2.7 µm for the cellulose filter paper and 1 µm for nylon, cellulose has a ~172,000 Da molecular weight cutoff, while nylon filter has a ~63,000 molecular weight cutoff (Table 4.1).

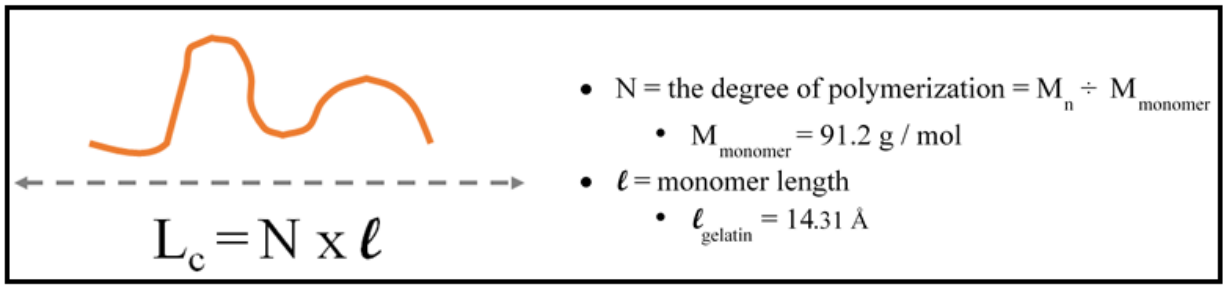

Figure 4.3. Gelatin contour length. The contour length, L_c, is the length of a fully extended gelatin chain[15] obtained from the degree of polymerization and monomer length.

Table 4.1. Theoretical molecular weight cutoff of gelatin based on company stated pore size

Sample	$b_{gelatin}$ (Å)	$L_{c\_Cellulose}$ (Å)	N	M_n (Da)$_{Cellulose\ cutoff}$	L_{c_Nylon} (Å)	N	M_n (Da)$_{Nylon\ cutoff}$
Gelatin	14.31	27000.0	1886.8	172075.5	10000.0	698.8	63731.7

4.5.3 NP Physicochemical Properties

4.5.3.1 Size, Charge, Chemical Bonding, Crosslinking and Encapsulation

SB225 particle diameters were at least 55 nm smaller using FISH desolvation compared to two-step desolvation, and FISH prepared VA300 particles were at least 165 nm smaller compared to two-step (Figure 4.4A, 4.4B). Additionally, low PDIs (< 0.2) indicate monodispersed sizes.[16] Importantly, drastic reductions in NP diameter were obtained by acting on the gelatin itself, instead of changing experimental protocols, as typically reported. Altogether, a population average (including both gelatin and filter types) of 168 ± 17 nm indicates high consistency.

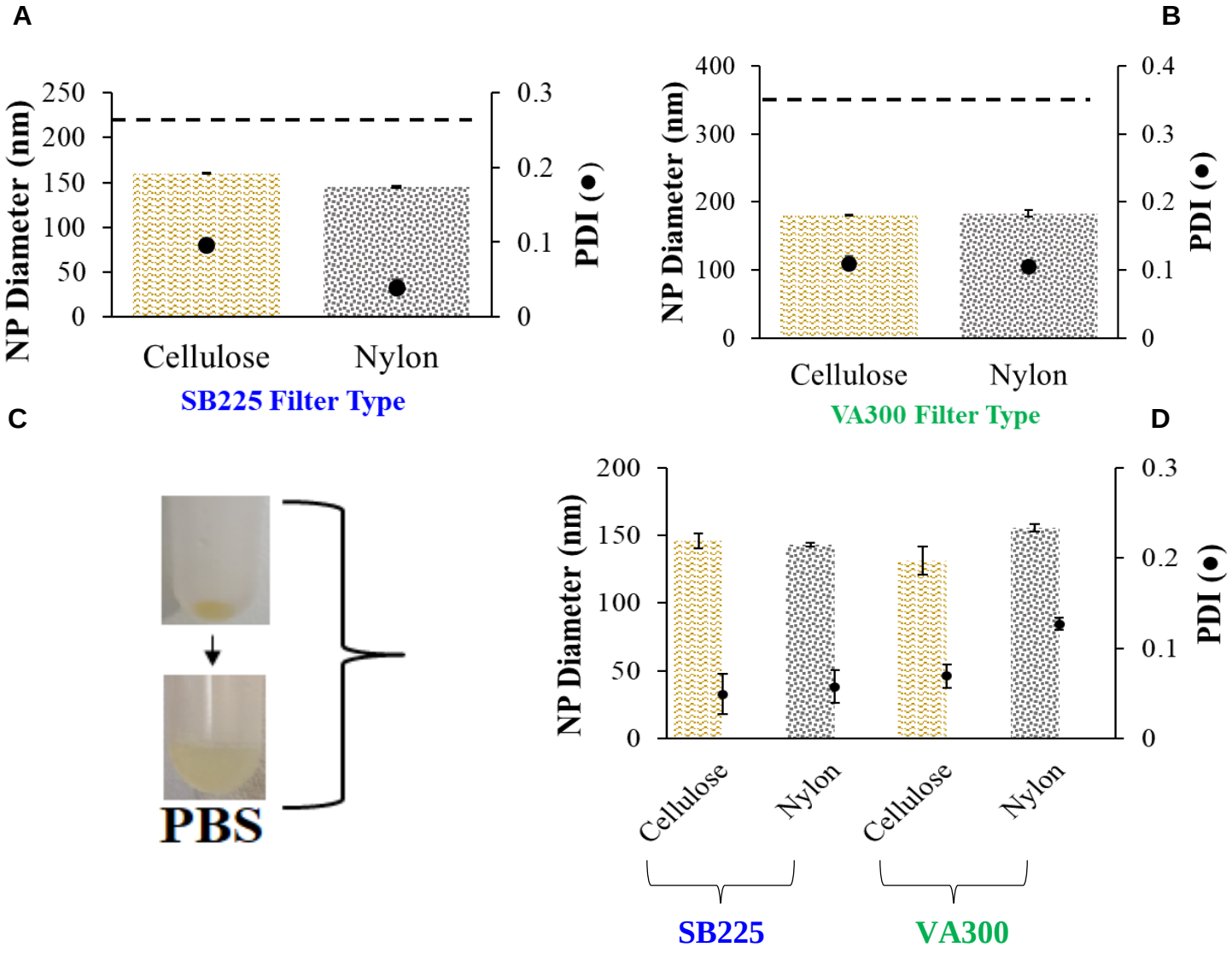

Figure 4.4 FISH desolvation gelatin diameters. (A) Average diameter measurements of SB225 and (B) VA300 gelatin NPs in distilled water (pH ~2.5). Dashed line represents respective gelatin diameters prepared using two-step desolvation reported in Chapter 3. (C) NP dispersion in PBS following centrifugation (D) lead to slight decreases in overall size. Entire data set reveal 143 ± 12 nm diameters and low PDIs (< 0.2). n ≥ 6 total measurements from two separate trials.

NPs were next centrifuged and dispersed in PBS to better mimic food grade preparations using phosphate.[17] While centrifugation causes many polymeric NPs to aggregate and cluster,[18] removal of acetone prior to high speed separation allowed NP dispersion via brief vortex with no visible aggregates in the solution (Figure 4.4C). Similar sizes were confirmed by each sample's low PDI (Figure 4.4D) and the population average PDI was calculated to be 0.07 ± 0.03. Compared to NPs dispersed in water, PBS dispersion actually caused slight size decreases (population average: 143 ± 12 nm) likely due to ionic compaction of gelatin chains reducing their interaction between water.[19] The population size deviation was low (± 12 nm) as was the deviation within respective samples (≤ 10 nm). To statistically compare gelatin means, all SB225 NP diameters were compared to all VA300 NP diameters and revealed an effect size (ES) estimate of 0.21 (see Calculation 4.1). Hence, negligible significance exists between the two group's diameters since ES ~ 0.20.[20]

Calculation 4.1:

Group 1: Average SB225 NP Diameter (cellulose and nylon) = 144.7 ± 4.2 nm
Group 2: Average VA300 NP Diameter (cellulose and nylon) = 142.3 ± 16.2 nm
Average NP Population Diameter (SB225 and VA300): 143 ± 11.6 nm

Effect Size = (Group 1 – Group 2) ÷ (NP Population Diameter Standard Deviation) = 0.207

The PDI values were well below the 0.2 threshold set by the polymer NP community; however, FISH desolvation is a technique that has never been reported before, so additional confirmation of the narrow sample volume distributions was deemed beneficial. Figure 4.5 shows representative plots of each solution with one peak, verifying the sample is a composed of a highly narrow volume of particles. Therefore, both filters are effective at reducing gelatin macroscale heterogeneity. As a result, filtration of NPs after synthesis, a common method to remove unwanted larger NP sizes (and consequently their encapsulated, precious bioactive molecules) [7, 21] is not needed using FISH desolvation. Also, representative TEM images indicate NPs are less than 200 nm with mostly uniform morphology in the dry state (Fig. 4.5E, 4.5F).

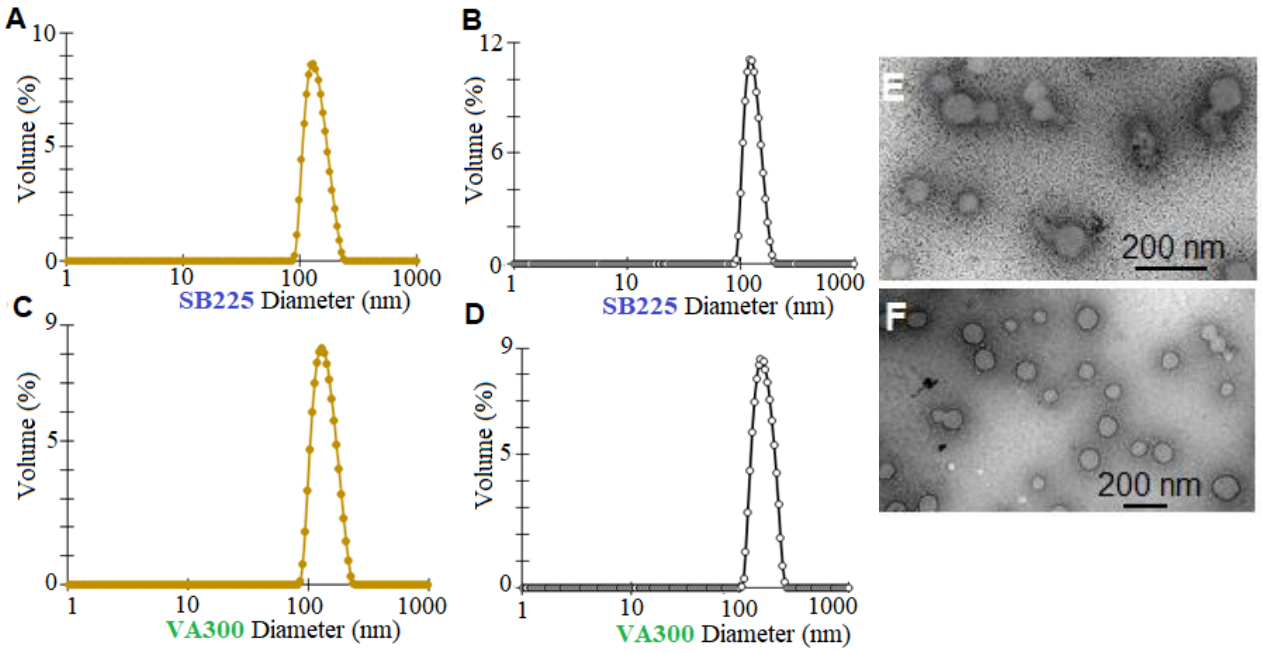

Figure 4.5. Representative volume distributions indicate each sample is composed of only one component slightly greater than 100 nm. FISH desolvation (A,C) cellulose filtered and (B,D) nylon filtered obtained similar volume profiles. (E) TEM images of SB225 NPs and (F) VA300 NPs. Images taken between 120-200 kV.

As previously discussed in the Introduction, charge is an important property for determining appropriate NP function and stability. SB225 NPs have nearly a 2x increase in zeta potential compared to VA300 NPs (Figure 4.6A, 4.6B). Type B gelatin is processed via alkaline hydrolysis where zero net charge might exist between 4.7 to 5.4 pH [22] while Type A gelatin undergoes acidic hydrolysis that can produce zero net charge between 7 to 9 pH environments.[22] The expected difference in charge following NP dispersion in PBS (pH 7.4) confirms each gelatin's functional integrity following manipulation into NPs.

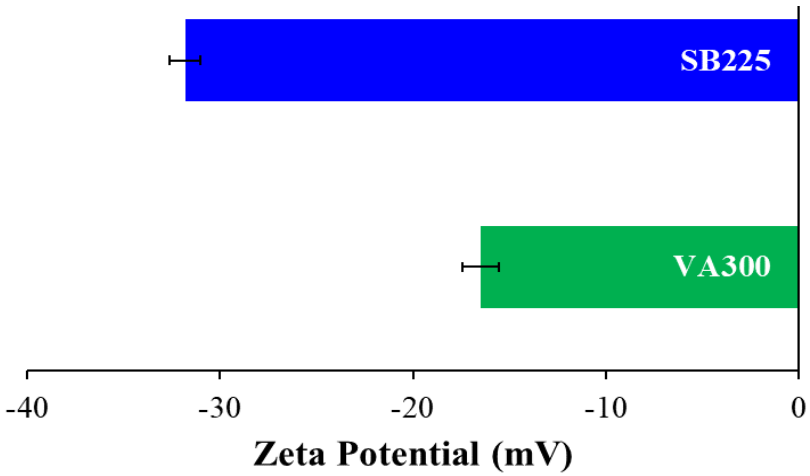

Figure 4.6. NP charge in PBS. (A) SB225 and (B) VA300. n = 5 measurements.

The TNBS assay was used to determine NP crosslinking extent. Uncrosslinked gelatin obtained a linear calibration curve between lysine amine groups and overall absorbance (Figure 4.7A). Higher amounts of free lysine react with TNBS producing darker orange hues. NP reaction with TNBS produced a faint yellow hue (Figure 4.7B) indicating low concentration of free amine groups likely due to glutaraldehyde crosslinking. Similar NP crosslinking extents were estimated for SB225 (91 ± 0.8%) and VA300 (87 ± 0.7%) using the moles of available lysine (Figure 4.8). SB225 and VA300 NPs produced via two-step desolation were only crosslinked between 40 to 62% (Chapter 3, Figure 3.4) indicating FISH desolvation creates more chemically stable NPs. FTIR (Figure 4.9) confirmed analogous chemical structures for the NPs, which corroborate TNBS crosslinking.

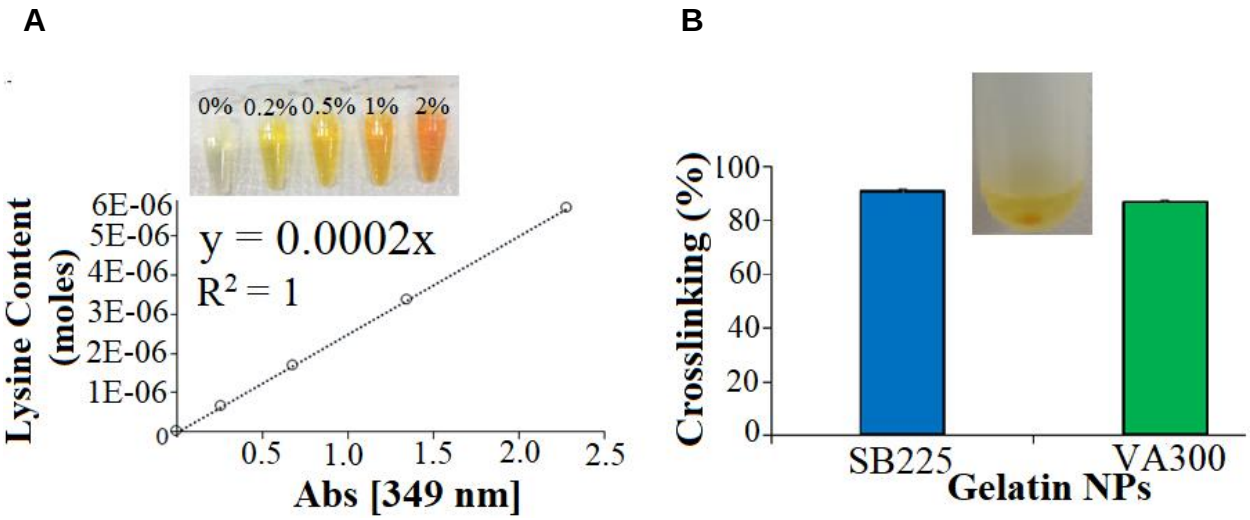

Figure 4.7 Gelatin free amine group detection. (A) TNBS assay calibration curve of uncrosslinked gelatin (0 % to 2 %) revealing linear relationship between lysine mole content and wt. %. (B) High relative crosslinking extent of NPs. Representative picture insert shows TNBS and NP interaction produces a faint yellow hue. Dark yellow feature is centrifuged NP pellet. n =3 measurements.

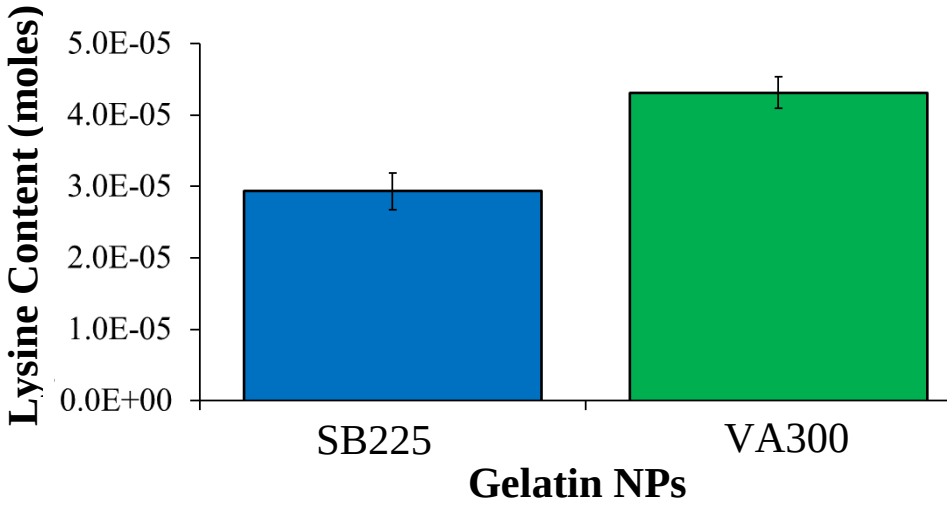

Figure 4.8 Available moles of lysine calculated from TNBS calibration curve of gelatin concentrations. VA300 NPs have ~1.4 more available free lysine than SB225 NPs, so their estimated crosslinking extent is slightly lower (Figure 4.7B).

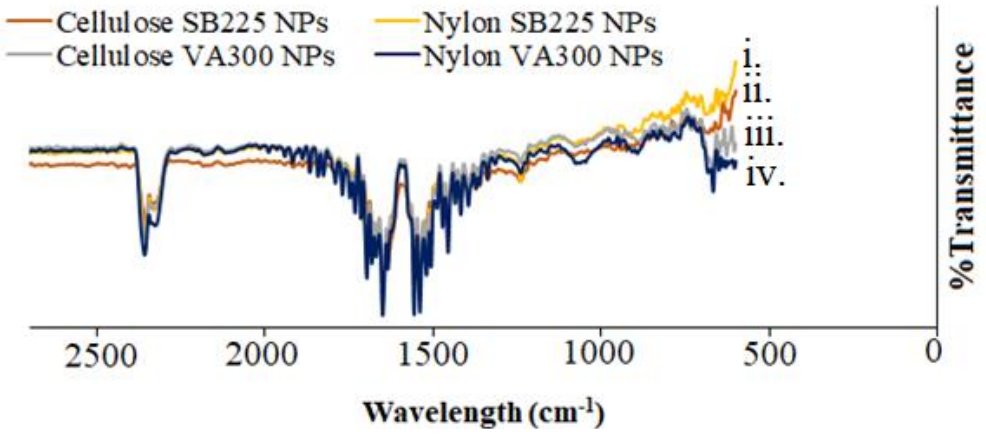

Figure 4.9. NP FTIR profiles. i. Nylon SB225, ii. Cellulose SB225, iii. Cellulose VA300, iv. Nylon VA300. All gelatin NPs have analogous chemical structures identified by amide I (C=0, 1648 cm^{-1}), amide II (N-H, 1540 cm^{-1}), amide III (N-H, 1238 cm^{-1}) and Schiff Base formation (C=N, 1456 cm^{-1}). Schiff Base formation indicates gelatin lysine amine ($-NH_2$) crosslinking with glutaraldehyde (-CHO).[23,24]

4.5.4 Rhodamine 110 Encapsulation

Incorporation of a model fluorescent bioactive, rhodamine 110, obtained ~80% encapsulation efficiency for SB225 and VA300 NPs (Figure 4.10A). Though glutaraldehyde induced crosslinking leads to gelatin autofluorescence,[25] rhodamine 110 encapsulated NPs (+Rho) obtained significantly higher fluorescence values than unloaded NPs (- Rho) (Figure 4.10B). SB225 and VA300 rhodamine 110 encapsulated NPs retained single volumes peaks (Figure 4.11) with a population average of 140 ± 2 nm. Maximum retention of the model bioactive is obtained as consistent sizes eliminate the need for particle filtration post synthesis.

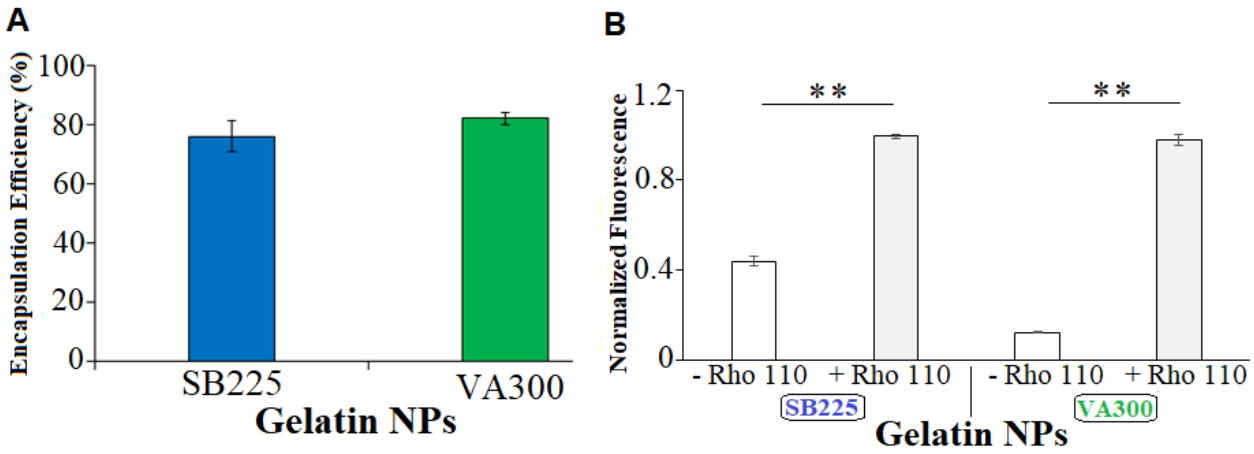

Figure 4.10 Rhodamine 110 encapsulation analysis. (A) Gelatin NP encapsulation efficiencies. (B) Gelatin NP fluorescence measurements. Results normalized by each gelatin type maximum. **p < 0.01. n = 3 for all measurements.

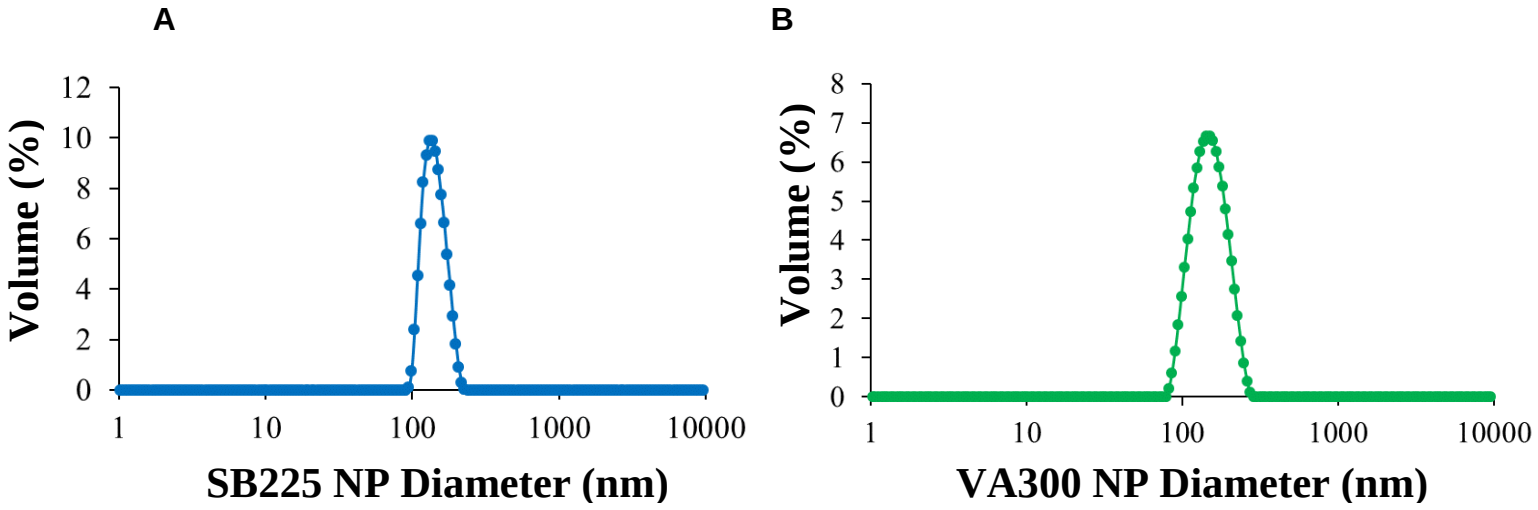

Figure 4.11. Representative volume distributions of NPs with rhodamine 110 encapsulated. (A) SB225 and (B) VA300.

4.6 Conclusions

In summary, this chapter showed a highly consistent method to prepare gelatin NPs based on reducing chain dispersity. Using FISH desolvation, a population average of 143 ± 12 nm indicated consistency between and within gelatin types. While SB225 and VA300 NPs had different charge intensities in PBS, indicative of their respective isoelectric points, TNBS assay and FTIR showed similarities in chemical crosslinking and bonding. In all, the concept of obtaining more homogenous molecular weight samples by using filtration prior to NP synthesis, is anticipated to reduce variability in NP properties for a variety of food based biopolymers. Therefore, this unique approach offers a simple platform to generate highly reproducible biopolymer NPs with practical implementations for food bioactive encapsulation and sustainable packaging formulations.

References

1. Nitta, S. K.; Numata, K., Biopolymer-Based Nanoparticles for Drug/Gene Delivery and Tissue Engineering. *International Journal of Molecular Sciences* **2013,** *14* (1), 1629-1654.
2. McClements, D. J., Encapsulation, protection, and release of hydrophilic active components: Potential and limitations of colloidal delivery systems. *Advances in Colloid and Interface Science* **2015,** *219* (Supplement C), 27-53.
3. Blanco, E.; Shen, H.; Ferrari, M., Principles of nanoparticle design for overcoming biological barriers to drug delivery. *Nature biotechnology* **2015,** *33* (9), 941-51.
4. Pathak, M., Chapter 5 - Nanoemulsions and Their Stability for Enhancing Functional Properties of Food Ingredients A2 - Oprea, Alexandra Elena. In *Nanotechnology Applications in Food*, Grumezescu, A. M., Ed. Academic Press: 2017; pp 87-106.
5. Djagny, K. B.; Wang, Z.; Xu, S., Gelatin: A Valuable Protein for Food and Pharmaceutical Industries: Review. *Critical Reviews in Food Science and Nutrition* **2001,** *41* (6), 481-492.
6. Elzoghby, A. O., Gelatin-based nanoparticles as drug and gene delivery systems: reviewing three decades of research. *Journal of controlled release : official journal of the Controlled Release Society* **2013,** *172* (3), 1075-91.
7. Geh, K. J.; Hubert, M.; Winter, G., Optimisation of one-step desolvation and scale-up of gelatine nanoparticle production. *Journal of microencapsulation* **2016,** *33* (7), 595-604.
8. Khan, S.; Schneider, M., *Nanoprecipitation versus two step desolvation technique for the preparation of gelatin nanoparticles*. 2013; Vol. 8595.
9. Azarmi, S.; Huang, Y.; Chen, H.; McQuarrie, S.; Abrams, D.; Roa, W.; Finlay, W. H.; Miller, G. G.; Lobenberg, R., Optimization of a two-step desolvation method for preparing gelatin nanoparticles and cell uptake studies in 143B osteosarcoma cancer cells. *Journal of pharmacy & pharmaceutical sciences : a publication of the Canadian Society for Pharmaceutical Sciences, Societe canadienne des sciences pharmaceutiques* **2006,** *9* (1), 124-32.
10. Hudson, D.; Margaritis, A., Biopolymer nanoparticle production for controlled release of biopharmaceuticals. *Critical reviews in biotechnology* **2014,** *34* (2), 161-79.
11. Lu, Z.; Yeh, T.-K.; Wang, J.; Chen, L.; Lyness, G.; Xin, Y.; Wientjes, M. G.; Bergdall, V.; Couto, G.; Alvarez-Berger, F.; Kosarek, C. E.; Au, J. L. S., PACLITAXEL GELATIN NANOPARTICLES FOR INTRAVESICAL BLADDER CANCER THERAPY. *The Journal of urology* **2011,** *185* (4), 1478-1483.
12. Klier, J.; Fuchs, S.; May, A.; Schillinger, U.; Plank, C.; Winter, G.; Coester, C.; Gehlen, H., Erratum to: A Nebulized Gelatin Nanoparticle-Based CpG Formulation is Effective in Immunotherapy of Allergic Horses. *Pharmaceutical Research* **2012,** *29* (7), 2030-2030.
13. Hickey, J. W.; Santos, J. L.; Williford, J.-M.; Mao, H.-Q., Control of polymeric nanoparticle size to improve therapeutic delivery. *Journal of Controlled Release* **2015,** *219* (Supplement C), 536-547.
14. Kuo, W.-T.; Huang, J.-Y.; Chen, M.-H.; Chen, C.-Y.; Shyong, Y.-J.; Yen, K.-C.; Sun, Y.-J.; Ke, C.-J.; Cheng, Y.-H.; Lin, F.-H., Development of gelatin nanoparticles conjugated with phytohemagglutinin erythroagglutinating loaded with gemcitabine for inducing apoptosis in non-small cell lung cancer cells. *Journal of Materials Chemistry B* **2016,** *4* (14), 2444-2454.
15. Bohidar, H. B.; Rawat, K., Biological Polyelectrolytes: Solutions, Gels, Intermolecular Complexes and Nanoparticles. In *Polyelectrolytes: Thermodynamics and Rheology*, P. M, V.; Bayraktar, O.; Picó, G. A., Eds. Springer International Publishing: Cham, 2014; pp 113-182.
16. Wang, H.; Hansen, M. B.; Löwik, D. W. P. M.; van Hest, J. C. M.; Li, Y.; Jansen, J. A.; Leeuwenburgh, S. C. G., Oppositely Charged Gelatin Nanospheres as Building Blocks for Injectable and Biodegradable Gels. *Advanced Materials* **2011,** *23* (12), H119-H124.
17. Lampila, L. E., Applications and functions of food-grade phosphates. *Annals of the New York Academy of Sciences* **2013,** *1301*, 37-44.

18. Hu, B.; Xie, M.; Zhang, C.; Zeng, X., Genipin-structured peptide-polysaccharide nanoparticles with significantly improved resistance to harsh gastrointestinal environments and their potential for oral delivery of polyphenols. *Journal of agricultural and food chemistry* **2014,** *62* (51), 12443-52.
19. Wang, Y.; Heinze, T.; Zhang, K., Stimuli-responsive nanoparticles from ionic cellulose derivatives. *Nanoscale* **2016,** *8* (1), 648-657.
20. Hojat, M.; Xu, G., A visitor's guide to effect sizes: statistical significance versus practical (clinical) importance of research findings. *Advances in health sciences education : theory and practice* **2004,** *9* (3), 241-9.
21. Robertson, J. D.; Rizzello, L.; Avila-Olias, M.; Gaitzsch, J.; Contini, C.; Magoń, M. S.; Renshaw, S. A.; Battaglia, G., Purification of Nanoparticles by Size and Shape. *Scientific Reports* **2016,** *6*, 27494.
22. Calejo, M. T.; Hasirci, N.; Bagherifam, S.; Lund, R.; Nystrom, B., CHAPTER 6 Stimuli-Responsive Structures from Cationic Polymers for Biomedical Applications. In *Cationic Polymers in Regenerative Medicine*, The Royal Society of Chemistry: 2015; pp 149-177.
23. Jadhav, N. R., Tone, J. S., Irny, P. V., & Nadaf, S. J. (2013). Development and characterization of gelatin based nanoparticles for targeted delivery of zidovudine. International Journal of Pharmaceutical Investigation, 3(3), 126–130. http://doi.org/10.4103/2230-973X.119213
24. Fathollahipour, S.; Abouei Mehrizi, A.; Ghaee, A.; Koosha, M., Electrospinning of PVA/chitosan nanocomposite nanofibers containing gelatin nanoparticles as a dual drug delivery system. *Journal of biomedical materials research. Part A* **2015,** *103* (12), 3852-62.
25. Collins, J. S.; Goldsmith, T. H., Spectral properties of fluorescence induced by glutaraldehyde fixation. *The journal of histochemistry and cytochemistry : official journal of the Histochemistry Society* **1981,** *29* (3), 411-4.

Chapter 5

Gelatin Nanoparticle Desolvation with Peptide Encapsulation and Glyceraldehyde Crosslinking for Traumatic Brain Injury Treatment

This chapter is currently in final preparation for submission to journal

Abstract:

Fundamental research has advanced our knowledge regarding the physical damage that occurs following a traumatic brain injury. Because the secondary injury phase can persist for days and weeks, researchers believe it might be susceptible to treatment interventions, such as by neuroprotective agents. Protective agents can spur brain healing and vascular remodeling to potentially reduce TBI symptoms and death. Gelatin nanoparticles (NPs) are attractive materials to encapsulate potential TBI treatments as they can form 100-200 nm structures and maintain a negative charge in physiological pH environments, essential physicochemical properties for optimal NP efficacy. While gelatin NP research has been applied to treat brain injuries, typical NP sizes are above 200 nm using emulsion techniques and the use of potentially toxic crosslinkers for particle stability decrease their translational ability. Here, the use of glyceraldehyde as a non-toxic crosslinker is revealed by measuring brain cell viability. The brain cells tested were able to well tolerate higher concentrations of glyceraldehyde compared to glutaraldehyde. Gelatin NPs were formed using desolvation and crosslinked with glyceraldehyde to be fully under 200 nm, monodispersed and negatively charged. Furthermore, incorporation of a new small molecule peptide within the NPs obtained slower cumulative release profiles compared to the plain peptide control. In all, applying concise experimental methods and adequately characterizing new NP formulations is expected to facilitate nanoscale property reproducibility and enable greater translation of drug delivery devices to industry use.

5.1 Introduction

Every year in the United States, an estimated 1.7 million people experience a force to the head that disrupts normal brain function, formally known as a traumatic brain injury (TBI).[1] Common occurrences are due to falls, motor vehicle accidents and sports activities that affect children, young adults, and the elderly. These traumatic events are the leading cause of death in the first forty years of life[2] and are projected to become the third leading cause of death and disability world-wide by 2020.[3] Fundamental research has advanced our knowledge regarding the physical damage that occurs at the moment of trauma when tissues and blood vessels are stretched, compressed, and torn (the "primary injury"),[4] and the resulting biochemical cascades and cellular changes (the "secondary injury").[5] Because the secondary injury can persist for days and weeks, researchers believe it might be susceptible to intervention, such as by neuroprotective agents, spurring brain healing and vascular remodeling to potentially reduce TBI symptoms and death.[6-7] Notably, the EphA4 pathway has been implicated as one significant contributor to secondary injury progression.[8-9] Frugier *et al.* determined there was increased phosphorylation of the EphA4 protein in mouse models and human brain tissue from patients who died after closed head injury.[8] After blocking EphA4 phosphorylation in astrocyte culture, his team determined there was no increase in human reactive astrocytes, cell proliferation, or stellate morphology, which suggests that blocking EphA4 activation may represent a therapeutic approach to improving recovery after brain trauma.[8, 10]

One potential neuroprotective peptide, known by its first three amino acid sequences as VTM (full sequence: VTMEAINLAFPG), binds to an EphA4 protein receptor, preventing subsequent phosphorylation.[11] Further, Theus showed systemic VTM delivery using an implantable pump reduced cortical tissue damage, spurred greater arteriogenesis, and substantially decreased lesion volume compared to the saline control in a moderately contused mouse model (Figure 5.1, unpublished data).[12]

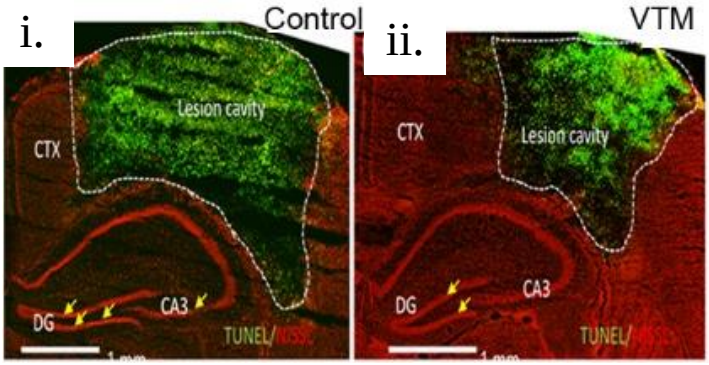

Figure 5.1. TBI animal model comparison. Murine lesion volume of (i.) saline control and (ii.) VTM minipump infusion (10 mg/kg/day or 300 µg/day) after 3 days post-TBI. Scale bar is 1 mm. Direct approval obtained from M. Theus for image use.

Similar to other peptides however, VTM is rapidly degraded by enzymes[11] and must pass through the restrictive blood-brain barrier,[13] prompting the need for continuous administration for adequate peptide to reach the brain. Though intranasal administration offers more direct brain access as it bypasses the blood-brain barrier,[14] the mucosal barrier and epithelial cell membrane restricts efficient transport for peptides.[15] To address these challenges, nanoparticles (NPs) have been shown to protect therapeutics against premature degradation, extend circulation in the body and enter the brain.[14] Additionally, the capability to produce NPs with properties for successful delivery via systemic *and* intranasal administration increases their overall translational potential. Gelatin NPs are attractive particles to encapsulate potential TBI treatments as they can form 100–200 nm particles and maintain a negative charge in physiological pH environments.[16] Size and charge are NP properties shown to prolong circulation in animal models, which increases the likelihood of permeation into the brain following injury.[17] Furthermore, negatively charged NPs have shown higher brain uptake rates than their positively charged counterparts.[18] For intranasal delivery applications, gelatin exhibits non-covalent bioadhesive interactions including: (1) hydrogen bonding between gelatin carboxylic acid and mucosa hydroxyl groups; (2) hydrophobic interactions between gelatin and mucosal glycoproteins attributed to leucine, isoleucine, methionine, and valine; (3) hydrophilic interactions in aqueous environments which initiate bioadhesion,[19] and (4) electrostatic interactions between positively charged mucosal segments without risk of permanent entrapment.[20]

One substantial determinant impeding gelatin NP translation, is successful production of gelatin NPs between 100-200 nm using crosslinkers significantly less toxic than glutaraldehyde. NP compositions should not adversely affect the normal physiology or normal structure of organs or tissues of humans and animals.[21] The use of toxic agents in NP preparations counters the overall formulation's intended therapeutic potential. Additionally, after brain injury, a class of enzymes known as matrix metalloproteinases (MMPs), including MMP-2 (gelatinase A), MMP-3 (stromelysin-1), and MMP-9 (gelatinase B), are produced by cerebrovascular endothelial cells, astrocytes, microglia, and neurons.[22] Consistent with these findings, the upregulation of MMP-2 and MMP-9 was shown in specimens of human plasma, interstitial fluid, and brain tissue from TBI patients,[22] which further indicates NP degradation components should be as tolerable as possible.

Glyceraldehyde is a monosaccharide sugar shown to be less toxic than glutaraldehyde (Chapter 2.2.2.2); however, glyceraldehyde crosslinked gelatin NPs are typically greater than 200 nm using desolvation.[23] Previous studies have used water-in-water emulsion, a tedious method requiring surfactants, typically low concentrations of gelatin, and additional reagents for gelatin NP stability to encapsulate potential therapeutic agents and showed protective efforts in brain injured murines.[16, 24] This chapter sets out to provide (1) direct evidence of higher glyceraldehyde tolerance compared to glutaraldehyde, specifically using brain cells; (2) formation of glyceraldehyde crosslinked gelatin NPs using desolvation within the following design criteria:

- Diameter: 150 ± 20 nm
- PDI: 0.17 ± 0.03
- Zeta Potential: -20 ± 10 mV,

(3) VTM-RhoB release rates and (4) recommendations to consider when preparing gelatin NPs to help improve experimental reproducibility. With regard to the design criteria, the goal was to at least replicate the gelatin glyceraldehyde crosslinked NPs shown successful in literature for brain injury applications, but here using desolvation instead of the tedious emulsion techniques.

5.2 Materials and Methods

5.2.1 Materials

The CellTiter 96® AQueous One Solution Cell Proliferation Assay, known as [3-(4,5-dimethylthiazol-2-yl)-5-(3-carboxymethoxyphenyl)-2-(4-sulfophenyl)-2H-tetrazolium;MTS assay] was obtained from Promega (Madison, WI), phosphate buffered saline (PBS, with Ca^{2+} and Mg^{2+}) and 75 cm^2 tissue culture treated flasks were obtained from Thermo Fisher Scientific (Waltham, MA). Antibiotic-Antimycotic solution and 0.05% trypsin was obtained from Life Technologies (Carlsbad, CA). D, L-Glyceraldehyde (≥ 90%) was obtained from Sigma Aldrich (St. Louis, MO). Vyse Type B 275 bloom strength gelatin (VB275) was generously provided by Vyse Gelatin Company (Schiller Park, IL). Glutaraldehyde (25%), acetone, and TNBS assay (4%) solution, were obtained from Fisher Scientific or Sigma Aldrich. VTM RhodamineB (VTM-RhoB, ~2700 Da) was synthesized from Dr. John Matson's lab (Chemistry Department, Virginia Tech). Float-A-Lyzer G2 Dialysis Devices (10 mL volume) with 8-10kD molecule weight cutoff were purchased from Spectrum Laboratories, Inc. (Rancho Dominguez, CA).

Cell Types, Culture Media and Supplements:

BV-2 mouse derived immortalized microglia: BV-2 cells were generously obtained from Dr. Yong Lee (School of Biomedical Engineering and Sciences, Virginia Tech).

C6 rat derived immortalized astrocytes and SH-SY5Y primary human neuroblastomas: C6 and SY5Y cells were generously provided by Dr. Pamela VandeVord (School of Biomedical Engineering and Sciences, Virginia Tech). Dulbecco's Modified Eagles Medium (DMEM) horse serum and fetal bovine serum (FBS) were obtained from Thermo Fisher Scientific (Waltham, MA).

Wild Type Endothelial Cells (wtECs) – primary mouse derived and isolated from post-natal day 1-5 brain: wtECs were generously provided by Dr. Michelle Theus (Department of Biomedical Sciences & Pathobiology, Virginia Tech). Complete mouse endothelial cell medium (basal medium with growth factor supplement) was obtained from Cell Biologics (kit M1168). Gelatin solution (Type B 2%, tissue culture grade suitable for cell culture) was obtained from Sigma Aldrich (St. Louis, MO).

5.2.2 Methods

5.2.2.1 Glyceraldehyde Thermal Analysis and Stock Solution Preparation

Glyceraldehyde (~5.5 mg) was added to a thermal gravimetric analyzer (TGA, Q50 TA Instruments New Castle, DE, USA) and heated isothermally under nitrogen purge at 10°C / min until ~170 °C. For the cellular toxicity experiments, glyceraldehyde (1.42 g) was added to distilled water (3 mL) and heated to ~60 °C to obtain a soluble 5.24 M solution. PBS was used for further dilution to 5.24 mM for glyceraldehyde and 2.62 mM for glutaraldehyde. Solutions were stored cold (~5 °C) and prior to use were placed in a water bath (37 °C). For NP crosslinking experiments, 5.24 M glyceraldehyde was diluted to 2.62 M using distilled water.

5.2.2.2 Cellular Toxicity

All cells were expanded in a 37 °C, 5% CO_2 incubator and split 3~6 days depending on confluence. The toxicity experiments were performed after seeding each cell type in serum free medium (100 µL) on 96 tissue culture treated wells for 24 h. Cell medium will be referred to as "control" in the results section containing bar graph cell viabilities. Each molecule (1.0 µL of control, glutaraldehyde or glyceraldehyde) was incubated in the cells for 2.5 h to represent the first few hours when clinical decisions are being made regarding patient care, known as the hyper acute

phase.[25] Englert *et al*. also assessed cell viability after crosslinker incubation for 2 h (Chapter 2.2.2.2).[26] In this chapter, five wells were used per molecule and conducted three separate times (n=3) for each cell type. Standard curves with respective cells (~5,000 to ~22,000) were made in each experiment ($R^2 \geq 0.90$). MTS absorbance was measured using a microplate reader (BioTex Multi-Mode, Winooski, VT) at 490 nm after reaction (2.5-4 h maximum). Statistical significance was determined in Minitab 18 via a one-way ANOVA with Tukey's post hoc test at $p<0.05$. Viability measurements were standardized by dividing each experimental run by the maximum value in the data set and multiplying by 100%. Data represent mean ± standard deviation. Specific experimental methods with slight distinctions per cell type are detailed in the following sections.

Wild Type Endothelial Cells (wtECs):

Prior to wtECs expansion, 0.2% tissue culture grade gelatin was added (for ≥30 min) and then removed from the culture flask. Following expansion in complete medium, wtECs were centrifuged and plated in a 96 well plate with serum free medium (~9,500 cells/well). Prior to plating, the wells were coated with 0.2% gelatin as described for the culture flasks. After 24 h, the serum medium was removed and fresh serum free medium was added along with respective molecules. The solutions were removed, rinsed with PBS, serum free medium added (100 µL) followed by MTS (10 µL). Reaction occurred for 4 h and absorbance read.

BV-2 Microglia:

Following expansion in complete medium (DMEM, 5% FBS, 1% Antibiotic – Antimycotic), cells were centrifuged and plated in a 96 well plate with serum free medium (~8,700 cells / well). After 24 h, the medium was removed and fresh serum free medium (100 µL) was added followed by respective molecules. After 2.5 h, MTS (20 µL) was added, reaction occurred for 4 h and absorbance was read. Controls consisted of BV-2 cells in serum free medium only and crosslinkers in serum free media only.

C6 Astrocytes:

Following expansion in complete medium (86.5% DMEM/F-12, 10% horse serum, 2.5% FBS, 1% Antibiotic – Antimycotic), cells were centrifuged and plated in a 96 well plate with serum free medium (~8700 cells / well). After 24 h, the medium was removed and fresh serum free medium

(100 µl) was added followed by respective molecules. After 2.5 h, the solutions were removed, rinsed with PBS, serum free medium added (100 µL) followed by MTS (10 µL). Reaction occurred for 2.5 h and absorbance was read.

SH-SY5Y Neuroblastomas:
Following expansion in complete medium (DMDM/F-12, 10% FBS, 1.0% Antibiotic-Antimycotic), cells were centrifuged and plated (~9500/well) in a 96 well plate with complete medium. After 24 h, the medium was removed and fresh serum free medium was added along with respective molecules as described above. After 2.5 h, the solutions were removed, rinsed with PBS, serum free medium added (100 µL) followed by MTS (5 µL). Reaction occurred for 4 h and absorbance read.

5.2.2.3 Gelatin NP Preparations
Similar to Chapter 3, VB275 NPs were prepared by two-step desolvation. Briefly, gelatin (1.25 g) was dissolved in distilled water (40 °C, 25 mL), acetone added (25 mL) and left to precipitate for 24 h. The liquid gelatin fraction was decanted, additional distilled water was added (25 mL), pH adjusted to 2.5 (1 M HCl), dropwise acetone added and solution crosslinked with glyceraldehyde (250 µL of 2.62 M or 5.24 M). After crosslinking, NPs were purified three distinct routes: (1) rotary evaporation as described in Chapter 3.3, (2) centrifugation at 100,000 x g as described in Chapter 4.3.1, and (3) lyophilization (LABCONCO, Kansas City, MO) where 2 mL pre-purified NP solution was added to 4 mL PBS, frozen for 1 day followed by 2 day lyophilization (-60 °C, <0.09 mbar).

VTM-RhoB peptide (1 mM, 1 mL) was introduced into NPs using two distinct routes: (1) adding peptide to the NP solution after pH adjustment, stirring for 10 min and procedure followed as above. (2) Adding the peptide to lyophilized NPs (0.054 g) dispersed in PBS for one day swelling. VB275 NPs were also prepared via FISH desolvation using the procedure described in Chapter 4.3.1. Briefly, gelatin (0.7 g) was dissolved in distilled water (40°C, 25 mL) and filtered using Whatman grade 50 cellulose filter paper. Additional distilled water (17 mL) was added to the filtrate with heating and stirring as previously described. The pH was lowered to 2.5 (1M HCl), dropwise acetone added (~90 mL, 3 mL/min) followed by glutaraldehyde (250 µL, 2.62 M) or

glyceraldehyde (250 µL, 5.24 M). NPs were centrifuged as described above and dispersed in PBS (~7 mL)

5.2.2.4 Characterization

Dynamic Light Scattering:

To determine initial glyceraldehyde crosslinking, a lower concentration to mimic glutaraldehyde was used (2.62 M, 250 µL) and only the pre-purified NP Z-Average mean (known as "diameter" or "size") along with the polydispersity index (PDI) was obtained. For the samples with higher glyceraldehyde to equal the number of glutaraldehyde *aldehyde* groups, NP diameter, PDIs, volume distributions and charges were carried out using a Malvern ZetaSizer Nano ZS90 (λ = 633 nm, protein analysis method) after 10x dilution in deionized water or PBS as indicated. At least three measurements of each samples were obtained ($n \geq 3$). All measurements are reported as mean ± standard deviation.

Extent of crosslinking:

TNBS assay was used to determine percent crosslinking of VB275 glyceraldehyde NPs as described in Chapters 3.3.3. Briefly, NPs in distilled water (0.494 g) were added to TNBS and $NaHCO_3$, reacted for 2 h at ~40 °C, centrifuged (100,000 x g, 30 min) to remove the NP pellet and absorbance measured at 349 nm after 1 mL dilution. Three measurements were obtained (n = 3). Data represent mean ± standard deviation

Fourier Transform Infrared Spectroscopy (FTIR) and Circular Dichroism:

FTIR measurements (32 scans) of VB275 glutaraldehyde or glyceraldehyde crosslinked NPs (~5% v/v, 15 µL) in aqueous solution were carried out using a Nicolet iS5 with iD7 ATR (Thermo Fisher Scientific, Waltham, MA). Aqueous background was automatically subtracted from each sample. For circular dichroism, the exact instrument and settings used as described in Chapter 3.3.4. Briefly, after centrifugation VB275 glyceraldehyde crosslinked NPs were diluted in distilled water (100 µL NPs: 125 µL H_2O) for sufficient signal in the circular dichrometer. A stock solution of VTM-RhoB (1 mM, 200 µL) was analyzed as well. n = 3 measurements per sample.

NP Fluorescence and VTM-RhoB Encapsulation Efficiency (%):

Fluorescence of blank and VTM-RhoB encapsulated NPs (7 mL) was obtained after centrifugation as described above and pellet dispersion in PBS (3 mL). The NP suspension was analyzed using the microplate reader described above with excitation: 560 nm, emission: 625 nm and sensitivity setting kept at 100. n ≥ 3 measurements and data represent mean ± standard deviation. Encapsulation efficiency was determined for the VTM-RhoB sample actually incorporated during NP synthesis. After crosslinking, the NPs (7 mL) were centrifuged twice using the conditions described above, followed by syringe filtration (0.10 μm) to ensure NPs were adequately removed from solution. The supernatant was then analyzed via fluorescence using the microplate reader and settings just described (n≥3 measurements, data represent mean ± standard deviation). VTM-RhoB NP encapsulation efficiency was determined by finding the concentration of peptide in solution using a calibration curve and performing the following calculation (Eq. 5.1)[27]:

$$Encapsulation\ Efficiency\ (\%) = \frac{\text{Total amount of peptide added} - \text{Leftover peptide in supernatant}}{\text{Total amount of peptide added}}\ x\ 100\%$$

Release Study:

The release profiles of VTM-RhoB were evaluated by three float-a-lyzer dialysis devices that were prepared using the package instructions. Next, four different solutions were added separately to the inside plastic tube of the dialysis membrane. The solutions were: (1) Free Peptide (1 mM, 1 mL + 9 mL PBS); (2) Dry NPs (lyophilized suspension containing swelled 1 mM, 1mL VTM-RhoB + 9 PBS); (3) Wet NPs (1 mM, 1 mL VTM-RhoB incorporated during NP synthesis, centrifuged and dispersed in 10 mL PBS); (4) Blank NPs (no VTM-RhoB incorporated, centrifuged and dispersed in 10 mL PBS). The plastic membranes were added to an outer shell containing PBS (27 mL) and the entire device submerged in a large volumetric container. Temperature was kept at ~37 °C with gentle agitation (110 rpm). At specific time points, the outer shell (100 μL, n ≥ 3 measurements per sample, data represent mean ± standard deviation) was analyzed for fluorescence using the microplate reader as described above. The outer shell solutions were completely removed and fresh PBS (27 mL) was added back.

5.3 Results and Discussion

5.3.1 Glyceraldehyde Thermal Characterization

Prior to glyceraldehyde thermal manipulation to improve aqueous solubility, it was necessary to determine temperature degradation. Figure 5.2 shows glyceraldehyde degradation onset temperature at ~110 °C with 5% degradation occurring at ~130 °C. This profile is similar to Shen *et al.* who determined the first onset of glyceraldehyde degradation occurred at ~142 °C.[28] Since <100 °C would be applied to glyceraldehyde (due to water boiling temperature), it's thermal stability was sufficient. At ~60 °C with stirring, glyceraldehyde became translucent indicating solubility was achieved.

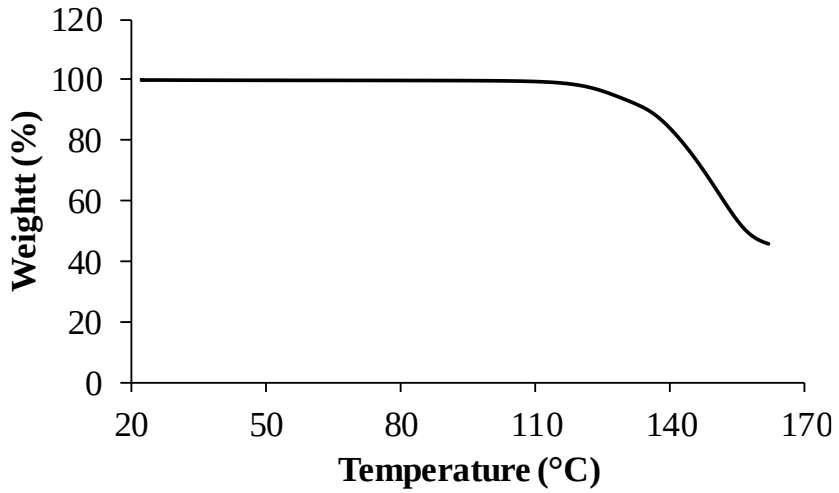

Figure 5.2. TGA thermal profile of glyceraldehyde.

5.3.2 MTS Assay and Description of Immortalized Cells

In vitro cytotoxicity testing has become an integral aspect of characterizing the toxic potential of new chemical entities due to its convenience, cost effectiveness and predictive means.[29] In particular, MTS is a tetrazolium salt that forms a colored soluble formazan (dye) upon reduction by viable cells in culture medium.[30] This conversion is likely accomplished by NADPH or NADH produced by dehydrogenase enzymes in metabolically active cells.[31] Upon cell death, cells rapidly lose the ability to reduce tetrazolium products; thus, the colored formazan product is proportional to the number of viable cells in culture.[30] Because different cell types have different levels of

metabolic activity, the MTS method is popular as its absorbance can be recorded periodically during early stages of incubation, allowing for multiple readings to assist in assay development.[32] For any cytotoxicity assay, the major factors critical for reproducibility and success include: 1) using a tightly controlled and consistent source of cells to set up experiments and 2) appropriate characterization of reagent concentration and incubation time for each experiment.[32] Therefore, minimal adjustments in cell seeding and MTS incubation time were made between cell types to obtain adequate measurements for statistical analysis.

The use of immortalized cell lines, where cells are infected with a retrovirus to continuously divide, are routinely used to acquire large numbers of cells without time consuming techniques and low cell numbers, at times associated with primary derived cells (non-transfection).[33] Primary or immortalized cells were used based on availability, ease of culture and their respective scientific efficacies described in the literature. The following sections will provide brief background regarding each cell type and present the crosslinker toxicity data. While important, the specific mechanisms of cell death are quite multifaceted and were not investigated.

5.3.3 Cellular Cytotoxicity Data

wtECs:

Endothelial cells constitute a major component of the blood-brain-barrier, intracerebral blood vessels and lamina propria of the olfactory mucosa.[34-35] As a result, toxicity should be limited to maintain their homeostatic role in the brain, such as regulating blood flow and angiogenesis.[36]
Primary rat brain wtECs showed significantly higher viability in glyceraldehyde compared to glutaraldehyde (Figure 5.3). There was no statistical difference in viability between glyceraldehyde and the control (serum free medium). This suggests that in general, higher concentrations of glyceraldehyde are well tolerated to wtECs than glutaraldehyde. This data confirms the study by Khan *et al.* (described in Chapter 2) showing glutaraldehyde toxicity in human endothelial cells.[37]

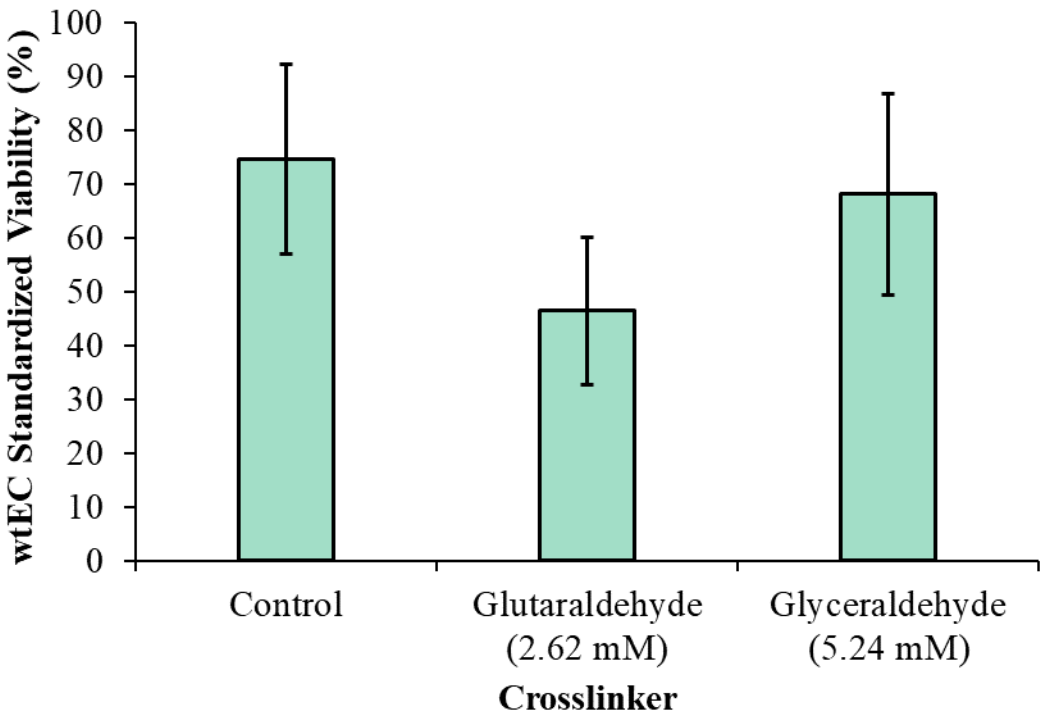

Figure 5.3. Incubation in glutaraldehyde caused significantly lower wtEC viability compared to the control and glyceraldehyde. † $p<0.05$ via one-way ANOVA. Data represent mean ± standard deviation.

BV-2 Microglia:

Microglia are the immune cells of the CNS and make up 10-15% of all mouse brain cells.[38] Human microglia renew at a median rate of 28% per year with data predicting complete renewal in the human cortex occurs during the lifespan of an individual,[39] similar to mice.[40] In regard to TBI, microglia cells offer a dual role releasing factors that modulate both secondary injury and recovery after injury via pro- and anti-inflammatories.[41]

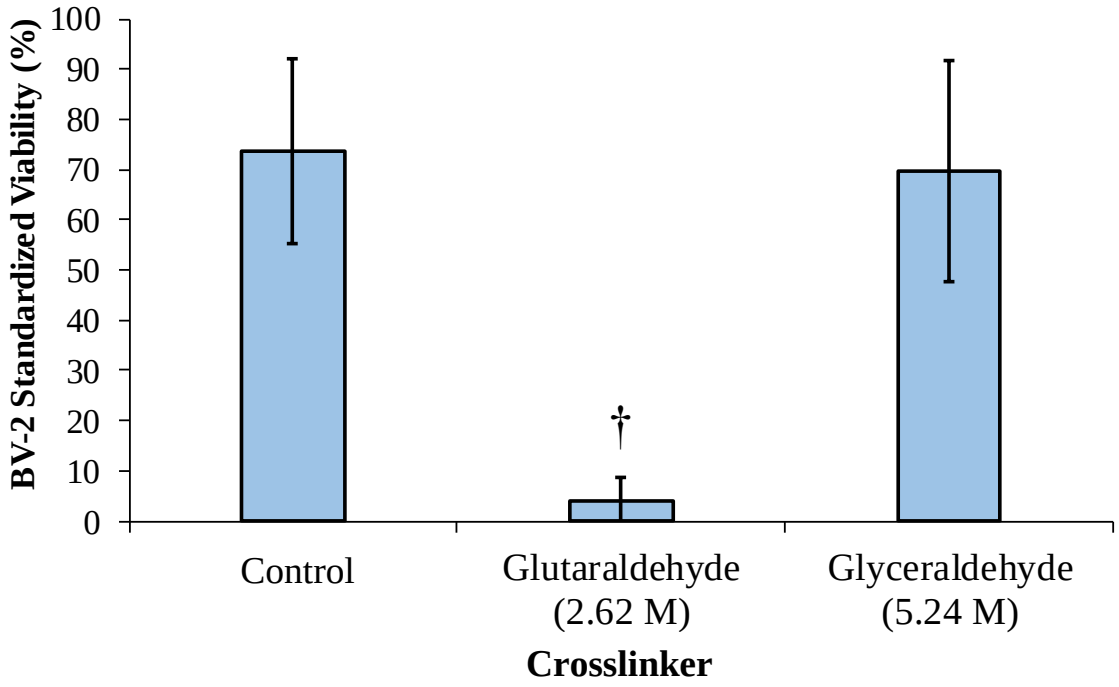

Figure 5.4. Incubation in glutaraldehyde caused significantly lower BV-2 cell viability compared to the control and glyceraldehyde. † $p<0.05$ via one-way ANOVA. Data represent mean ± standard deviation.

BV-2 microglia viability was significantly higher for glyceraldehyde incubated cells compared to those incubated in glutaraldehyde (Figure 5.4). Viability between the control and glyceraldehyde were not statistically different. This suggests that in general, higher concentrations of glyceraldehyde are well tolerable for BV-2 microglia cells. BV-2 microglia were the only cell type (out of those tested in this dissertation) that showed significant viability differences between the crosslinkers at the concentration used for NP stability.

BV-2 microglia are an immortalized cell line infected with an v-raf/v-myc recombinant retrovirus[42] and utilized frequently as a substitute for primary microglia.[43] Henn *et al.* showed that BV-2 microglia retain many qualities of primary microglia including 90% upregulation of inflammation-related genes (though less pronounced) were also found in primary microglial, along with protein expression after stimulation with lipopolysaccharide.[43] Their group also showed that BV-2 microglia obtained normal regulation of nitric oxide production and functional response to cytokine interferon gamma (IFN-γ), which are important parameters for appropriate interaction

with T cells and neurons.[43] Additionally it was shown that stimulation of BV-2 cells with lipopolysaccharide, and cell medium incubation with primary cortical astrocytes, caused increases in interleukin-6, which indicated BV-2 capacity to initiate a complex biological process typically observed through *in vivo* conditions.[43] While inflammatory upregulation studies were beyond the scope of this dissertation, literature has shown the characteristics indicate BV-2 cells are an appropriate model for primary microglia.

C6 Astrocytes:

Astrocytes account for more than half the cells in the brain and are the most numerous cell type within the central nervous system (CNS).[44] They perform a variety of tasks, from axon guidance and synaptic support, to the control of the blood brain barrier and blood flow.[45] Furthermore, astrocytes express numerous receptors that enable their response to growth factors, cytokines, small molecules and toxins. As such, their response can include the secretion of neurotrophic factors for the proliferation and maturation of neuroblasts to influence neuronal development and neuron activity. With respect to TBI, reactive astrocytes represent the main cell type responsible for creating the glial scar – the barrier between damaged and healthy tissue, which prevents the innervation of new neurons into damaged regions while also preventing further cellular degeneration and continued inflammatory responses.[46] Similar to microglia, astrocytes regulate acute phase responses of neuroinflammation, secreting pro-inflammatory and anti-inflammatory substances.[44]

As with the microglia cells, C6 viability was significantly higher for glyceraldehyde incubated cells compared to those incubated in glutaraldehyde (Figure 5.5). Viability between the control and glyceraldehyde were not statistically different. This suggests that in general, higher concentrations of glyceraldehyde are more tolerable for C6 astrocytes. The C6 astrocyte cell line was derived from cloning rat glial tumor induced by N-nitrosomethylurea.[47] Since its establishment, the C6 cell line are widely used as an astrocyte- like cell to study astrocytic function, S100B protein secretion and oxidative stress.[48] Furthermore, Mead *et al.* showed that primary rat astrocytes along with the C6 cell line and the human astrocytoma cell line (1321N1) obtained similar responses to toxic substances including altered morphology.[49] Additionally, for toxic substances the correlation coefficients of the EC50 values between primary cells and the C6 or

1321N1 cells were r > 0.5, and between the C6 and 1321N1 cells r > 0.9.[49] In all, these studies indicate that C6 astrocytes are an appropriate model for primary and human cultures, which might also show tolerability to higher concentrations of glyceraldehyde compared to glutaraldehyde.

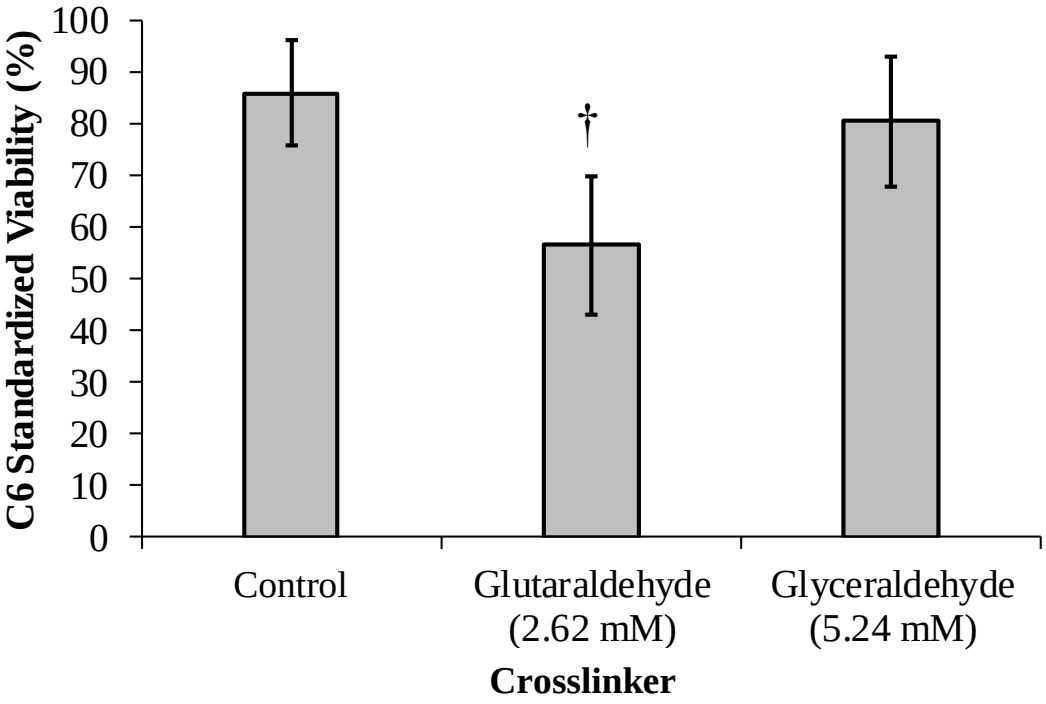

Figure 5.5. Incubation in glutaraldehyde caused significantly lower C6 cell viability compared to the control and glyceraldehyde. † $p<0.05$ via one-way ANOVA. Data represent mean ± standard deviation.

SH-SY5Y Neuroblastomas:

Neurons are cells that send and receive electrical impulses and chemical signals to and from the brain. The ability of the adult brain to generate new neurons provides optimism that damaged brain regions can be repaired and highlights it is advantageous to protect mature neurons that cannot be produced again.[50] Research has shown that after brain injury, proliferation of subventricular zone cells occurs, forming neuroblasts, which migrate along blood vessels to the damaged region.[51] Therefore, the ability to prevent further neuronal cell death may enable greater functional recovery after injury.[52] Similar to the cell types described above, SH-SY5Y viability was significantly higher for glyceraldehyde incubated cells compared to those incubated in glutaraldehyde (Figure

5.6). Viability between the control and glyceraldehyde were not statistically different. This suggests that in general, higher concentrations of glyceraldehyde are well tolerable for SH-SY5Y neuroblastomas. The SH-SY5Y cell line was originally derived from metastatic bone tumor biopsy and as they are human-derived, a variety of human-specific proteins are expressed.[53] In this particular study, the SH-SY5Y cells were not differentiated into a more mature, neuron-like phenotype for the following reasons summarized by Kovalevich *et al.* : (1) both undifferentiated and differentiated SH-SY5Y cells have been utilized for *in vitro* experiments requiring neuronal-like cells.[53] Neuronal differentiation obtains increased electrical excitability of the plasma membrane, formation of synaptophysin-positive functional synapses, and induction of neuron-specific enzymes, neurotransmitters, and neurotransmitter receptors.[53] (2) Undifferentiated *SH-SY5Y* cells continuously proliferate, express immature neuronal markers, and are thus considered to be most reminiscent of immature catecholaminergic neurons.[53] The main interest of Aim 3 was to compare crosslinker toxicity instead of investigating the neuron's functional response due to the crosslinkers. Additionally, catecholaminergic neurons can give rise to the nigrostriatal pathway,[54] which is crucial to a large array of behavior ranging from voluntary to higher cognitive processes.[55] Thus, the undifferentiated model was deemed highly sufficient for the focus described.

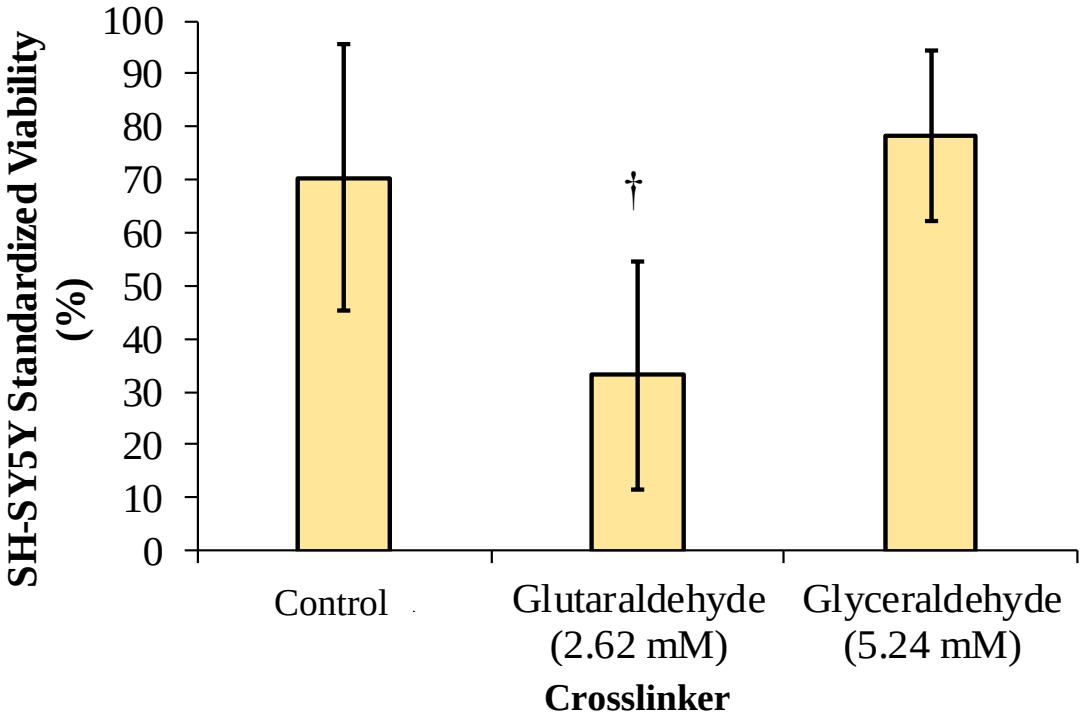

Figure 5.6. Incubation in glutaraldehyde caused significantly lower SH-SY5Y cell viability compared to the control and glyceraldehyde. †$p < 0.05$ via one-way ANOVA. Data represent mean ± standard deviation.

5.3.4 NP Physicochemical Properties

NP Crosslinker Comparison:

Glyceraldehyde (2.62 M) was first used to crosslink the NPs to compare their diameters using the same *concentration* as glutaraldehyde (2.62 M). As shown in Figure 5.7, after the first day of crosslinking, NPs were 182 ± 2.7 nm with overall decreases in size until the study was concluded on day 7. NPs had an average diameter of 129 ± 1.15 nm at day 5, with virtually no size change at day 7, which suggests 5 days would be adequate to crosslink the NPs at this concentration and volume. Glutaraldehyde is an efficient crosslinker in terms of faster reaction time with gelatin, likely due to its di-aldehyde structure as opposed to glyceraldehyde's single aldehyde group.

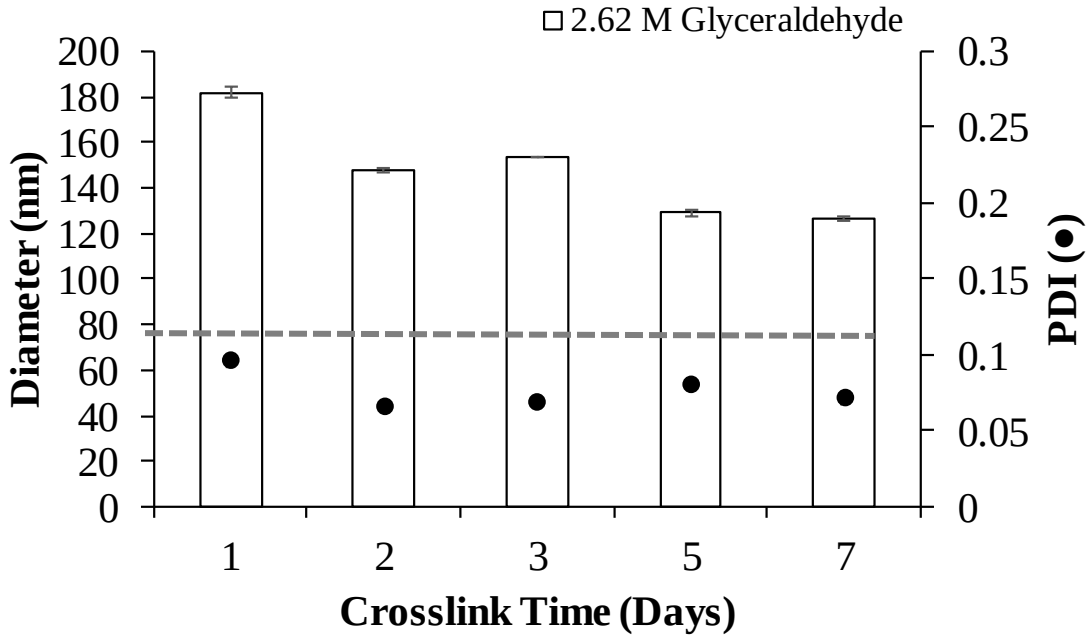

Figure 5.7. Pre-purified VB275 NP diameters decrease with additional crosslink time and have low PDI values. n = 3 measurements per day shown. Data represent mean ± standard deviation. Grey dashed line represents VB275 NP average diameter using glutaraldehyde (2.62 M).

Next, VB275 NPs were crosslinked with a 5.24 M concentration of glyceraldehyde to mimic the number of total aldehydes as glutaraldehyde in the same 250 µL volume. After 24 h crosslink time, Figure 5.8 shows VB275 NPs crosslinked with glyceraldehyde have ~100 nm diameters, which is ~35 nm larger than glutaraldehyde crosslinked NPs. However, upon rotovap to remove acetone,

glyceraldehyde crosslinked NPs swelled to over 2x their original diameter and agglomerate (PDI: 0.27 ± 0.07). Extensive literature review has found limited mention of characterizing gelatin NP diameter prior to NP purification (only 1 study currently found).[56] It is necessary to determine the pre-purified diameter (after selected crosslink time, but just prior to further manipulation) to determine the resulting affect the purification steps might have on the NP solutions. This might allow for reproducible NP purification methods.

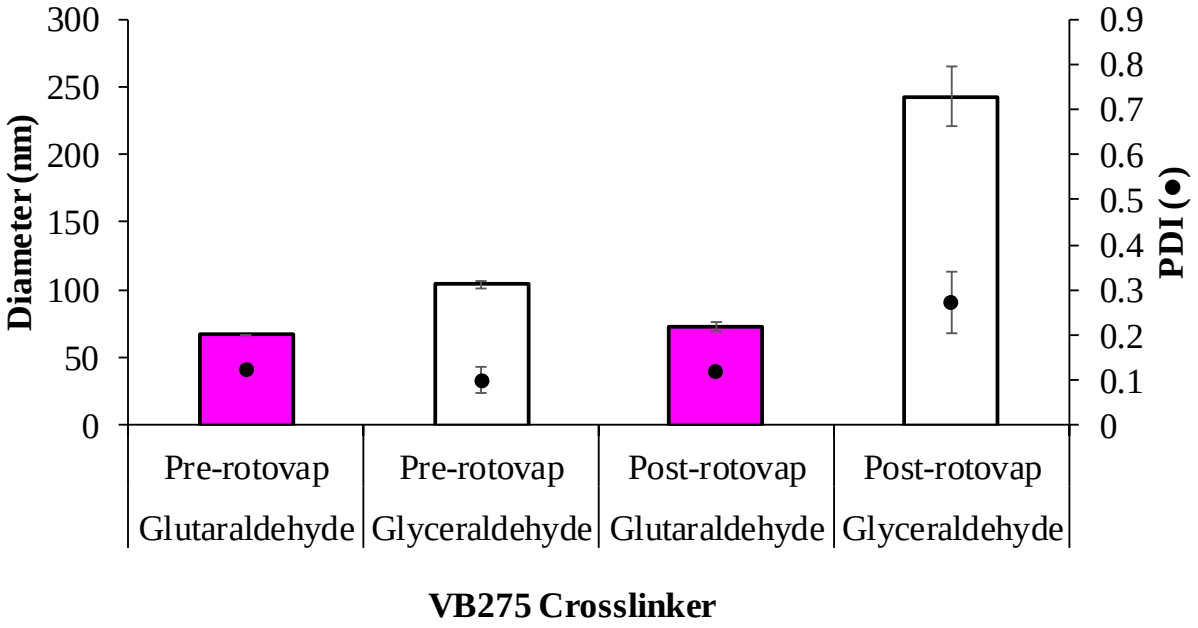

Figure 5.8. VB275 NPs crosslinked with glyceraldehyde swell and agglomerate upon rotary evaporation to remove acetone. n = 3 measurements per sample. Data represent mean ± standard deviation. Small standard deviations might seem invisible on some individual graphs, but all are added.

Additional characterization of the pre / post rotovap NP volume distributions indicate drastic changes in the NP population for glyceraldehyde (Figure 5.9). Larger diameters and agglomerated constructs from the glyceraldehyde crosslinked NPs after rotovap suggests the gelatin chains are crosslinked to a lesser extent and perhaps more flexible compared to glutaraldehyde crosslinking. These phenomena could lead to greater susceptibility to increased temperatures combined with mechanical force during rotovap (36 °C, 40 rpm). Table 5.1 includes an overview of the quantitative volume distributions in each NP sample.

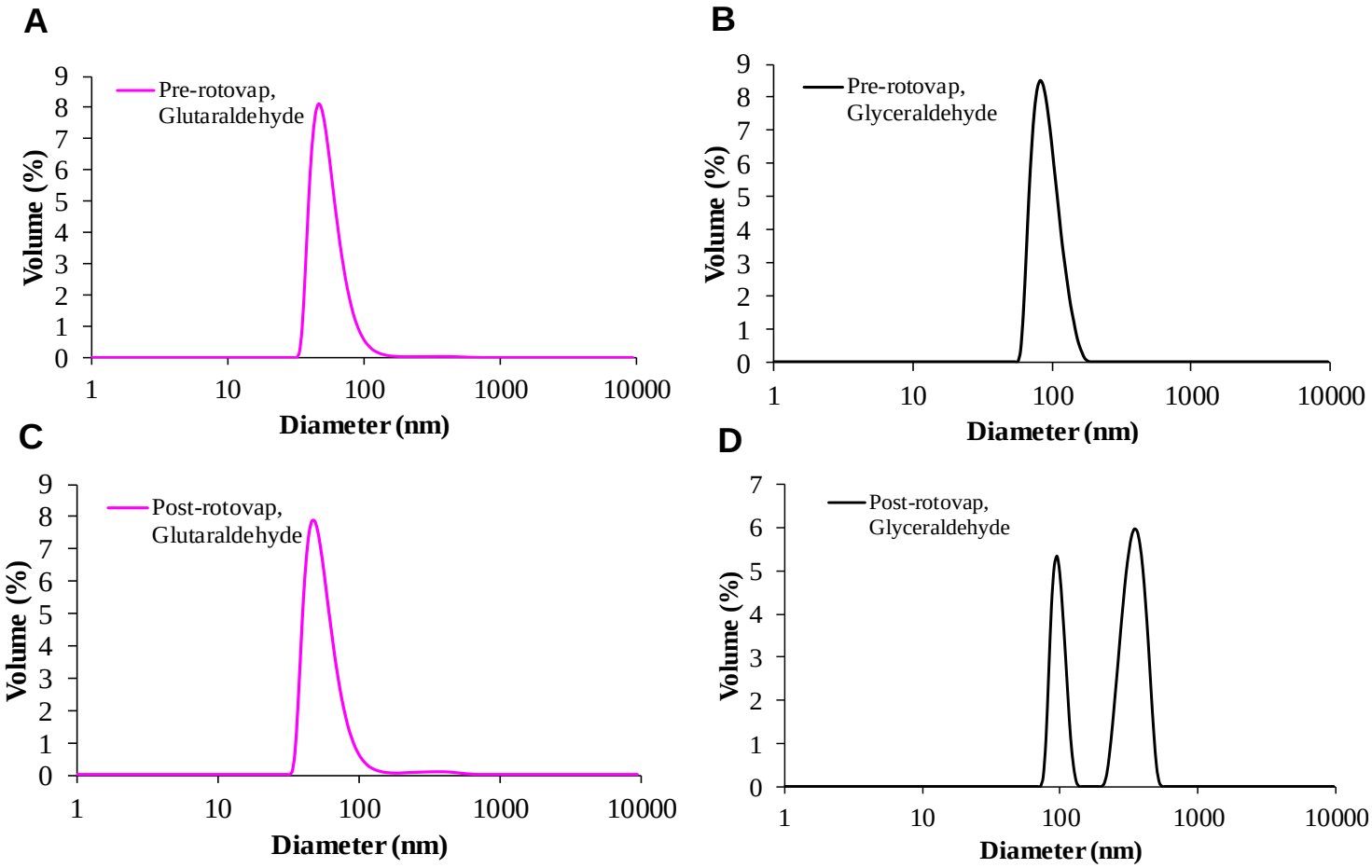

Figure 5.9. Representative volume distributions of VB275 NPs. Removal of acetone via rotovap, causes instability in the glyceraldehyde crosslinked NPs leading to multiple populations in the sample.

Table 5.1. Quantitative Volume Proportions in Pre and Post Rotovap Solutions

NP Solution	Peak 1 Size (nm)	Volume (%)	Peak 2 (nm)	Volume (%)
(A) Pre-rotovap, Glutaraldehyde	56 ± 17	99	-	-
(B) Pre-rotovap, Glyceraldehyde	92 ± 20	100	-	-
(C) Post-rotovap, Glutaraldehyde	57 ± 17	98	349 ± 107	< 2
(D) Post-rotovap, Glyceraldehyde	342 ± 66	65	96 ± 11	34

Previously discussed in Chapter 2, limited study on gelatin NP formation using desolvation with glyceraldehyde crosslinking exist; however, one recent study by Geh *et al.* determined Type B 300 bloom strength gelatin produced ~200-250 nm diameters.[23] Their diameters were obtained after NP centrifugation and dispersion in water, but no centrifugation speed or time was provided.[23] A few studies have prepared crosslinked gelatin NPs using glyceraldehyde via the emulsion process for TBI treatment.[24, 57] Zhao *et al.* formed gelatin-poloxamer NPs crosslinked with glyceraldehyde via water-in-water emulsion and obtained diameters of 210 ± 10.2 nm and a PDI of 0.19 for one study[57] and 172 ± 1.3 nm with a 0.11 ± 0.01 PDI for another.[16] Unfortunately, no information regarding gelatin type (animal source, bloom strength) and purification method was included except the NPs were dispersed in hydrogenated soy phosphatidylcholine, trehalose and cholesterol.[16, 57] Lu *et al.* characterized their NPs after lyophilization and dispersion in distilled water and obtained 136 ± 1.32 nm and 0.15 ± 0.02 PDI.[24] No information regarding gelatin type or lyophilization process was included.

NP Purification Methods and Subsequent Physicochemical Properties:

In an effort to reduce swelling and agglomeration after glyceraldehyde crosslinking, the following three separate methods were applied: (1) Lyophilization; (2) Rotovap at room temperature (25 °C) with 40 rpm; (3) Centrifugation. The qualitative and quantitative data will be presented first, followed by a description of the lyophilization and centrifugation processes.

Table B shows that all methods obtained diameters between ~120-135 nm with PDIs of ~0.20. Since the PDI values lie toward the upper end of the research community threshold, it was beneficial to view each sample's volume proportions. Figure 5.10 reveals single peaks indicative of one NP population with all measurements under 200 nm (Figure 5.10C). Therefore, the new purification methods were deemed successful and further characterization occurred along with VTM-RhoB encapsulation in the next sections.

Table 5.2. NP Diameter and PDI after Purification Methods

Purification	Diameter (nm)	PDI
Lyophilization	123 ± 2.4	0.19 ± 0.03
Rotovap_25 °C	129 ± 3.2	0.19 ± 0.02
Centrifugation	134 ± 1.3	0.20 ± 0.01

n = 3 measurements, Data represent mean ± standard deviation

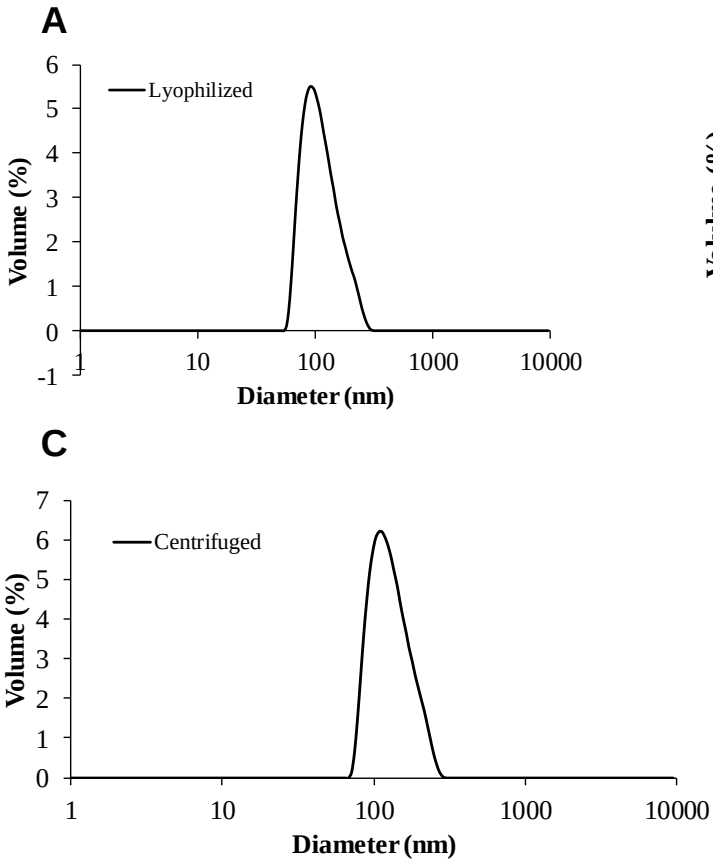

Quantitative Volume Proportions

Purification	Peak 1 (nm)	Volume (%)
Lyophilization	119 ± 41	100
Rotovap_25 °C	117 ± 34	100
Centrifugation	131 ± 26	100

Figure 5.10. Representative volume distributions of VB275 NPs following purification. All methods reveal a single peak, which is confirmed in the quantitative volume proportions table.

Common for various other pharmaceuticals, NP formulations can be stored as a dry powder using lyophilization (also known as freeze drying), to increase their long-term stability. For example, Abraxane is an FDA approved formulation composed of albumin NPs incorporating the anti-cancer drug paclitaxel, which is stored as a powder.[58] While NP lyophilization is commonly reported, experimental protocols are severely lacking in detail concerning the applied freeze-

drying cycle or particle characteristics before and after lyophilization.[59] Additionally, the freeze-drying step has been shown to induce NP aggregation and irreversible NP fusion, likely from mechanical ice crystallization stresses acting on the NPs.[60] Therefore, cryoprotectants are used for stability. In this study, lyophilized gelatin NPs were dispersed in PBS and heating was required, likely due to their chemical induced crosslinking. Figure 5.11 shows the lyophilized product and the resulting solution after heating and stirring to obtain the diameters and distributions discussed above.

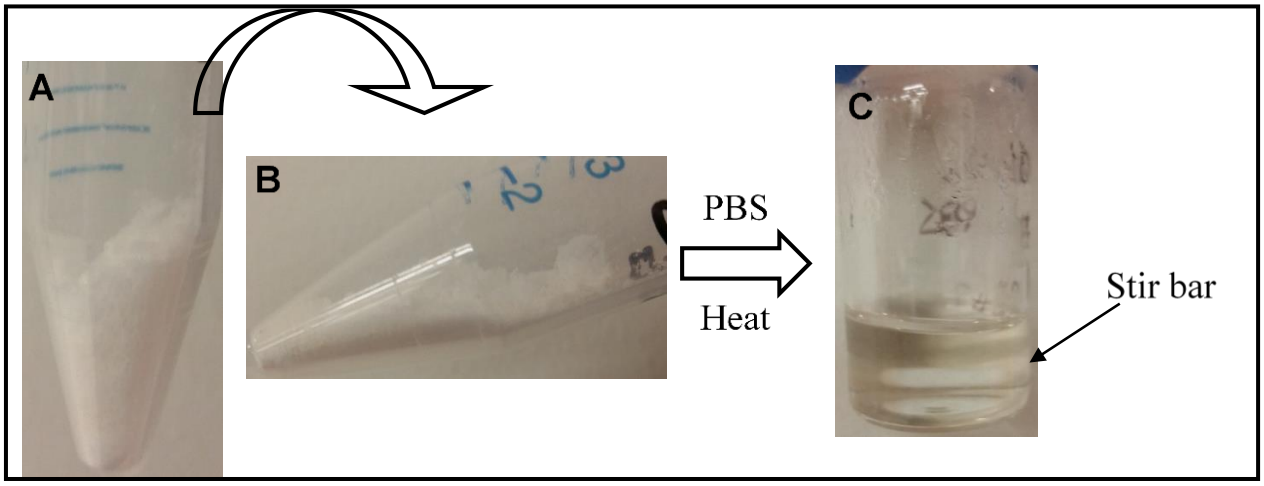

Figure 5.11. (A) Post lyophilized powder is (B) not a solid mass. (C) Powder sample (0.054 g) is dispersible in PBS with heating (~65 °C) and stirring (250 rpm).

Chapter 4 showed that high speed centrifugation of FISH prepared NPs crosslinked with glutaraldehyde was possible at 100,000 x g, 7 mL, 15 min. Using the same method, centrifugation of the glyceraldehyde crosslinked NPs produced a pellet, but dispersion in aqueous solution was not possible. Additional modifications to centrifuge speed, time and temperature occurred, yet every pellet remained gelled (Figure 5.12A). This likely indicates, the solution was crosslinked for too long. A new batch of NPs were produced and crosslinked for under 24 h (19-23 h). The solution was centrifuged (12 min, other conditions kept constant) and produced a clear pellet which was highly dispersible in PBS (Figure 5.12B) and obtained diameters and distributions discussed above (Figure 5.12).

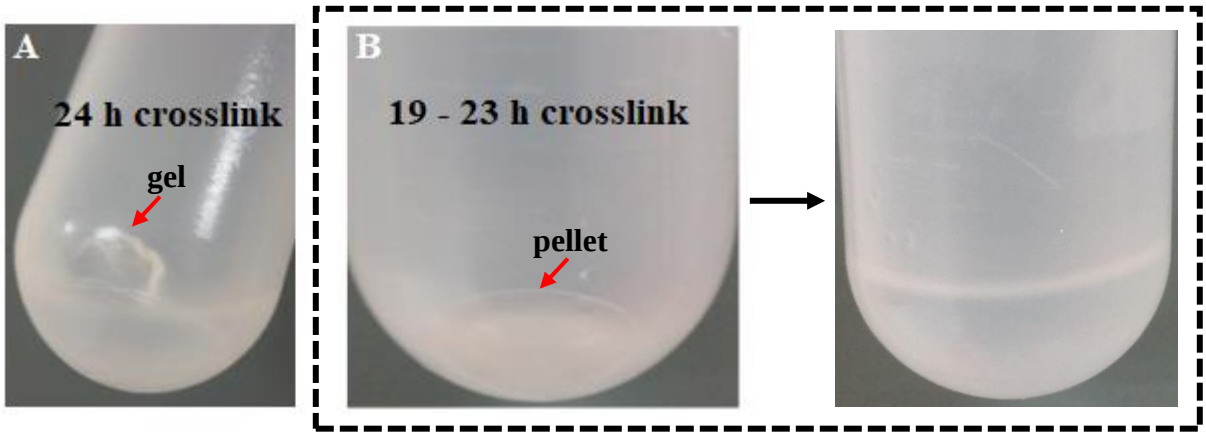

Figure 5.12. (A) Representative gelled NP pellet after 24 h glyceraldehyde crosslinking and centrifugation. (B) NP pellet after 19-23 h crosslink and centrifugation easily disperses in 5 mL PBS.

Interestingly, glyceraldehyde crosslinked NPs appear white and translucent in comparison to the yellow to golden color indicative of glutaraldehyde crosslinking (Figure 4.3C). In glutaraldehyde crosslinking, the color change is due to the formation of aldimine linkages (–CH=N–) between the free amino groups of lysine or hydroxyl lysine amino acid residues of the protein and the aldehyde groups of glutaraldehyde.[61] Glyceraldehyde crosslinking was discussed in Chapter 2.2.2.2, and the results presented indicate distinct differences. While glyceraldehyde only contains one aldehyde group, a relatively high degree of lysine amine interaction takes place (Figure 5.13A), which confirms the loss of lysine correlates well for glyceraldehyde (along with glutaraldehyde) crosslinking.[62] However, glyceraldehyde crosslinked VB275 NPs by ~14% less extent compared to glutaraldehyde (Figure 5.13B). These results suggest that new crosslinkers with one aldehyde group might also be able to chemically induce sufficient gelatin crosslinking. Additionally, the TNBS assay was performed using the rotovapped VB275 glyceraldehyde sample to maintain experimental consistency. The high degree of crosslinking with low standard deviation is indicative of a consistent NP population confirming the dynamic light scattering data presented beforehand (Figure 5.10).

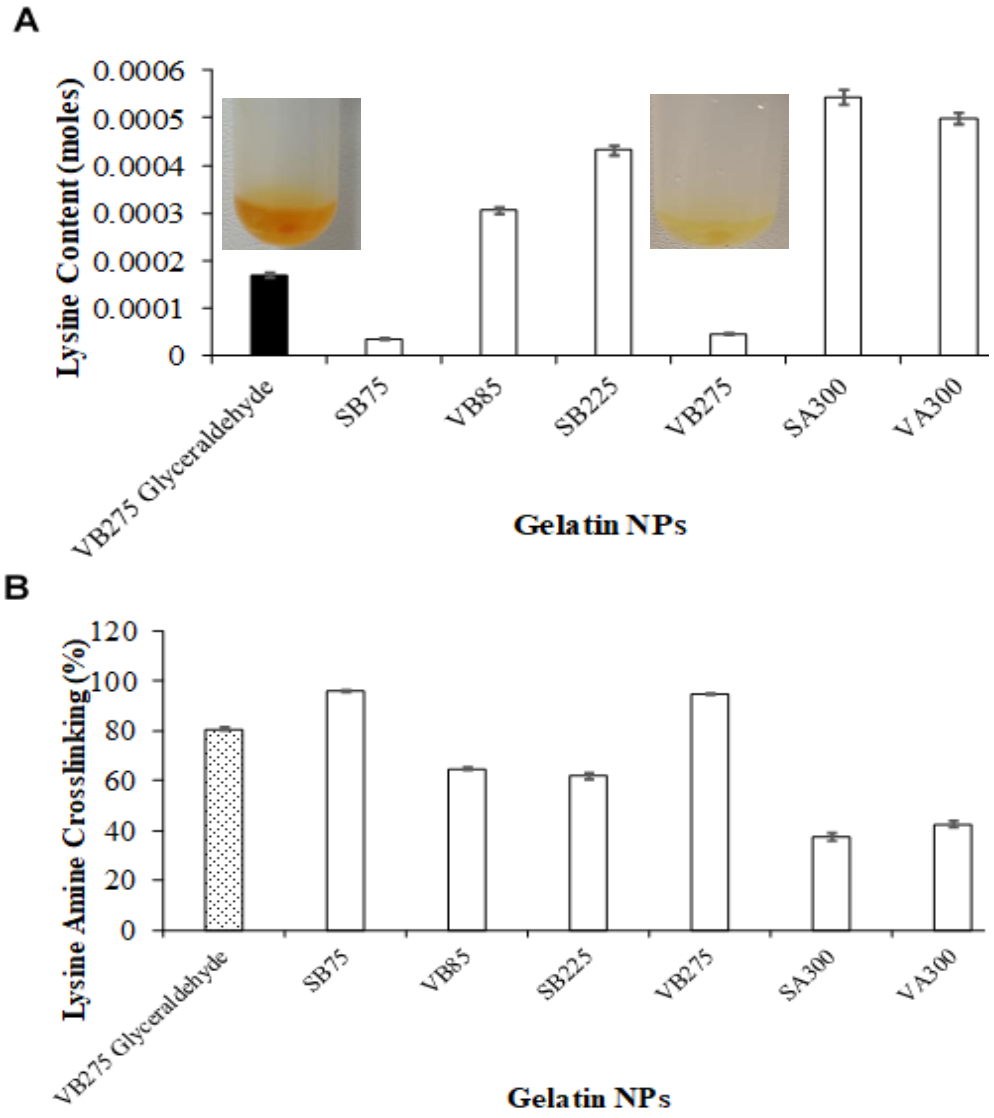

Figure 5.13. Gelatin NP Crosslinking Comparison. (A) Free lysine detection based on low (yellow) to higher (orange) concentrations. Black bar is the new glyceraldehyde data while open boxes are values already presented in Figure 3.3. (B) NP crosslinking extent. n = 5 measurements for the new sample. Data represent mean ± standard deviation.

FTIR was used to further compare gelatin chemical interactions between the respective crosslinkers. Figure 5.14 reveals the glutaraldehyde crosslinked sample has greater band intensities compared to glyceraldehyde. Bond stretching at 1640 cm^{-1} is a characteristic of Amide I C=O, the 1540 cm^{-1} band represents Amide II N-H bending, and bond bending at 1200 cm^{-1} represents amide

III C-N, which are all characteristics of gelatin.[63] The 1450 cm^{-1} peak reveals Schiff Base formation and is shown more prominently in the glutaraldehyde sample.[64] Characteristic C-O-C bonds are indicative of the 1020 cm^{-1} peak. Overall, the spectra indicate that the glyceraldehyde crosslinked NPs contain less intense chemical bonding interactions compared to glutaraldehyde, and might undergo additional molecular rearrangements to sufficiently crosslink functional groups for stability, which the scientific community has proposed via the reaction scheme shown in Chapter 2.

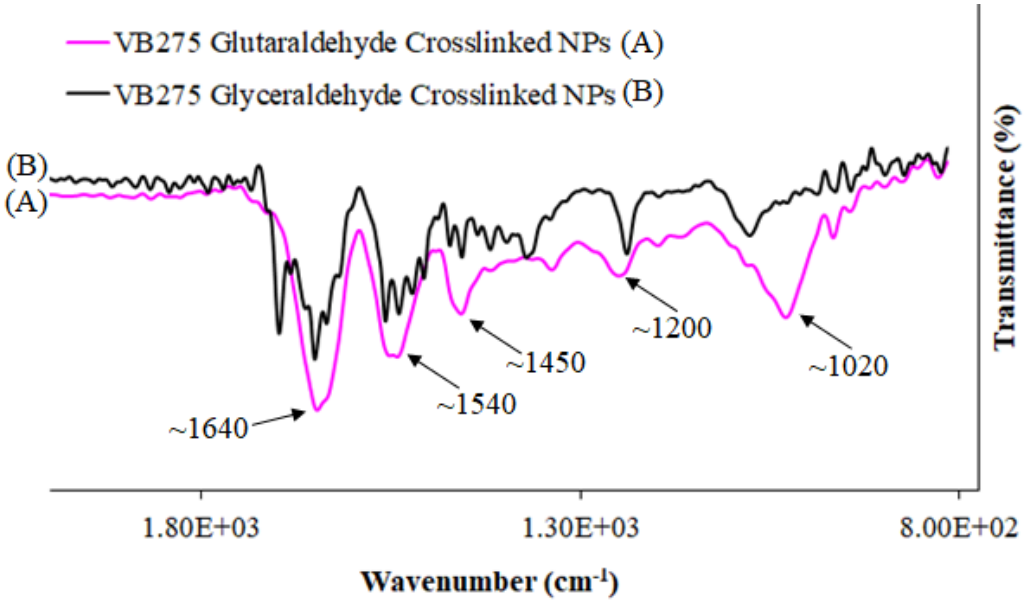

Figure 5.14. FTIR spectra of crosslinked gelatin NPs with glutaraldehyde vs glyceraldehyde.

5.3.5 Characterization of Glyceraldehyde Crosslinked VB275 NPs Containing VTM-RhoB Physicochemical Properties and VTM-RhoB Encapsulation:

VTM-RhoB (1 mM, 1 mL) was incorporated into VB275 NPs via two separate methods. The first included incubation of VTM-RhoB into lyophilized VB275 NPs for 1 day and the second method consisted of adding the peptide (for 10 min mix) prior to NP formation and crosslinking (see 5.2.2.3 for complete experimental procedures). VTM-RhoB that was incorporated into the NPs after lyophilization showed no increases in diameter or PDI following the one day swelling (Table 5.2). Table 5.3 contains diameters for VTM-RhoB incorporated before NP formation. After crosslinking and prior to centrifugation, the NPs were originally ~200 nm. After centrifugation

and dispersion in PBS their size decreased by ~50 nm (Table 5.3). The shrinkage in diameter after dispersion in PBS is described by Wang *et al.* as the likely ionic compaction of gelatin chains, which reduces the interaction between water.[65] Madan *et al*. also obtained nearly 50 nm reductions in Type B gelatin NP diameter after dispersion in PBS.[66] Additional diameter reductions might also be due to the lesser extent of gelatin hardening by glyceraldehyde since it only has one aldehyde group. As a result, the chains might be softer and more environmentally responsive to changes in pH or ionic strength. Compared to blank NPs (Table 5.2), there is an ~15 nm increase with VTM-RhoB incorporation. The post centrifuged NPs obtained a highly monodisperse size distribution indicated by the PDI value, in part due to the interaction between the peptide and gelatin. VTM-RhoB (1 mg / mL) has a negative charge in distilled water (-66.5 ± 1.5 mV, n=4 measurements) and Figure 3.6 showed that Type B macroscale gelatin maintains a nearly neutral charge in distilled water (-2.8 ± 0.9 mV). Electrostatic interactions between charged gelatin segments and VTM-RhoB likely initiate stability even after acidic pH adjustment.

Table 5.3. VB275 Glyceraldehyde VTM-RhoB NPs

Centrifugation	Diameter (nm)	PDI
Pre	202 ± 1.7	0.11 ± 0.03
Post	149 ± 1.8	0.05 ± 0.03

n = 3 measurements. Data represent mean ± standard deviation.

Similar to macroscale gelatin (Figure 3.5), circular dichroism confirms VTM-RhoB is a random coil in acidic pH environments (Figure 5.15), so van der waals interactions such as hydrogen bonding could integrate within the final structure to promote overall stability. Glyceraldehyde crosslinked gelatin maintains random coil morphology (Figure 5.15). Molecular weight differences between the gelatin protein vs VTM-RhoB (a small molecule peptide) likely contribute to their dissimilar signal intensities, yet both have similar secondary structure morphology indicative of a negative peak at ~200 nm.

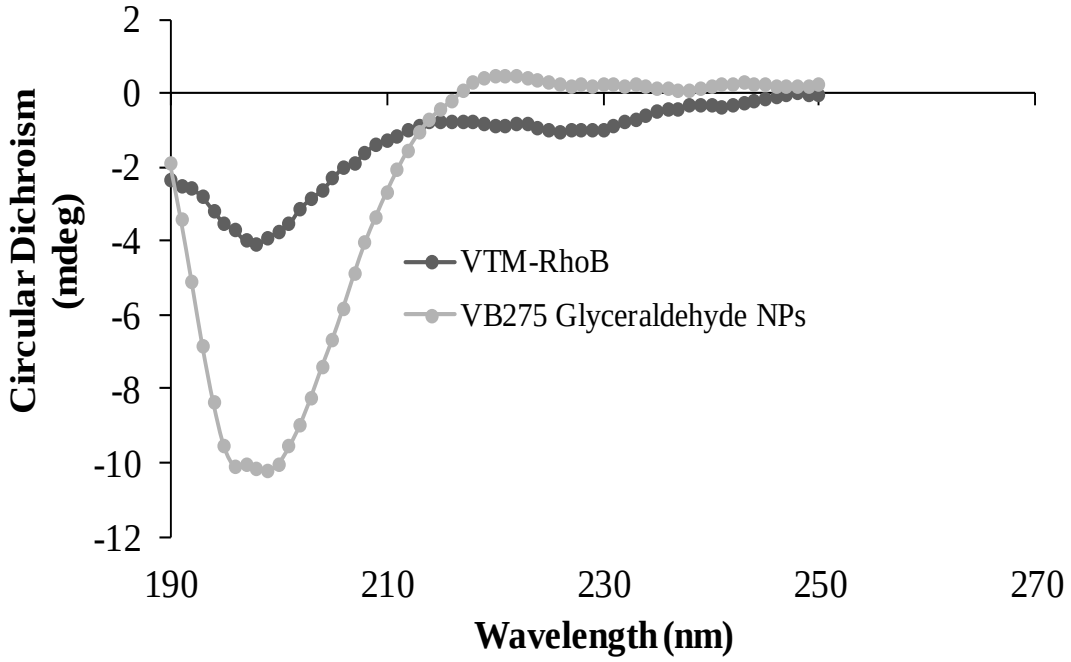

Figure 5.15. Circular dichroism spectra of VTM-RhoB and VB275 glyceraldehyde crosslinked NPs. n = 3 scans.

Post centrifuged NPs also maintain a single volume peak similar to blank NPs (Figure 5.16A) and maintain negative charges above gelatin Type B pI ~5.2 (Figure 5.16B).

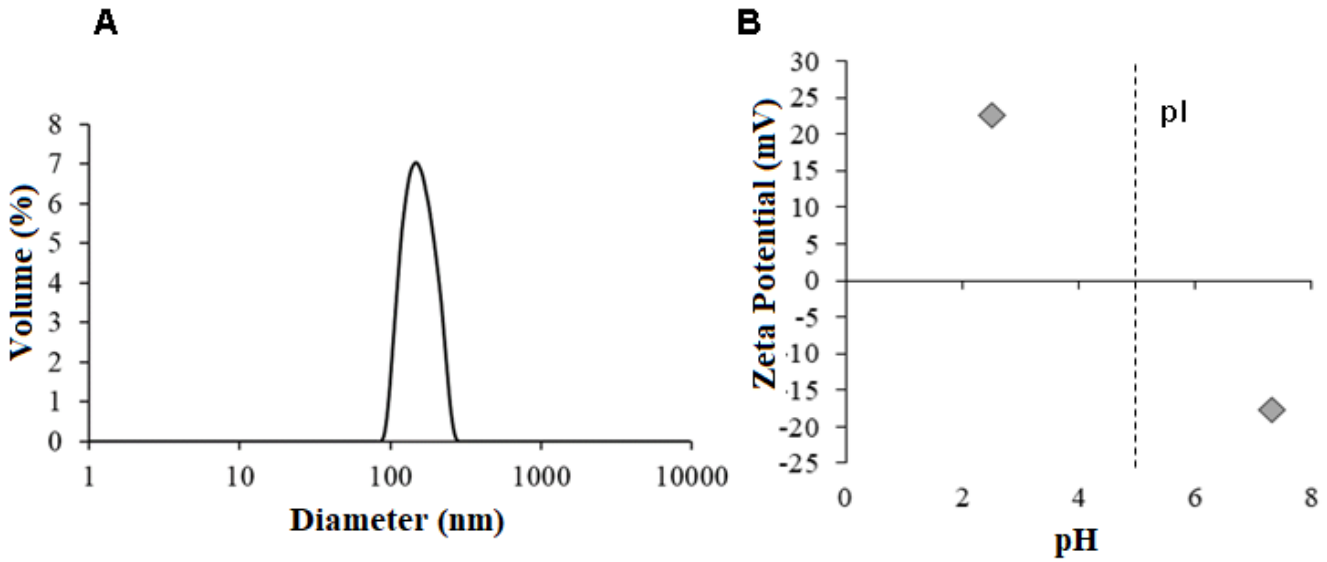

Figure 5.16. (A) Representative volume distribution of VB275 NPs encapsulating VTM-RhoB and crosslinked with glyceraldehyde. (B) Zeta potential of VB275 NPs in water (pH ~2.5 and ~7.3). n = 5 measurements. Data represent mean ± standard deviation. Error bars added but may be difficult to see.

A VTM-RhoB calibration curve was produced to determine the encapsulation efficiency and reveal a linear relationship between peptide concentration and fluorescence (Figure 5.17).

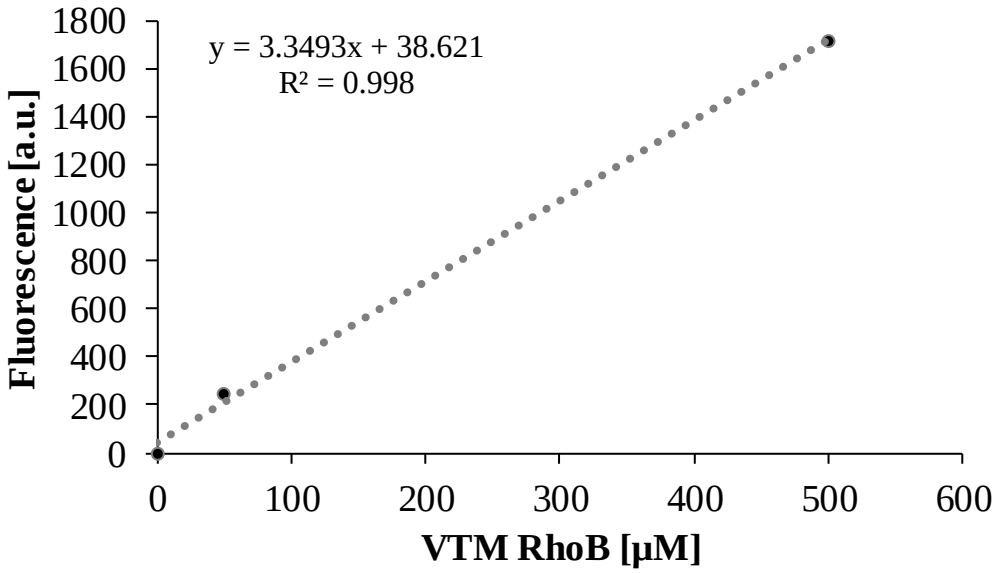

Figure 5.17. VTM-RhoB standard curve after dissolving samples in acidic distilled water (pH 2.5) to mimic NP supernatant. n = 2 measurements averaged per concentration. 100 sensitivity.

Encapsulation Efficiency was calculated to be 64 ± 7% indicating high incorporation of peptide within the NPs. Fluorescence measurements of NPs encapsulated with VTM-RhoB compared to blank VB275 NPs showed significantly higher signals, confirming encapsulation (Figure 5.18).

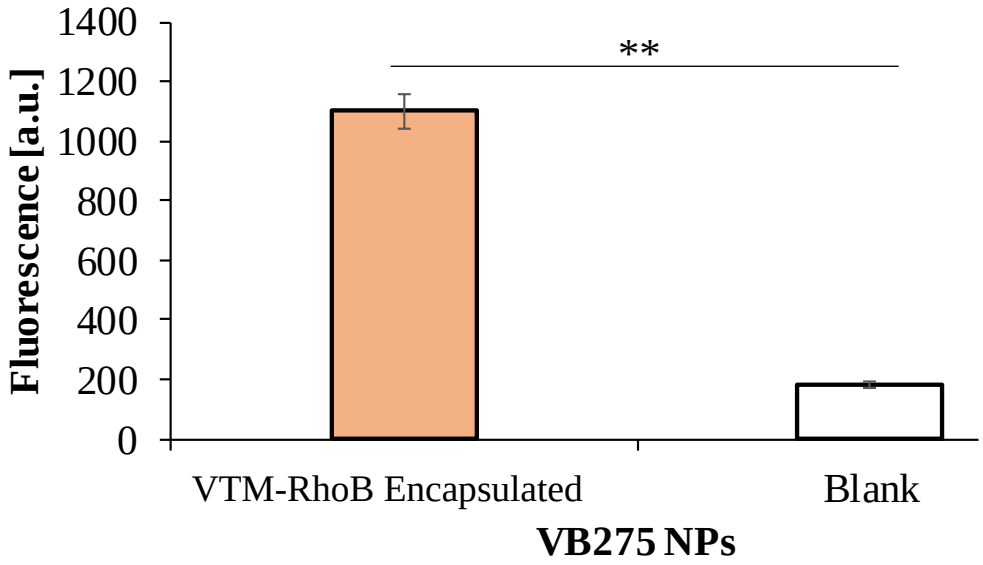

Figure 5.18. Fluorescence measurements comparing encapsulated vs. blank NPs. n = 3-4 measurements. **p < 0.001 via two-sample t-test.

In vitro Release Studies of Glyceraldehyde Crosslinked NPs Containing VTM-RhoB:

In vitro release kinetics reveal distinct profiles for the free peptide (VTM-RhoB control) compared to the NPs (Figure 5.19). Again, VTM-RhoB was incorporated during NP synthesis for the wet NPs in contrast to post lyophilized swelling of the dry NPs in VTM-RhoB solution. The control displays a higher cumulative release over six days compared to the NPs, which maintained slower peptide release (Figure 5.19). After day one, there was a significant difference in peptide release between the control and the wet NPs only (denoted by asterisk * in Figure 5.19). This indicates the wet NPs maintain limited burst release indicative of higher crosslinked NPs, which are less susceptible to aqueous based swelling.[67-68] On day two, the first complete exchange of PBS occurred and no significant difference in cumulative peptide release was obtained for the groups (Figure 5.19).

The following explanations provide insight why both NP groups obtained a similar cumulative release as the control on day two: (1) Their small ~130-150 nm diameters enable greater contact and interaction with PBS, so peptide that is internally near the surface will easily diffuse from the NP,[69] which is further enhanced after complete buffer exchange meant to help establish sink conditions.[70] (2) Following buffer exchange, smaller molecular weight substances (such as unbound dye) become less entangled in polymer networks enabling faster diffusion out of the polymer compared to their larger molecular weight counterparts.[69] VTM-RhoB is a chemically conjugated molecule consisting of modified VTM (~1700 Da) and fluorescent rhodamine B dye (~480 Da). Due to the conjugation process, unbound or non-covalently attached rhodamine B will likely constitute a fraction of the entire sample. It is possible that unbound rhodamine B readily diffuses out of the control, wet NP and dry NP groups accounting for similar cumulative release concentrations after the first PBS exchange. Gel electrophoresis to estimate molecular weight and / or mass spectrometry to determine amino acid composition could be used to confirm VTM-RhoB purity obtained from collaborators.

From the third day onward, fresh PBS was added daily yet there was no statistical difference in cumulative release between the NPs; however, the control was significantly higher to both NPs (denoted by house ⌂ Figure 5.19). Overall, the data indicates both NPs provide an effective steric barrier to retain VTM-RhoB within their polymer networks. Electrostatic interactions between negatively charged gelatin segments (COO-) and positively charged peptide amine groups is one potential route known to retard release.[69] Similar NP release profiles also indicates limited VTM-RhoB chemical crosslinking with gelatin during NP synthesis. Limited crosslinking of the *peptide* is typically desired to retain the peptide's inherent structure and purported biological activity. Additionally, peptide – gelatin covalent bonding makes it difficult to release adequate peptide[71] as significant aqueous and / or enzymatic degradation is required.

Gelatin degradation was determined to be minimal since the control group of plain (non-encapsulated) crosslinked NPs revealed similar fluorescence measurements as PBS. Overall, similar cumulative release concentrations for VTM-RhoB incorporated during NP synthesis or swelling after lyophilization establish both methods are effective at peptide retention likely from entrapment within the gelatin network.[72]

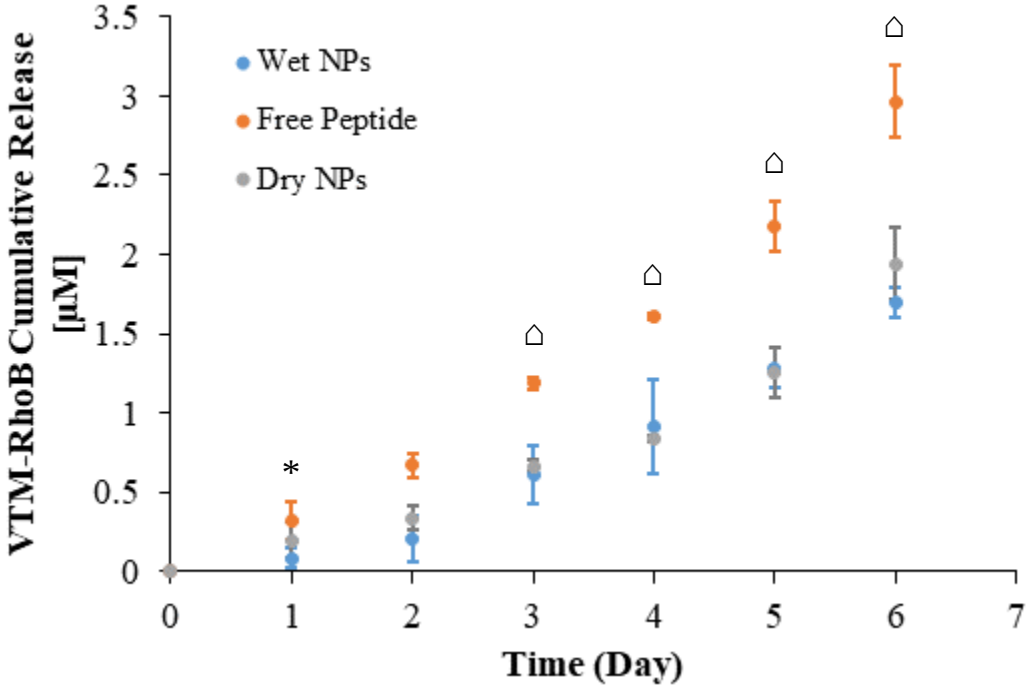

Figure 5.19. Release profiles of peptide formulations from VB275 NPs crosslinked with glyceraldehyde. n ≥ 2 measurements per sample. *p < 0.05 for the Wet NPs vs the Free Peptide only and ⌂p < 0.05 for the NPs (Wet and Dry) vs the Free Peptide with statistical significance determined via one-way ANOVA.

5.3.6 VB275 FISH Desolvation NP Synthesis

In order to determine if glyceraldehyde crosslinking is also impacted by gelatin macroscale molecular weight dispersity, FISH desolvation was performed using VB275 gelatin and NPs were crosslinked with glutaraldehyde (the control) or glyceraldehyde for comparison. Shown in Figure 5.20. after glutaraldehyde crosslinking and NP centrifugation, FISH desolvation produced ~100 nm particles, which is ~30 nm higher than two-step desolvation (indicated by the dashed line, actual values shown in Figure 5.8). Based on the correlation analysis in Chapter 3, the cellulose fiber filter paper used likely generates a higher molecular weight dispersity compared to two-step. This suggests that VB275 has lower molecular weight fractions that are easily removed via acetone precipitation from two-step, but are not adequately removed from FISH due to the presence of larger filter paper pore diameters. Direct comparison of VB275 macroscale molecular weight and molecular weight dispersity using size exclusion chromatography (SEC) after the first desolvation in two-step vs after vacuum filtration would provide helpful insight regarding sample differences

prior to NP synthesis. While VB275 NP diameters are larger using FISH desolvation, their PDI values remain narrow revealing size uniformity. As expected, glutaraldehyde crosslinking maintains uniform diameters even after centrifugation (Figure 5.20).

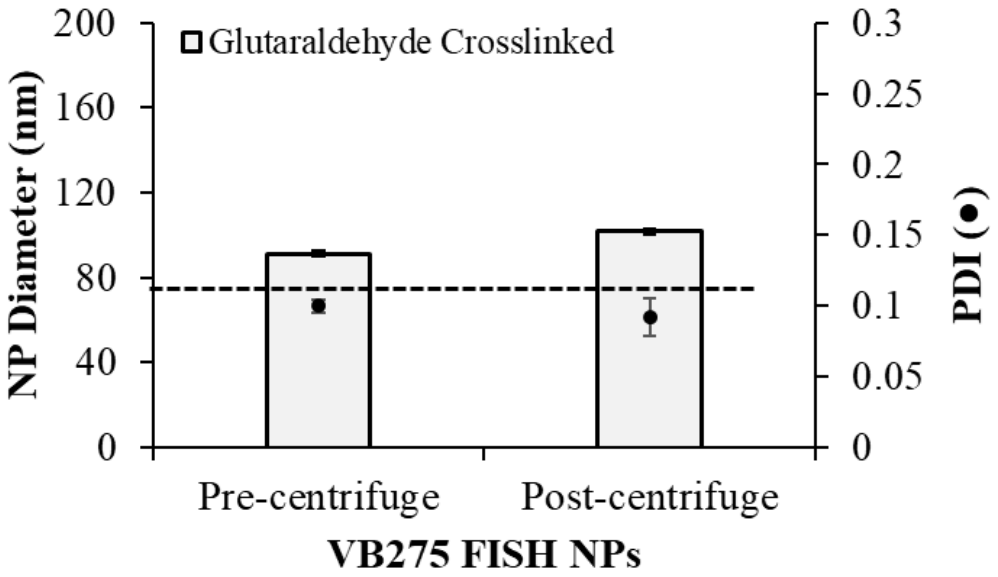

Figure 5.20. VB275 NPs prepared via FISH desolvation and glutaraldehyde crosslinked. Post-centrifuge NPs were dispersed in PBS. n = 3 measurements. Data represent mean ± standard deviation. Dashed line represents average VB275 NP diameter prepared via two-step desolvation.

Figure 5.21 shows diameters and PDI values for glyceraldehyde crosslinked NPs. After NP centrifugation, FISH desolvation produced ~160 nm particles, which is ~30 nm higher than two-step desolvation (indicated by the dashed line, actual values in Table 5.2). The data indicates glyceraldehyde crosslinking is similarly influenced by molecular weight dispersity. Glyceraldehyde crosslinked VB275 NPs prepared using FISH desolvation also maintain low PDI values after centrifugation confirming a narrow size distribution. Comparing the post-centrifuged NP diameters crosslinked with glutaraldehyde vs glyceraldehyde reveal an ~60 nm diameter increase for the particles crosslinked with glyceraldehyde (Figure 5.20, 100 nm and Figure 5.21, ~160 nm). Interestingly, there was also an ~60 nm increase in NP diameter after glyceraldehyde crosslinking using two-step desolvation (Table 5.2 rotovap) compared to glutaraldehyde (Figure 5.20 dashed line). Overall, this further reveals gelatin molecular weight dispersity impacts di-

aldehyde and monoaldehyde crosslinking and if the sample dispersity can be controlled, then the ability to predict NP diameters using various chemical crosslinkers is possible.

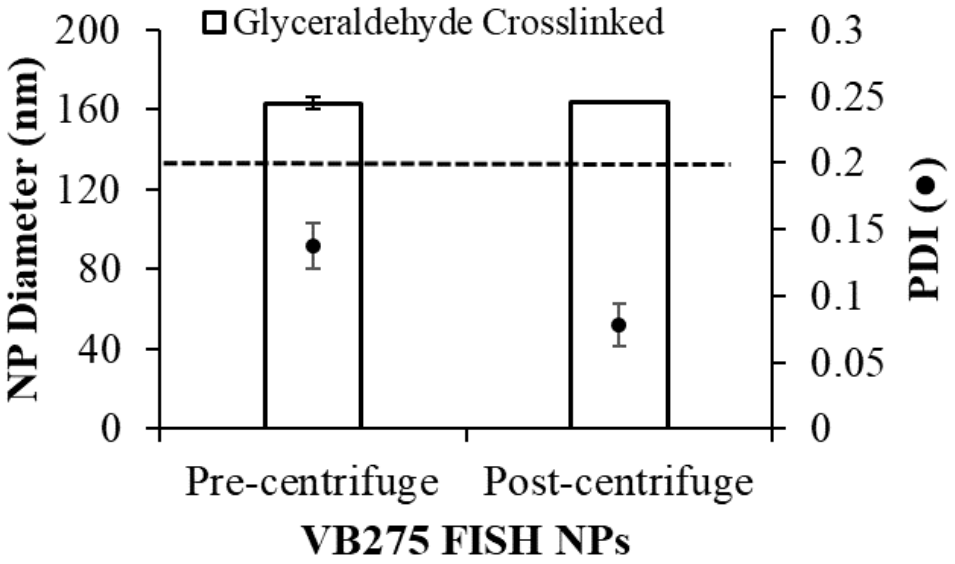

Figure 5.21. VB275 NPs prepared via FISH desolvation and glyceraldehyde crosslinked. Post-centrifuge NPs were dispersed in PBS. n = 3 measurements. Data represent mean ± standard deviation. Dashed line represents average VB275 NP diameter prepared via two-step desolvation. Error bars added but may be difficult to see.

5.4 Conclusions

This chapter provided additional insight regarding the use of glyceraldehyde as a non-toxic chemical crosslinker and the experimental processes for gelatin NP stability. Numerous brain cells were well tolerated with higher concentrations of glyceraldehyde compared to glutaraldehyde. Controlling gelatin NP swelling after glyceraldehyde crosslinking was a prominent feature in this chapter. Recommendations were provided such as the need to clearly characterize pre-purified NP diameters before purification along with clear protocols used in NP purification. Lyophilization, centrifugation and room temperature rotovap were effective at maintaining NP diameters after purification. The incorporation of VTM-RhoB seemed to drastically increase NP stability by preventing aggregation, possibly due to structural similarity between the peptide and gelatin. Peptide incorporation allowed the NP formulation to be well under the size and PDI results typical of emulsion based methods. Finally, increased NP diameters after VB275 FISH desolvation reveal

both glyceraldehyde and glutaraldehyde is influenced by molecular weight dispersity. Gelatin with a higher molecular weight dispersity results in larger NP diameters independent of aldehyde crosslinker composition. Therefore, properly characterizing gelatin macroscale properties prior to investigating new crosslinker NP stability will be advantageous for future experiments.

References

1. Faul M, X. L., Wald MM, Coronado VG, Traumatic Brain Injury in the United States: Emergency Department Visits, Hospitalizations and Deaths 2002–2006. *Atlanta (GA): Centers for Disease Control and Prevention, National Center for Injury Prevention and Control* **2010**.
2. Popescu, C.; Anghelescu, A.; Daia, C.; Onose, G., Actual data on epidemiological evolution and prevention endeavours regarding traumatic brain injury. *Journal of Medicine and Life* **2015,** *8* (3), 272-277.
3. The Lancet, N., The changing landscape of traumatic brain injury research. *The Lancet Neurology* **2012,** *11* (8), 651.
4. Giustini, A.; Pistarini, C.; Pisoni, C., Chapter 34 - Traumatic and nontraumatic brain injury. In *Handbook of Clinical Neurology*, Barnes, M. P.; Good, D. C., Eds. Elsevier: 2013; Vol. 110, pp 401-409.
5. Lozano, D.; Gonzales-Portillo, G. S.; Acosta, S.; de la Pena, I.; Tajiri, N.; Kaneko, Y.; Borlongan, C. V., Neuroinflammatory responses to traumatic brain injury: etiology, clinical consequences, and therapeutic opportunities. *Neuropsychiatric disease and treatment* **2015,** *11*, 97-106.
6. Xiong, Y.; Mahmood, A.; Chopp, M., Emerging treatments for traumatic brain injury. *Expert opinion on emerging drugs* **2009,** *14* (1), 67-84.
7. Xiong, Y.; Mahmood, A.; Chopp, M., Angiogenesis, neurogenesis and brain recovery of function following injury. *Current opinion in investigational drugs (London, England : 2000)* **2010,** *11* (3), 298-308.
8. Frugier, T.; Conquest, A.; McLean, C.; Currie, P.; Moses, D.; Goldshmit, Y., Expression and Activation of EphA4 in the Human Brain After Traumatic Injury. *Journal of Neuropathology & Experimental Neurology* **2012,** *71* (3), 242-250.
9. Boyd, A. W.; Bartlett, P. F.; Lackmann, M., Therapeutic targeting of EPH receptors and their ligands. *Nature Reviews Drug Discovery* **2013,** *13*, 39.
10. Coulthard, M. G.; Morgan, M.; Woodruff, T. M.; Arumugam, T. V.; Taylor, S. M.; Carpenter, T. C.; Lackmann, M.; Boyd, A. W., Eph/Ephrin Signaling in Injury and Inflammation. *The American Journal of Pathology* **2012,** *181* (5), 1493-1503.
11. Lamberto, I.; Qin, H.; Noberini, R.; Premkumar, L.; Bourgin, C.; Riedl, S. J.; Song, J.; Pasquale, E. B., Distinctive Binding of Three Antagonistic Peptides to the Ephrin-Binding Pocket of the EphA4 Receptor. *The Biochemical journal* **2012,** *445* (1), 47-56.
12. Theus Michelle, M. J., Whittington A., Engineering Health 2016 ICTAS JFA - Full Proposal Virginia Tech: 2016; Vol. 120000, pp 1-9.
13. Upadhyay, R. K., Drug Delivery Systems, CNS Protection, and the Blood Brain Barrier. *BioMed Research International* **2014,** *2014*, 869269.
14. Kozlovskaya, L.; Abou-Kaoud, M.; Stepensky, D., Quantitative analysis of drug delivery to the brain via nasal route. *Journal of controlled release : official journal of the Controlled Release Society* **2014,** *189*, 133-40.
15. Diaz-Arrastia, R.; Kochanek, P. M.; Bergold, P.; Kenney, K.; Marx, C. E.; Grimes, C. J. B.; Loh, L. T. C. Y.; Adam, L. T. C. G. E.; Oskvig, D.; Curley, K. C.; Salzer, C. W., Pharmacotherapy of Traumatic Brain Injury: State of the Science and the Road Forward: Report of the Department of Defense Neurotrauma Pharmacology Workgroup. *Journal of Neurotrauma* **2014,** *31* (2), 135-158.
16. Zhao, Y.-Z.; Li, X.; Lu, C.-T.; Lin, M.; Chen, L.-J.; Xiang, Q.; Zhang, M.; Jin, R.-R.; Jiang, X.; Shen, X.-T.; Li, X.-K.; Cai, J., Gelatin nanostructured lipid carriers-mediated intranasal delivery of basic fibroblast growth factor enhances functional recovery in hemiparkinsonian rats. *Nanomedicine: Nanotechnology, Biology and Medicine* **2014,** *10* (4), 755-764.
17. Thompson, B. J.; Ronaldson, P. T., Chapter Six - Drug Delivery to the Ischemic Brain. In *Advances in Pharmacology*, Davis, T. P., Ed. Academic Press: 2014; Vol. 71, pp 165-202.
18. Lockman, P. R.; Koziara, J. M.; Mumper, R. J.; Allen, D. D., Nanoparticle Surface Charges Alter Blood–Brain Barrier Integrity and Permeability. *Journal of Drug Targeting* **2004,** *12* (9-10), 635-641.

19. Sharma, P. P.; Sharma, A.; Solanki, P. R., Recent Trends of Gelatin Nanoparticles in Biomedical Applications. In *Advances in Nanomaterials*, Husain, M.; Khan, Z. H., Eds. Springer India: New Delhi, 2016; pp 365-381.
20. Roy, S.; Pal, K.; Anis, A.; Pramanik, K.; Prabhakar, B., Polymers in Mucoadhesive Drug-Delivery Systems: A Brief Note. *Designed Monomers and Polymers* **2009,** *12* (6), 483-495.
21. Li, X.; Wang, L.; Fan, Y.; Feng, Q.; Cui, F.-z., Biocompatibility and Toxicity of Nanoparticles and Nanotubes. *Journal of Nanomaterials* **2012,** *2012*, 19.
22. Chodobski, A.; Zink, B. J.; Szmydynger-Chodobska, J., Blood-brain barrier pathophysiology in traumatic brain injury. *Translational stroke research* **2011,** *2* (4), 492-516.
23. Geh, K. J.; Hubert, M.; Winter, G., Optimisation of one-step desolvation and scale-up of gelatine nanoparticle production. *Journal of microencapsulation* **2016,** *33* (7), 595-604.
24. Lu, C. T.; Jin, R. R.; Jiang, Y. N.; Lin, Q.; Yu, W. Z.; Mao, K. L.; Tian, F. R.; Zhao, Y. P.; Zhao, Y. Z., Gelatin nanoparticle-mediated intranasal delivery of substance P protects against 6-hydroxydopamine-induced apoptosis: an in vitro and in vivo study. *Drug design, development and therapy* **2015,** *9*, 1955-62.
25. Lawrence, T. P.; Pretorius, P. M.; Ezra, M.; Cadoux-Hudson, T.; Voets, N. L., Early detection of cerebral microbleeds following traumatic brain injury using MRI in the hyper-acute phase. *Neuroscience Letters* **2017,** *655*, 143-150.
26. Englert, C.; Blunk, T.; Muller, R.; von Glasser, S. S.; Baumer, J.; Fierlbeck, J.; Heid, I. M.; Nerlich, M.; Hammer, J., Bonding of articular cartilage using a combination of biochemical degradation and surface cross-linking. *Arthritis research & therapy* **2007,** *9* (3), R47.
27. Kuo, W.-T.; Huang, J.-Y.; Chen, M.-H.; Chen, C.-Y.; Shyong, Y.-J.; Yen, K.-C.; Sun, Y.-J.; Ke, C.-J.; Cheng, Y.-H.; Lin, F.-H., Development of gelatin nanoparticles conjugated with phytohemagglutinin erythroagglutinating loaded with gemcitabine for inducing apoptosis in non-small cell lung cancer cells. *Journal of Materials Chemistry B* **2016,** *4* (14), 2444-2454.
28. Shen, D.; Yao, S.; Wu, S.; Liu, Q.; Xiao, R., Kinetic study on the thermo-oxidative degradation of glyceraldehyde under different oxygen concentrations. *Journal of Analytical and Applied Pyrolysis* **2015,** *113*, 665-671.
29. Niles, A. L.; Moravec, R. A.; Riss, T. L., In Vitro Viability and Cytotoxicity Testing and Same-Well Multi-Parametric Combinations for High Throughput Screening. *Current Chemical Genomics* **2009,** *3*, 33-41.
30. Terry Riss, M. O. B., Richard Moravec. Choosing the Right Cell-Based Assay for Your Research *Cell Notes* [Online], 2003, p. 6-12.
31. *CellTiter 96® AQueous One Solution Cell Proliferation Assay Technical Bulletin*; Promega Corporation: 2012; pp 1-12.
32. Riss, T. L.; Moravec, R. A.; Niles, A. L.; Duellman, S.; Benink, H. A.; Worzella, T. J.; Minor, L., Cell Viability Assays. In *Assay Guidance Manual*, Sittampalam, G. S.; Coussens, N. P.; Brimacombe, K.; Grossman, A.; Arkin, M.; Auld, D.; Austin, C.; Baell, J.; Bejcek, B.; Chung, T. D. Y.; Dahlin, J. L.; Devanaryan, V.; Foley, T. L.; Glicksman, M.; Hall, M. D.; Hass, J. V.; Inglese, J.; Iversen, P. W.; Kahl, S. D.; Kales, S. C.; Lal-Nag, M.; Li, Z.; McGee, J.; McManus, O.; Riss, T.; Trask, O. J., Jr.; Weidner, J. R.; Xia, M.; Xu, X., Eds. Eli Lilly & Company and the National Center for Advancing Translational Sciences: Bethesda (MD), 2004.
33. Stansley, B.; Post, J.; Hensley, K., A comparative review of cell culture systems for the study of microglial biology in Alzheimer's disease. *Journal of Neuroinflammation* **2012,** *9*, 115-115.
34. Djupesland, P. G.; Messina, J. C.; Mahmoud, R. A., The nasal approach to delivering treatment for brain diseases: an anatomic, physiologic, and delivery technology overview. *Therapeutic delivery* **2014,** *5* (6), 709-33.
35. Hussar, P.; Tserentsoodol, N.; Koyama, H.; Yokoo-Sugawara, M.; Matsuzaki, T.; Takami, S.; Takata, K., The glucose transporter GLUT1 and the tight junction protein occludin in nasal olfactory mucosa. *Chemical senses* **2002,** *27* (1), 7-11.

36. Salmeron, K.; Aihara, T.; Redondo-Castro, E.; Pinteaux, E.; Bix, G., IL-1alpha induces angiogenesis in brain endothelial cells in vitro: implications for brain angiogenesis after acute injury. *Journal of neurochemistry* **2016,** *136* (3), 573-80.
37. Khan, A. A.; Paul, A.; Abbasi, S.; Prakash, S., Mitotic and antiapoptotic effects of nanoparticles coencapsulating human VEGF and human angiopoietin-1 on vascular endothelial cells. *International Journal of Nanomedicine* **2011,** *6*, 1069-1081.
38. Lawson, L. J.; Perry, V. H.; Gordon, S., Turnover of resident microglia in the normal adult mouse brain. *Neuroscience* **1992,** *48* (2), 405-15.
39. Réu, P.; Khosravi, A.; Bernard, S.; Mold, J. E.; Salehpour, M.; Alkass, K.; Perl, S.; Tisdale, J.; Possnert, G.; Druid, H.; Frisén, J., The Lifespan and Turnover of Microglia in the Human Brain. *Cell Reports 20* (4), 779-784.
40. Askew, K.; Li, K.; Olmos-Alonso, A.; Garcia-Moreno, F.; Liang, Y.; Richardson, P.; Tipton, T.; Chapman, M. A.; Riecken, K.; Beccari, S.; Sierra, A.; Molnár, Z.; Cragg, M. S.; Garaschuk, O.; Perry, V. H.; Gomez-Nicola, D., Coupled Proliferation and Apoptosis Maintain the Rapid Turnover of Microglia in the Adult Brain. *Cell Reports 18* (2), 391-405.
41. Loane, D. J.; Byrnes, K. R., Role of microglia in neurotrauma. *Neurotherapeutics* **2010,** *7* (4), 366-377.
42. Bocchini, V.; Mazzolla, R.; Barluzzi, R.; Blasi, E.; Sick, P.; Kettenmann, H., An immortalized cell line expresses properties of activated microglial cells. *Journal of neuroscience research* **1992,** *31* (4), 616-21.
43. Henn, A.; Lund, S.; Hedtjarn, M.; Schrattenholz, A.; Porzgen, P.; Leist, M., The suitability of BV2 cells as alternative model system for primary microglia cultures or for animal experiments examining brain inflammation. *Altex* **2009,** *26* (2), 83-94.
44. Markiewicz, I.; Lukomska, B., The role of astrocytes in the physiology and pathology of the central nervous system. *Acta neurobiologiae experimentalis* **2006,** *66* (4), 343-58.
45. Blackburn, D.; Sargsyan, S.; Monk, P. N.; Shaw, P. J., Astrocyte function and role in motor neuron disease: a future therapeutic target? *Glia* **2009,** *57* (12), 1251-64.
46. Silver, J.; Miller, J. H., Regeneration beyond the glial scar. *Nature Reviews Neuroscience* **2004,** *5*, 146.
47. Benda, P.; Lightbody, J.; Sato, G.; Levine, L.; Sweet, W., Differentiated rat glial cell strain in tissue culture. *Science (New York, N.Y.)* **1968,** *161* (3839), 370-1.
48. Quincozes-Santos, A.; Bobermin, L. D.; Latini, A.; Wajner, M.; Souza, D. O.; Gonçalves, C.-A.; Gottfried, C., Resveratrol Protects C6 Astrocyte Cell Line against Hydrogen Peroxide-Induced Oxidative Stress through Heme Oxygenase 1. *PLoS ONE* **2013,** *8* (5), e64372.
49. Mead, C.; Pentreath, V. W., Evaluation of toxicity indicators in rat primary astrocytes, C6 glioma and human 1321N1 astrocytoma cells: can gliotoxicity be distinguished from cytotoxicity? *Archives of Toxicology* **1998,** *72* (6), 372-380.
50. Pfisterer, U.; Khodosevich, K., Neuronal survival in the brain: neuron type-specific mechanisms. *Cell Death &Amp; Disease* **2017,** *8*, e2643.
51. Fuchs, E.; Fl; #xfc; gge, G., Adult Neuroplasticity: More Than 40 Years of Research. *Neural Plasticity* **2014,** *2014*, 10.
52. Viscomi, M. T.; D'Amelio, M.; Cavallucci, V.; Latini, L.; Bisicchia, E.; Nazio, F.; Fanelli, F.; Maccarrone, M.; Moreno, S.; Cecconi, F.; Molinari, M., Stimulation of autophagy by rapamycin protects neurons from remote degeneration after acute focal brain damage. *Autophagy* **2012,** *8* (2), 222-235.
53. Kovalevich, J.; Langford, D., Considerations for the Use of SH-SY5Y Neuroblastoma Cells in Neurobiology. *Methods in molecular biology (Clifton, N.J.)* **2013,** *1078*, 9-21.
54. Cirrito, J. R.; Holtzman, D. M., 12 - ANTI-AMYLOID-β IMMUNOTHERAPY AS A TREATMENT FOR ALZHEIMER'S DISEASE A2 - Kordower, Jeffrey H. In *CNS Regeneration (Second Edition)*, Tuszynski, M. H., Ed. Academic Press: San Diego, 2008; pp 295-318.

55. Paladini, C. A.; Tepper, J. M., Chapter 17 - Neurophysiology of Substantia Nigra Dopamine Neurons: Modulation by GABA and Glutamate. In *Handbook of Behavioral Neuroscience*, Steiner, H.; Tseng, K. Y., Eds. Elsevier: 2017; Vol. 24, pp 335-359.
56. Won, Y. W.; Kim, Y. H., Recombinant human gelatin nanoparticles as a protein drug carrier. *Journal of controlled release : official journal of the Controlled Release Society* **2008,** *127* (2), 154-61.
57. Zhao, Y.-Z.; Li, X.; Lu, C.-T.; Xu, Y.-Y.; Lv, H.-F.; Dai, D.-D.; Zhang, L.; Sun, C.-Z.; Yang, W.; Li, X.-K.; Zhao, Y.-P.; Fu, H.-X.; Cai, L.; Lin, M.; Chen, L.-J.; Zhang, M., Experiment on the feasibility of using modified gelatin nanoparticles as insulin pulmonary administration system for diabetes therapy. *Acta Diabetologica* **2012,** *49* (4), 315-325.
58. Miele, E.; Spinelli, G. P.; Miele, E.; Tomao, F.; Tomao, S., Albumin-bound formulation of paclitaxel (Abraxane(®) ABI-007) in the treatment of breast cancer. *International Journal of Nanomedicine* **2009,** *4*, 99-105.
59. Zillies, J. C.; Zwiorek, K.; Hoffmann, F.; Vollmar, A.; Anchordoquy, T. J.; Winter, G.; Coester, C., Formulation development of freeze-dried oligonucleotide-loaded gelatin nanoparticles. *European journal of pharmaceutics and biopharmaceutics : official journal of Arbeitsgemeinschaft fur Pharmazeutische Verfahrenstechnik e.V* **2008,** *70* (2), 514-21.
60. Fonte, P.; Soares, S.; Costa, A.; Andrade, J. C.; Seabra, V.; Reis, S.; Sarmento, B., Effect of cryoprotectants on the porosity and stability of insulin-loaded PLGA nanoparticles after freeze-drying. *Biomatter* **2012,** *2* (4), 329-339.
61. Jeong, L.; Park, W. H., Preparation and Characterization of Gelatin Nanofibers Containing Silver Nanoparticles. *International Journal of Molecular Sciences* **2014,** *15* (4), 6857-6879.
62. Gerrard, J. A., Maillard crosslinking of food proteins. I: the reaction of glutaraldehyde, formaldehyde and glyceraldehyde with ribonuclease. *Food chemistry* **2002,** *v. 79* (no. 3), pp. 343-349-2002 v.79 no.3.
63. Acar, H.; Çınar, S.; Thunga, M.; Kessler, M. R.; Hashemi, N.; Montazami, R., Study of Physically Transient Insulating Materials as a Potential Platform for Transient Electronics and Bioelectronics. *Advanced Functional Materials* **2014,** *24* (26), 4135-4143.
64. Jadhav, N. R.; Tone, J. S.; Irny, P. V.; Nadaf, S. J., Development and characterization of gelatin based nanoparticles for targeted delivery of zidovudine. *International journal of pharmaceutical investigation* **2013,** *3* (3), 126-30.
65. Wang, H.; Hansen, M. B.; Löwik, D. W. P. M.; van Hest, J. C. M.; Li, Y.; Jansen, J. A.; Leeuwenburgh, S. C. G., Oppositely Charged Gelatin Nanospheres as Building Blocks for Injectable and Biodegradable Gels. *Advanced Materials* **2011,** *23* (12), H119-H124.
66. Madan, J.; Dhiman, N.; Sardana, S.; Aneja, R.; Chandra, R.; Katyal, A., Long-circulating poly(ethylene glycol)-grafted gelatin nanoparticles customized for intracellular delivery of noscapine: preparation, in-vitro characterization, structure elucidation, pharmacokinetics, and cytotoxicity analyses. *Anti-cancer drugs* **2011,** *22* (6), 543-55.
67. Bueno, V. B.; Bentini, R.; Catalani, L. H.; Petri, D. F. S., Synthesis and swelling behavior of xanthan-based hydrogels. *Carbohydrate Polymers* **2013,** *92* (2), 1091-1099.
68. Azimi, B.; Nourpanah, P.; Rabiee, M.; Arbab, S., Producing Gelatin Nanoparticles as Delivery System for Bovine Serum Albumin. *Iranian Biomedical Journal* **2014,** *18* (1), 34-40.
69. McClements, D. J., Encapsulation, protection, and release of hydrophilic active components: Potential and limitations of colloidal delivery systems. *Advances in Colloid and Interface Science* **2015,** *219*, 27-53.
70. Mello, V. A. d.; Ricci-Júnior, E., Encapsulation of naproxen in nanostructured system: structural characterization and in vitro release studies. *Química Nova* **2011,** *34*, 933-939.
71. Wang, L. Y.; Gu, Y. H.; Zhou, Q. Z.; Ma, G. H.; Wan, Y. H.; Su, Z. G., Preparation and characterization of uniform-sized chitosan microspheres containing insulin by membrane emulsification and a two-step solidification process. *Colloids and surfaces. B, Biointerfaces* **2006,** *50* (2), 126-35.

72. Lu, X.-Y.; Wu, D.-C.; Li, Z.-J.; Chen, G.-Q., Chpater 7 - Polymer Nanoparticles. In *Progress in Molecular Biology and Translational Science*, Villaverde, A., Ed. Academic Press: 2011; Vol. 104, pp 299-323.

Chapter 6

Conclusions and Future Work

6.1 Conclusions

Gelatin nanoparticles (NPs) are appealing natural based materials to encapsulate and protect numerous molecules for the food and pharmaceutical industries. Decades of research has refined gelatin NP preparation methods based on aggregation and chemical crosslinking to produce particles with relatively narrow size distributions within respective batches. While the research community has presented impressive applications of gelatin NPs, the lack of gelatin NP property reproducibility using different gelatin batches along with limited knowledge on alternative non-toxic crosslinkers for stability, were two important areas this dissertation addressed.

The first part of this dissertation provided insight as to why similar gelatin samples (this dissertation framed gelatin samples as similar blooms obtained from different manufacturers) produced both statistically significant and non-significant NP physicochemical properties. Interestingly, the lowest bloom gelatin and a high bloom gelatin from different manufacturers consistently produced sub-100 nm particles, while another low bloom and middle bloom gelatin consistently produced ~200 nm particles. A new approach to develop correlations between macroscale and nanoscale properties revealed a high association between gelatin pre-crosslinked PDI and NP diameter in particular, using the experimental conditions outlined. This research is particularly helpful since gelatin macroscale dispersity is usually not reported prior to NP preparation nor is the first desolvation time length, which can have a dramatic result on the remaining precipitate and consequently the NP diameter. NPs were prepared without varying experimental conditions (for example temperature, pH and crosslinker concentration) already described in the literature. It is worth noting that gelatin macroscale dispersity is a major property that must be controlled, but is not the only factor that must be considered.

From the new correlation analysis, the second part of this dissertation postulated that if the macroscale dispersity could be reduced between two gelatin samples (independent of bloom or Type A / Type B) then similar diameters could be obtained. To demonstrate this, a brand new

technique to prepare gelatin NPs was produced known as filtration initiated selective homogeneity (FISH) desolvation. SB225 and VA300 that differed by >120 nm in diameter using two-step desolvation, had diameters within ±12 nm upon vacuum filtration and dispersion in phosphate buffered saline (PBS). Though their diameters and extent of crosslinking were highly similar, the NPs obtained different charge profiles in PBS due to their distinct isoelectric points (pIs). Low polydispersity indices (PDIs) revealed the NP population was highly monodispersed, which was further substantiated by a single narrow volume peak below 200 nm in each gelatin sample. Therefore, filtering NPs to obtain a narrow size distribution is not required for FISH desolvation, allowing for maximum retention of encapsulated molecules. FISH desolvation produces NPs with greater physicochemical consistency and reduces the preparation time by 24 h compared to the two-step desolvation procedure described in this dissertation. Actually, the first desolvation step, which is rarely reported in literature with regard to length of time, is completely removed in FISH, likely reducing the amount of experimental variation in future studies.

The third part of this dissertation addressed the use of an alternative crosslinker to glutaraldehyde and the experimental methods to obtain NPs that meet specific design criteria for prospective traumatic brain injury treatment. Glyceraldehyde is a monosaccharide and literature has reported its non-toxicity in comparison to glutaraldehyde. To further our knowledge, this section revealed that not only were brain cells more tolerant to glyceraldehyde than glutaraldehyde, but they were so at higher concentrations. This was the first study to directly show that significantly higher cell viability was obtained for brain cells spiked with higher concentrations of glyceraldehyde compared to lower glutaraldehyde concentrations. With regard to gelatin, this study was the first to directly compare gelatin NP diameters using the same molar concentration and the same number of aldehyde groups of glutaraldehyde and glyceraldehyde. Experimental processing obtained distinct differences between the chemically crosslinked NPs most likely due to their unique covalent bonding with gelatin. For example, substantial swelling and agglomeration was prominent in the glyceraldehyde crosslinked NPs upon heated rotary evaporation. As a result, NPs must be characterized just prior to purification to determine how the respective processes might affect NP diameter and PDI. Various methods were able to reduce swelling and agglomeration including centrifugation and lyophilization. Gelatin NPs were prepared and met design criteria after incorporation of a new potential therapeutic peptide to treat TBI. The peptide, known as

VTM, was incorporated using two distinct routes and maintained similar cumulative release profiles with both preparations. Finally, glyceraldehyde also showed an association between NP diameter and macroscale dispersity, so this interaction is likely independent of crosslinker "type" referred here as di-aldehyde glutaraldehyde or monoaldehyde glyceraldehyde.

Overall, applying materials science principles to characterize macroscale and nanoscale gelatin provided new insights regarding NP formation and control of physicochemical properties. This work is expected to allow for smoother translations into the manufacturing of new gelatin nanoscale formulations.

6.2 Future Work

This research provided insight into gelatin NP formation and crosslinking, which will enable further exciting NP explorations. For example, the ability to predict and control NP physicochemical properties is needed for successful translation to industry. In this research, gelatin macroscale dispersity was highly correlated to NP diameter. Future studies might determine if other natural (or synthetic) polymers have macroscale properties, such as dispersity, that correlate to their nanoscale properties. Obtaining various dispersities of albumin, chitosan, hyaluronic acid along with highly utilized polyethylene glycol (PEG) and poly(lactic-co-glycolic) acid (PLGA), and characterizing and forming NPs might offer additional insight to macroscale and nanoscale correlations. Additionally, filtering gelatin samples prior to NP formation obtained highly consistent nanoscale properties. As previously described, other natural based polymers are also formed into NPs using desolvation and might benefit from greater molecular weight homogeneity prior to NP preparation.

Emulsion techniques are widely utilized by the scientific community to prepare NPs. With respect to gelatin, emulsion based methods generally require numerous experimental modifications to prepare NPs with narrow size distributions compared to the more limited factors described in the literature for desolvation. Since emulsion typically does not remove gelatin fractions prior to NP formation, vacuum filtration prior to emulsion based NP production might reveal that molecular weight homogeneity is applicable to a range of gelatin NP preparation techniques and should be a considered within the gelatin NP community.

While this work incubated glyceraldehyde by itself within brain cells, for pharmaceutical applications, NPs crosslinked with glyceraldehyde (and glutaraldehyde for comparison) should be incubated with applicable cell types (for example brain cells if using to treat TBI) at various concentrations to determine tolerable toxicity thresholds. Prior to *in vivo* applications which increase translational potential by proving NP formulation efficacy, the biological activity of the potential therapeutic peptide (VTM) must be accessed to confirm its function is maintained. This would consist of applying VTM that has been released from the NPs to an EphA4 assay to monitor decreased phosphorylation over time.

Currently, gelatin for food and the pharmaceutical applications is derived almost exclusively from animal products.[1] However, the products obtained through these processes are heterogeneous mixtures of polypeptides with different sizes and charges, conditions that affect the products' gel-forming capacity in bulk industry applications[2] and also the NP diameter shown in this dissertation. In addition to the risk of associated infectious diseases, such as bovine spongiform encephalopathy, animal-derived gelatin may cause immune hypersensitivity when consumed by humans.[2] Therefore, the use of plant based recombinant gelatin to byass the macroscale variations in animal gelatin is in its infancy. While it is claimed gelatin derived from a microbial system affords easy control of gelatin size and charge,[2] current recombinant gelatin NPs have obtained diameters above 200 nm and / or PDIs $\geq$0.22.[3-4] Current studies have used vastly different molecular weight of recombinant gelatin along with distinct crosslinkers. It would be highly interesting to begin characterization of various recombinant gelatins along with NP preparation using controlled conditions to determine how nanoscale properties might correlate.

References

1. Gorgieva, S., Collagen- vs. gelatine-based biomaterials and their biocompatibility: Review and perspectives. InTech: 2011; pp 17-51.
2. Duan, H.; Umar, S.; Xiong, R.; Chen, J., New Strategy for Expression of Recombinant Hydroxylated Human-Derived Gelatin in Pichia pastoris KM71. *Journal of Agricultural and Food Chemistry* **2011,** *59* (13), 7127-7134.
3. Won, Y.-W.; Yoon, S.-M.; Sonn, C. H.; Lee, K.-M.; Kim, Y.-H., Nano Self-Assembly of Recombinant Human Gelatin Conjugated with α-Tocopheryl Succinate for Hsp90 Inhibitor, 17-AAG, Delivery. *ACS Nano* **2011,** *5* (5), 3839-3848.
4. Won, Y.-W.; Kim, Y.-H., Recombinant human gelatin nanoparticles as a protein drug carrier. *Journal of Controlled Release* **2008,** *127* (2), 154-161.